HYDROLOGIC AND BIOGEOCHEMICAL IMPLICATIONS OF FLOODING IN TWO CATCHMENTS UNDERLAIN BY CONTINUOUS PERMAFROST

by

JOSHUA C KOCH

B.A., Wesleyan University, 2001

M.S., University of Arizona, 2005

A thesis submitted to the

Faculty of the Graduate School of the

University of Colorado in partial fulfillment

of the requirement for the degree of

Doctor of Philosophy

Department of Civil, Environmental, and Architectural Engineering

2010

This thesis entitled:

Hydrologic and biogeochemical implications of flooding in two catchments underlain by continuous permafrost

written by Joshua C Koch
has been approved for the Department of Civil, Environmental, and Architectural Engineering

Diane M. McKnight

Robert Striegl

*Date*_____

The final copy of this thesis has been examined by the signatories, and we
Find that both the content and the form meet acceptable presentation standards
Of scholarly work in the above mentioned discipline.

Koch, Joshua C. (Ph.D., Civil, Environmental, and Architectural Engineering)

Hydrologic and biogeochemical implications of flooding in two catchments underlain by continuous permafrost

Thesis directed by Professor Diane M. McKnight

Abstract

Flooding is a critical driver of ecosystem productivity. By rapidly increasing stream stage and velocity, floods mix water and solutes from the stream, hyporheic zone, and floodplains/riparian areas. Such mixing may spur biogeochemical activity. In catchments underlain by permafrost, flooding is more common due to both the potential for rapid ice melting and minimal storage potential in frozen soils. High latitude environments are often underlain by permafrost and are also areas of biogeochemical interest, due to large stores of carbon (C) and nitrogen (N), and the potential for rapid cycling. The increased complexity in groundwater/surface water hydrology during floods requires rigorous hydrologic analysis before biogeochemical trends can be correctly interpreted. This research aims to accurately quantify the hydrology and biogeochemical cycling of C and N in two high-latitude catchments utilizing stream tracer additions, synoptic sampling, and surface water (sw), groundwater (gw), and coupled sw/gw flow models.

Two catchments, in Alaska and Antarctica represent very different ecosystems, both characterized by continuous permafrost and shallow aquifers. In Antarctica, coupled surface water / groundwater flow modeling and tracer additions identify sources of DOC (dissolved organic carbon) and locations of denitrification. Mass balance calculations identify heightened water / sediment interactions at high flows, and increased C and N uptake when solutes return to the stream during low flows. In Alaska, discharge correlates to DOC and nitrate concentrations, indicating leaching and flushing of organic material from the hillslope during high discharge, with a greater potential for microbial processing of this organic material during low flows. Multiple tracer additions demonstrate a seasonal trend, with the greatest C and N uptake early in the summer, potentially related to shallower flowpaths.

Differences between discharge, flooding, and C and N cycling in these two catchments indicate the importance of stream size and morphology. Using tracer dilution and major ion and uranium isotope chemistry, we identify preferential flow near and beneath the stream, indicating erosion of the stream bed via soil piping and thermokarsting. We propose that channel evolution will lead to decreased stream/catchment interactions and subsequently decreased C and N uptake potential in these high-latitude catchments.

Acknowledgements

This work could not have been completed without help and support from countless individuals. I would like to thank Jelle de Boer and Johan Varekamp for introducing me to research and providing me with the fundamentals of earth sciences. To Denis LeBlanc, who supervised the best job I ever had, went above and beyond to ensure that I was always learning and growing, and who facilitated my emigration to the great western states. To Rick Healy, Don Rosenberry, and Dean Anderson for providing me with diverse experience in the National Research Program of the USGS and for their constant and continued mentoring. To Paul Brooks for his tutelage, support, and encouragement as I wandered the deserts of southeast Arizona. To Rob Striegl and the Yukon River Basin project for taking me in, and allowing me to be part of a multi-faceted research project. And of course, I thank Diane McKnight, who welcomed me in to her academic family, taught me how to conduct rigorous scientific research, and how to be a diplomat and to foster positive interactions between diverse individuals and organizations.

I am grateful for the moral support of several individuals who helped maintain my sanity throughout this process. Thanks to Lars Peterson and Keith Musselman for teaching me to scale physical as well as metaphorical mountains, to Maneesh Sharma, Ben Hurwitz, and Dave Bihldorff for support and council as we continue navigating this strange world. Thanks to Charles and Eileen Koch for constant support and encouragement, Amee Koch for great conversations regarding life's mysteries, and of course, to Kathy Kelsey for all of her love and partnership in countless adventures.

CONTENTS

TABLES

Table

_ _

FIGURES

Figure

CHAPTER ONE

Biogeochemical implications of flooding

Introduction

Floods are important drivers of biogeochemical processes because of their ability to transport water, dissolved organic matter, and nutrients to and from reaction sites. Flooding is defined as an increase in discharge, which is related to an increase in stage and water velocity, and may influence stream and parafluvial biogeochemistry by altering the in-stream, hyporheic, and floodplain transport and storage of water and solutes.

Flooding alters the transport and availability of nutrients in stream ecosystems. The river continuum concept [*Minshall, et al.*, 1985] is a model of stream function, which proposes that stream ecosystems are structured to take advantage of solutes delivery from upstream. Inefficiencies in an upstream reach influence structure and function of a downstream reach. The advective flux in stream ecosystems leads to nutrient spiraling [*Newbold, et al.*, 1983], which is the idea that a nutrient molecule moving with stream water will eventually be utilized by biota, leading to chemical reduction and immobilization of the molecule until some later time. Increased flood wave velocity may effect stream ecosystems by increasing transport limitation, and subsequently inefficiencies of the upstream reach. Floods may also scour organic material from surfaces , thereby creating an organic matter pulse that will support greater productivity downstream [*Fisher, et al.*, 1998; *Marti, et al.*, 1997].

Flooding can affect ecosystems by exchanging stream water and solutes with storage zones including stream pools and eddies, the hyporheic zone, and the floodplain. Because different stores of water may have different oxidation states and nutrient

limitations, mixing of these zones can remove limitations and lead to heightened biogeoechemical cycling rates [*McClain, et al.*, 2003]. Increased stream stage may allow a stream to overflow its banks, increasing contact between the stream with the surrounding terrestrial riparian area [*Junk, et al.*, 1989]. Such flooding may remove ecosystem limitations by delivering necessary nutrients and flushing reaction products from both the terrestrial and aquatic systems. The hyporheic zone is the wetted area around and beneath a stream where surface water and subsurface waters mix, and has been recognized as an important location of biogeochemical activity [*Dent, et al.*, 2007; *Grimm and Fisher*, 1984; *McClain, et al.*, 2003]. Flooding may change stream-bed pressure heads and/or promote bank infiltration, thereby altering storage and exchange between the stream and hyporheic zone. The effect of flooding on hyporheic biogeochemistry has been observed in many systems [*Holmes, et al.*, 1998; *Meixner, et al.*, 2007; *Welter, et al.*, 2005].

This work adds to our knowledge of the biogeochemical effects of flooding by investigating stream ecosystems and flood events in high-latitude environments including interior Alaska and the coast of Antarctica. These systems are both arid environments and underlain by permafrost, which leads to frequent flooding. In the McMurdo Dry Valleys of Antarctica, soils and vegetation are minimal, providing an ideal setting for monitoring hyporheic interactions and stream microbial biogeochemistry with few confounding variables. The Alaskan interior does have soils and vegetation and is characterized by shallow flow, rapid runoff, and thermokarsting. High carbon content in boreal ecosystems are of particular interest because of the potential for respiration to create carbon dioxide and contribute to a climate warming feedback. Both of these

systems are vulnerable to climate change, which is expected to disproportionately affect polar systems . Our results increase knowledge of these individual systems and identify hydrologic, biogeochemical, and geomorphologic trends that are relevant to ecosystem productivity and climate change in permafrost-bound systems.

Methods

Aquatic ecosystem investigations are complicated by the fact that the location of solute reactivity is difficult to directly observe. Changes in solute concentrations may be used to indicate biogeochemical reactions, but are also related to hydrologic processes. It is necessary to accurately quantify hydrology first, in order to separate hydrologic and biogeochemical processes. We use a similar set of methods to address our research questions, focusing on tracer additions and surface water and groundwater flow modeling.

Hydrology

Flooding leads to inherently complex hydrologic interactions between disparate solute pools, requiring us to tailor our methods and models based on the particular research questions. We utilized tracer injections in both Alaskan and Antarctic streams. Tracers are useful for quantifying solute travel times, discharge along a reach, and the presence and magnitude of lateral inflows that add water to the stream. In many cases, a transient storage model (TSM) can add to this analysis by quantifying storage and exchange of the tracer in slow-velocity pools and the hyporheic zone [*Bencala and Walters*, 1983]. OTIS [*Runkel*, 1998], a popular TSM was used to analyze the Alaskan tracer data, but was less useful in Antarctica due to temporal variability in the transient

storage parameters (Chapter 1). Instead, the Antarctic tracer was modeled with the SFR2 package and MODFLOW, a coupled surface water routing and groundwater flow model [*Harbaugh*, 2005b; *Niswonger and Prudic*, 2005a], which allows for a more rigorous analysis of temporal variability in hyporheic dynamics In Alaska, temporally variability in storage was considered using the unsaturated flow model, VS2D [*Lappala, et al.*, 1993].

Biogeochemistry

This work utilizes carbon (C) and nitrogen (N) cycling to identify biogeochemical activity in our two study catchments. C and N are two of the most important elements to biogeochemical systems. Carbon is the primary element in biomass, and changes in stream concentrations, measured as dissolved organic carbon (DOC) may indicate assimilation by organisms or respiration. Respiration by heterotrophic bacteria creates carbon dioxide (CO_2) from DOC, and thus the rate of increase of CO_2 in incubations may be linked to microbial activity. The production of CO_2 from Alaskan soil DOC is of particular concern, because CO_2 is a greenhouse gas, and its emission may increase climate warming, thereby releasing more C and providing a climate warming feedback. We analyze C concentration and also quality, which provides information on C lability. Nitrogen is the primary limiting nutrient in many terrestrial and aquatic ecosystems. Nitrogen may be assimilated into biomass, but is also useful as an electron acceptor or donor due to its large range in oxidation states (+5 to -3). A shifting balance in the mass of disparate N species may indicate cycling, and subsequently ecosystem activity. The redox state of N molecules often provides information about the availability of oxygen and the moisture saturation of soils. By combining our hydrologic models with synoptic

C and N samples we can infer processes occurring in soil and stream flowpaths. We support our findings with mass balance calculations and laboratory incubations, which improve our understanding of the underlying processes that produce the observed chemical signatures.

Organization / Results Summary

Our results are split into five chapters and one appendix. Chapters 2 and 3 investigate hydrology and biogeochemistry in Huey Creek, in the McMurdo Dry Valleys of Antarctica, and consider the implications of diel floods on parafluvial storage and exchange, and subsequently on ecosystem productivity. Chapters 4 and 5 focus on the hydrology and biogeochemistry of Richarsdon Tributary, in the Yukon River Basin, Alaska. We quantify the seasonal variability in discharge, stream/catchment interactions, and C and N cycling and recognize the potential causes and consequences of soil piping and thermokarsting.

Chapter 2 [in review, *WRR*]: A glacial melt and catchment storage model is developed to explain the shape of an Antarctic stream hydrograph. Results indicate that flooding leads to large and rapid change in both stream/hyporheic storage and exchange rates.

Chapter 3 [*Koch, et al.*, 2010b]: Diel storage quantified in Chapter 2 flushes DOM from sediments, creating a pulse in the downstream reach as this DOM-rich water re-enters the stream. This DOM pulse and DOC and ammonium pulses emanating from further upstream are all lost in subsequent downstream reaches, indicating the potential for discharge-mediated rapid cycling of C and N in this ecosystem. Lithium concentrations

support the model developed in Chapter 2, and identify increased stream/sediment interactions at high discharge.

Chapter 4: This chapter investigates seasonality and export vs. processing of C and N on a hillslope in a boreal catchment in Alaska. Discharge correlates to DOC and nitrate concentration, indicating that generally, C and N are flushed from the catchment. Some uptake does occur in the smallest streams, and uptake rates increase at lower discharge. The catchment displays a seasonal trend of increasing C lability, and overall DOC and nitrate assimilation rates that decrease as the summer progresses.

Chapter 5: We use hydrologic analyses to show that the catchment is not drained uniformly, but that hydrologic connectivity and flux occur primarily in the near-stream environment. Tracer dilution and infiltration modeling suggest that the near stream environment is particularly important to hillslope drainage. Uranium concentrations and isotope activity ratios are used to delineate different modes of transport, and indicate the potential for preferential flow through soil pipes and thermokarst features in the parafluvial zone.

Chapter 6: Results from both Alaskan and Antarctic sites are combined to consider a broader trend in polar catchment hydrology. Here we review the tight coupling between heat and water cycles to explain the minimal catchment storage, flashy hydrographs, and potential for geomorphologic change in both streams. We identify critical discharge thresholds that control stream/catchment storage and exchange, and thus cycling and

uptake of C and N. We also compare the Antarctic and Alaskan stream, and recognize the significant loss in stream ecosystem dynamics that will result from thermokarsting and channel incision.

Conclusion

This dissertation expands classic stream ecosystem theory to include high-latitude streams that are underlain by permafrost. We consider how stream/catchment interactions are impacted by large and frequent floods in permafrost-bound systems, and how ecosystems function despite flashy hydrographs and rapid runoff. We compare and contrast these two systems to underscore the importance of stream/catchment and stream/hyporheic interactions, and propose that significant potential for channel incision and decreased stream productivity as polar systems get warmer.

References

Bencala, K. E., and R. A. Walters (1983), Simulation of Solute Transport in a Mountain Pool-and-Riffle Stream - a Transient Storage Model, *Water Resources Research*, *19*, 718-724.

Dent, C. L., et al. (2007), Variability in surface-subsurface hydrologic interactions and implications for nutrient retention in an arid-land stream, *Journal of Geophysical Research-Biogeosciences*, *112*.

Fisher, S. G., et al. (1998), Material spiraling in stream corridors: A telescoping ecosystem model, *Ecosystems*, *1*, 19-34.

Grimm, N. B., and S. G. Fisher (1984), Exchange between Interstitial and Surface-Water - Implications for Stream Metabolism and Nutrient Cycling, *Hydrobiologia*, *111*, 219-228.

Harbaugh, A. W. (2005), MODFLOW-2005, the U.S. Geological Survey modular ground-water model -- the Ground-Water Flow Process, US Geological Survey.

Holmes, R. M., et al. (1998), The impact of flash floods on microbial distribution and biogeochemistry in the parafluvial zone of a desert stream, *Freshwater Biology*, *40*, 641-654.

Junk, W. J., et al. (1989), The Flood Pulse Concept in River-Floodplain Systems, paper presented at Proceedings of the International Large River Symposium, Can. Spec. Publ. Fish. Aquat. Sci.

Koch, J. C., et al. (2010), Effect of unsteady flow on nitrate loss in an oligotrophic, glacial meltwater stream, *Journal of Geophysical Research G: Biogeosciences*, *115*.

Lappala, E. G., et al. (1993), Documentation of computer program VS2D to solve the equations of fluid flow in variably saturated porous media, US Geological Survey, Denver, CO.

Marti, E., et al. (1997), Pre- and post-flood retention efficiency of nitrogen in a Sonoran Desert stream, *Journal of the North American Benthological Society*, *16*, 805-819.

McClain, M. E., et al. (2003), Biogeochemical hot spots and hot moments at the interface of terrestrial and aquatic ecosystems, *Ecosystems*, *6*, 301-312.

Meixner, T., et al. (2007), Influence of shifting flow paths on nitrogen concentrations during monsoon floods, San Pedro River, Arizona, *Journal of Geophysical Research-Biogeosciences*, *112*.

Minshall, G. W., et al. (1985), Developments in stream ecosystem theory, *Can. J. Fish. Aquat. Sci.*, *42*, 1045-1055.

Newbold, J. W., et al. (1983), Phosphorus dynamics in a woodland stream ecosystem: a study of nutrient spiralling, *Ecology*, *64*, 1249-1265.

Niswonger, R. G., and D. E. Prudic (2005), Documentation of the streamflow-routing (SFR2) package to include unsaturated flow beneath streams - a modification of SFR1, 48 pp, US Geological Survey.

Runkel, R. L. (1998), One-dimensional tranpsort with inflow and storage (OTIS): a solute transport model for streams and rivers, U.S. Geological Survey, Denver, CO.

Welter, J. R., et al. (2005), Nitrogen transport and retention in an arid land watershed: Influence of storm characteristics on terrestrial-aquatic linkages, *Biogeochemistry*, *76*, 421-440.

CHAPTER 2:

Simulating unsteady flow, anabranching, and hyporheic dynamics in a glacial meltwater stream using a coupled surface water routing and groundwater flow model

J. C. Koch[1], D. M. McKnight[1], R. M. Neupauer[2]

1 – Institute of Arctic and Alpine Research, University of Colorado, Boulder, CO
2 – Civil, Environmental, and Architectural Engineering, University of Colorado, Boulder, CO

Flooding affects ecosystems by transporting water and solutes across aquatic-terrestrial interfaces, removing nutrient and organic substrate limitations and spurring biogeochemical activity. Few studies have considered the influence of flooding on surface water / groundwater interactions. This research examines the temporally-variable water storage and exchange in a stream in the McMurdo Dry Valleys (MDV) of Antarctica, where diel flood pulses occur due to glacial melt. Several MDV streams display truncated discharge peaks, suggesting water storage between the source glacier and the gaging station. We tested the hypothesis that stream braids and subsurface water storage contribute to the difference between glacial melt and stream outflow hydrographs by constructing a coupled surface water routing and subsurface water flow model. This model routes water into stream braids at high flows, and allows this water to infiltrate and return to the stream via subsurface flowpaths as flows recede. Our simulation demonstrates the importance of surface / subsurface water interactions in controlling the hydrograph shape. Maximum simulated discharge was sensitive to storage parameters including aquifer depth and the flooding threshold, while minimum discharge was

sensitive to hydraulic conductivity. Subsurface storage volume varied by 38 percent over a diel cycle and stream-subsurface exchange rates varied from 0 to 0.19 m^3/hr/m, with exchange from the stream to the subsurface during high flows, and vice versa at low flows. These results underscore how unsteady flow can increase hyporheic interactions and ecosystem productivity, and provide support for maintaining natural stream morphology and flow regimes.

Introduction

Low-order streams are disproportionately important to biogeochemical reactions, because of their large wetted perimeter and heightened interactions with the nearstream landscape [*Mulholland, et al.*, 2008; *Peterson, et al.*, 2001]. Much of this interaction occurs in the hyporheic zone, an area adjacent to the stream where surface and subsurface waters mix. Hyporheic interactions are controlled by variable pressure heads in the sediments surrounding a stream. Pressure variations are often caused by stream morphology including bedforms [*Boano, et al.*, 2007; *Cardenas, et al.*, 2004; *Harvey and Bencala*, 1993], riffles and pools [*Gooseff, et al.*, 2007; *Kasahara and Hill*, 2006; *Tonina and Buffington*, 2007], beaver dams [*Lautz, et al.*, 2006], cobbles [*Storey, et al.*, 2003], and meanders [*Cardenas, et al.*, 2004]. Storage and exchange of water and solutes between the stream and hyporheic zone lead to physical gradients in light, velocity, and temperature, and chemical differences in solute concentrations and oxidation state. Hyporheic biogeochemical activity contributes a substantial fraction of stream ecosystem function in many systems [*Gooseff, et al.*, 2004; *Grimm and Fisher*, 1984; *Holmes, et al.*, 1996; *Koch, et al.*, 2010; *McKnight, et al.*, 2004].

Flooding has been recognized as an important driver of biogeochemical reactions in many systems [*Holmes, et al.*, 1998; *Jones, et al.*, 1995a; b; *Junk, et al.*, 1989; *Koch, et al.*, 2010]. Unsteady flow stems from changes in discharge, and subsequently changes in water velocity, momentum, and stage. Such variability is ubiquitous in both natural and controlled streams and rivers, and may alter interactions between a stream, its floodplain, and the hyporheic zone. Unsteady flow may also alter subsurface pressure gradients [*Harvey and Bencala*, 1993], leading to variable hyporheic dynamics and affecting exchange of water and solutes between the surface and subsurface.

Surface / subsurface water interactions can be quantified using transient storage models (TSMs), which describe surface water flow with an advection - dispersion equation, and incorporate storage zones to simulate water and solutes stored in low-velocity zones such as pools and the hyporheic zone. OTIS (one-dimensional transport with inflows and storage) [*Runkel*, 1998] is a common TSM that simulates systems where continuous, bi-directional exchange between the stream and a storage zone dominates over gradient-based subsurface flow. OTIS describes storage with two variables: the cross sectional storage area, and the exchange rate between the stream channel and storage zone. OTIS has been coupled with a kinematic wave model to describe a conservative tracer transport [*Runkel, et al.*, 1998] in the same small, steep, unsteady glacial melt stream as simulated in this study.

Because TSMs do not simulate subsurface darcian flow, they are unable to physically represent changes in storage and exchange that may occur due to unsteady flow. Representation of hyporheic exchange in a given stream reach using a TSM is typically dependent on simulation of a tracer injection, which often only documents the

shortest storage zones and fastest exchange paths [*Harvey, et al.*, 1996]. TSM's can be manipulated to better approximate the residence times of stream water in the subsurface by including several storage areas [*Choi, et al.*, 2000], and incorporating decay functions to represent the long time scale over which solutes return to the stream from hyporheic flow paths [*Haggerty, et al.*, 2000].

Hyporheic dynamics can be more realistically simulated by using subsurface water flow models [*Cardenas, et al.*, 2004; *Gooseff, et al.*, 2006; *Lautz and Siegel*, 2006; *Storey, et al.*, 2003]. Such models are inherently complex, requiring knowledge of the medium through which the water is flowing and of the point- and reach-scale hydraulic gradients that drive hyporheic exchange. The additional field effort required to create and calibrate a groundwater flow model is often justified by the model's ability to represent stream-subsurface interactions and define hyporheic properties in systems with significant subsurface gradients, such as the system modeled by Lautz and Siegel [2006]. Groundwater flow models are able to consider the effects of varying hydraulic heads, which exert control on water crossing the stream/subsurface boundary. Therefore, they should also be capable of simulating the temporal and spatial variability in hyporheic dynamics that stem from unsteady streamflow.

Our study is based on a coupled conservative and reactive tracer experiment employed in the same stream as Runkel et al.'s [1998] study, under a similarly unsteady flow regime. Because our tracer results and hydrologic observations suggest complexity beyond what a TSM can reasonably model, we simulated unsteady stream flow and hyporheic dynamics using a coupled groundwater flow and surface water routing model. Our model is calibrated to achieve minimum error between the stream gage and

simulation hydrographs. We use our results to investigate the variability in hyporheic storage and exchange that stem from unsteady discharge and to consider the relevance of these dynamics to solute storage and biogeochemical processes.

Site Description

Huey Creek is located in the McMurdo Dry Valleys of Antarctica (Figure 1), which is one of the coldest and driest ecosystems on Earth. While ninety-eight percent of Antarctica is covered by ice sheets, the McMurdo Dry Valleys are representative of the ice-free desert oases on the coasts of the continent. The valleys are relatively free of snow and ice, receiving an average of less than ten centimeters of precipitation annually as snow [*Doran, et al.*, 2002]. Ninety-five percent of the valley surfaces are composed of arid soils [*Burkins, et al.*, 2001] derived from tills of granites, sandstones, dolerites, and meta-sedimentary rocks. There is no terrestrial vegetation, except for mosses near some stream channels and in wetted margins of lakes and ponds. A half meter below the surface the ground is permanently frozen.

Streams typically flow up to 14 weeks in the austral summer [*McKnight, et al.*, 1999], during which time the sun is above the horizon 24 hours per day. Water is derived from glacial melt [*Fountain, et al.*, 1999] and follows established channels into perennially ice-covered lakes on the valley floors. Incoming shortwave radiation and stream discharge fluctuate on a daily timescale with pulses of high discharge generated when the sun shines directly on glacier faces and surfaces [*Conovitz, et al.*, 1998]. Frozen soils and limited glacial melt preclude subsurface flow, except in stream hyporheic zones, where exchange between the stream and subsurface occurs on rapid timescales due to the high conductivity of the coarse – grained sediments.

Huey Creek is a high gradient stream in the Lake Fryxell Basin that drains a snowfield on the flank of the Commonwealth Glacier. This stream is characterized by a shallow channel with a narrow floodplain that is incised below the valley fill level. A previous tracer injection performed on Huey Creek was analyzed using a TSM to quantify hyporheic dynamics [*Runkel, et al.*, 1998]. Exchange rates ranged from 4.67 E-4 to 1.62 E-2 1/s, which are high relative to many reported values, and related to the high porosity of unconsolidated alluvial streambanks. Storage zone areas ranged from 0.8 to 3.07 m^2. The lack of groundwater inflows to Huey Creek is supported by tracer data from Runkel et al. [1998] and Koch et al. [2010].

During the daily high flow period the stream reach with the shallowest slope is dominated by anabranches (Figure 2), which are defined as multiple channels separated by semi-permanent alluvial islands [*Nanson and Knighton*, 1996]. Anabranches are common in streams with flood-dominated discharge regimes, and in Huey Creek fill with water during the daily high discharge pulse. These branches dry as the flood recedes and the reach becomes channelized again. The anabranches in Huey Creek are decimeter-wide, non-migratory braids, separated by gravel bars that route water laterally away from the main channel. The length of the anabranches range from meters to tens of meters. The high potential for water and solute storage in the surface and subsurface of the anabranching reach relative to channelized stream reaches leads to DOC pulses and heightened nitrogen cycling rates downstream of the anabranches [*Koch, et al.*, 2010].

Canada Stream is also located in the Lake Fryxell Basin and provides insight into the relationship between incoming solar radiation and downstream discharge. Canada and Huey are both located on the north side of the valley, and are fed from sources with

similar aspects. Canada Stream has a much larger source area (1.6 km^2 relative to 0.42 km^2). Because the source glaciers for Huey Creek and Canada Stream receive similar incoming solar radiation, we expect that the timing and relative magnitude of meltwater generation are similar. However, the routing of this meltwater downstream may be different, because Canada Stream is shorter than Huey Creek (1500 m versus 2160 m) and remains channelized for the entire distance between its source glacier and the stream gage. The shorter distance and lack of branches means that the Canada Stream hydrograph is likely more indicative of the effect of incoming solar radiation on meltwater generation than is the Huey Creek hydrograph. Therefore, the Canada Stream hydrograph may be useful in determining the relationship between incoming solar radiation and meltwater generation

Methods

We simulated Huey Creek discharge and subsurface flow through the anabranching reach for 48 hr coincident with the January 9th, 2006 tracer injection described by Koch et al [2010]. Coupled modeling of the surface and subsurface water flow was accomplished using MODFLOW [*Harbaugh*, 2005], which is a common groundwater flow model, and the SFR2 package [*Niswonger and Prudic*, 2005; *Niswonger, et al.*, 2008], which incorporates stream junctions, diversions, and exchange between surface and subsurface water. In SFR2, surface water flow is represented with the Kinematic Wave Approximation (KWA). The KWA is a simplification of the St. Venant equations and routes sub-critical flood waves while neglecting dynamic waves and backwater effects [*Woolhiser*, 1974]. This approximation functions best on streams

with high slopes, such as the one modeled in this study. The KWA is governed by a continuity equation that describes water movement in the channel and considers inputs/outputs:

$$\frac{\partial A}{\partial t} + \frac{\partial Q}{\partial L} = T\left(-q_{SS} - q_E - q_{BRANCH}\right), \qquad (1)$$

where A is cross section area, t is time, Q is stream discharge, L is the channel length, T is the width of the channel, q_{SS} represents exchange with the aquifer, q_E represents evaporative loss, and q_{BRANCH} represents water diversion to the anabranches. The continuity equation is coupled with a momentum equation, which was estimated using Manning's equation:

$$Q = \frac{C}{M} S^{1/2} A R^{2/3}, \qquad (2)$$

where C is a constant equal to 1 in SI units or 1.486 for English units, M is Manning's roughness, S is the channel slope, and R is the hydraulic radius. The flow of water between surface and subsurface pools (q_{ss}) was routed assuming Darcian flow through a saturated medium, with a hydraulic head gradient determined by the difference between the elevation of the stream stage and the water table:

$$q_{SS} = \frac{K}{z}\left(h - H\right), \qquad (3)$$

where K is hydraulic conductivity of the porous medium, z is stream bed thickness, h is stream stage, and H is hydraulic head in the aquifer. Subsurface water flow through the unconfined aquifer is governed by Darcy's law, and can be described using two-dimensional, isotropic, transient flow:

$$\frac{\partial}{\partial x_i}\left[HK\frac{\partial H}{\partial x_i}\right] + q_{SS} = S_y\frac{\partial H}{\partial t}, \qquad (4)$$

where x_i (i = 1, 2) represents spatial coordinates in two dimensions, and S_y is the volume of water released from a unit volume of aquifer per unit decline in hydraulic head.

Stream and anabranch boundaries and elevations were determined from a GPS survey that extended from the Huey Creek gage to 109 m above the anabranching reach (Figure 3). Stream boundaries for the upper-most reach were obtained from a GIS map available on the McMurdo Dry Valleys Long Term Ecological Research website (www.mcmlter.org). Depth to permafrost was determined by probing the subsurface with a metal rod, and was measured at several locations beneath the stream thalweg and parafluvial zone in the weeks surrounding the modeled time period.

Water Flow Simulations

The upstream boundary condition for our model was defined as a time-variable inflow derived from glacial melt, and was estimated using the relationship between incoming shortwave radiation (S_{radin}) measured at the Commonwealth Glacier meteorological station and Canada Stream discharge. This station was chosen because it has a similar aspect, elevation, and location as the snow field from which Huey Creek originates. The effect of S_{radin} on discharge was determined for Huey and Canada source

area - normalized hydrographs using regression analysis and incorporating a lag time. Surface water was routed using the stream flow routing package (SFR2) [*Niswonger and Prudic*, 2005]. Anabranching was simulated by allowing three stream segments in the anabranching zone to fill only when discharge in the main channel exceeded a set threshold. The GAGE package was used to quantify discharge at the location of the established gaging station on Huey Creek. Eight-point streambed cross sections were estimated from wading rod discharge measurements conducted at several locations in the stream, and incorporated into SFR2 to reproduce realistic channel morphology.

Our stream-subsurface water flow model was used to execute both steady state and transient simulations. The steady state simulation was run at a low discharge, to ensure that anabranches remained empty, providing a scenario with which to compare the effects of unsteady flow on water storage and exchange. The transient simulations routed water from the source glacier to the stream gage through 12 stream segments. Stream segment information and aquifer properties are summarized in Tables 1 and 2, respectively. Leakage from the stream to the subsurface was only allowed in the region of the stream where anabranching occurs (in reaches 3 through 10). Aquifer thickness was defined as 0.5 m, consistent with depth to ice observations in January, 2006. Lateral aquifer boundaries were simulated as no flow boundaries, such that all water entered and exited the anabranching zone through Huey Creek surface water, consistent with stream tracer results that estimated a 98 $^{+}$/- 2 % recovery of the injected conservative solute at the downstream end of the tracer reach [*Koch, et al.*, 2010]. Initial stream discharge at the upstream end of the model was set to 69 m^3/hr, and the water table was set to 0.1 m below the surface.

Table 1: Model Properties for SFR2.

Stream Reach	Leakage to Aquifer?	Type	Length (m)	Slope (m/m)	Roughness*
1	No	Channel	1451.24	0.2651	0.55
2	No	Channel	66.2864	0.2651	0.055
3	Yes	Channel	43.2386	0.0534	0.055
4	Yes	Channel	24.0607	0.0534	0.055
5	Yes	Branch	24.4767	0.0534	0.055
6	Yes	Channel	15.6561	0.0534	0.055
7	Yes	Channel	37.5312	0.0534	0.055
8	Yes	Branch	51.4194	0.0534	0.055
9	Yes	Branch	23.6665	0.0534	0.055
10	Yes	Channel	47.9498	0.0534	0.055
11	No	Channel	127.079	0.0570	0.055
12	No	Channel	205.066	0.0570	0.055

* - Calibrated value

Table 2: Model Properties for MODFLOW.

Parameter	Value	Units
Hydraulic Conductivity*	10	m/hr
Porosity	0.40	m^3/m^3
Specific yield	0.25	m^3/m^3
Minimum Diversion Discharge*	65	m^3/hr
Evaporation*	2.58	mm/hr

* - Calibrated value

Simulations were run for 48 hours, with outputs printed every hour. The effectiveness of each scenario was evaluated statistically by comparing the observed and simulated downstream hydrograph using the root mean squared error (RMSE),

$$RMSE = \sqrt{\left(\frac{1}{j} \sum_{i=1}^{n} \left(Y_o - Y_s \right)^2 \right)}, \qquad (5)$$

where j is the number of paired simulated and observed data points, Y_o is an individual flow observation, and Y_s is the corresponding simulated values of flow. The first four hours of simulation were not included in the statistical analyses to avoid errors resulting from inexact initial conditions. Model effectiveness was also evaluated by comparing the slope and intercept of simulated vs. observed discharge rates at each time step, and by comparing the relative shape and maximum and minimum discharges of the observed and simulated hydrographs.

The model was calibrated to minimize error between the simulated and observed (stream gage) hydrographs by varying several parameters:

1) subsurface hydraulic conductivity,
2) minimum discharge at which the anabranches began filling,
3) channel roughness, and
4) evaporation.

Once the best fit was achieved, the influence of particular model components was analyzed by modeling three intermediary scenarios:

1) kinematic wave routing and evaporation, but no subsurface flow or anabranch diversions,
2) kinematic wave routing, evaporation, and subsurface flow, but no anabranch diversions, and
3) kinematic wave routing, subsurface flow, and anabranch diversions, but no evaporation.

Anabranching zone head contours were plotted for the steady state model, and for the transient model during periods of rising and receding discharge in order to visualize differences in subsurface heads and hydraulic gradients between these situations.

Length - normalized storage volume in the anabranching reach (A_s) and flux of water between the main channel and the storage zone (q_s) were calculated to quantify temporal variability in hyporheic dynamics, and to compare surface / subsurface dynamics in our model to hyporheic parameters reported from tracer additions in other MDV streams. Length – normalized flux of water through the storage zone, q_s (m^3/hr/m), was defined by Harvey et al. [1996] as equal to the TSM storage zone exchange coefficient multiplied by the length – normalized stream volume. From our water flow model results, we calculated q_s for each time step as:

$$q_s = \frac{Q_{in} - Q_{out}}{L} - ET - T\frac{dh}{dt}, \qquad (6)$$

where Q_{in} is the flux into the anabranching reach from upstream, Q_{out} is the flux out of the downstream end of the anabranching reach, L is the length of the channel in the anabranching reach, and dh/dt is the change in stream stage with time. Because Q_{in} and

Q_{out} are measured in channelized sections above and below the anabranching reach that don't allow subsurface flow, this calculation includes the flux into the anabranches (q_{branch}) and aquifer (q_s), while excluding losses due to evaporation (q_E) and changes in channel volume ($\delta A/\delta t$). Length – normalized storage volume in the anabranching reach for each time step, A_S^i (m^3/m), was defined as:

$$A_s^i = \frac{V_S}{L} + \sum_{j=1}^{i} q_s^j \Delta t, \qquad (7)$$

where V_S is a known storage volume, and Δt is the time step. Storage volume in the anabranching reach (V_S) was calculated during low flow conditions when the anabranches are empty by using the volume of water stored in the aquifer:

$$V_S = nA_{aquifer}H - V_{channel}, \qquad (8)$$

where n is the aquifer porosity, $A_{aquifer}$ is the aquifer area, and $V_{channel}$ is the volume of the stream channel. Flux of water through the storage zone and length – normalized storage volume were compared to values from several tracer experiments conducted in the McMurdo Dry Valleys. When necessary, q_s for these studies was calculated by multiplying reported storage zone exchange coefficients by length – normalized stream volumes.

The effect of transient storage on denitrification rates was calculated assuming first order decay of nitrate in storage zones in the anabranching reach:

$$N = N_o e^{-\lambda t}, \qquad (9)$$

where N is the final nitrate concentration; N_o is the initial nitrate concentration, which was set at 18.3 μM consistent with the average background concentration measured in Huey Creek [*Koch, et al.*, 2010]; e is the exponential function; λ is the decay rate coefficient, which was estimated as the average of three hyporheic denitrification rates reported in a MDV stream by McKnight [2004]; and t is the storage zone residence time, which was adjusted to simulate two potential storage mechanisms in the anabranching reach. Solute residence time in the anabranch reach aquifer was estimated as 12 hr from chloride breakthrough through the anabranching reach reported by Koch et al. [2010]. Residence times in the near-stream hyporheic zone of the anabranching reach were calculated using the values published in Runkel et al. [1998] as 0.058 hr.

Results

Glacial Melt Hydrograph

Canada Stream and Huey Creek display similar hydrograph timing, but high discharge in Huey is significantly truncated relative to Canada (Figure 5A), which we hypothesize is due to storage in the surface and subsurface of Huey Creek's anabranching reach. Incoming solar radiation and discharge displayed correlations for Huey Creek and Canada Stream, with lags set at 2.75 hr and 3.75 hr, respectively (Figure 5B). There is significant hysteresis in the S_{radin}-discharge relationship for Huey Creek, which skews the regression due to the insensitivity of discharge to high S_{radin} values. To avoid this complexity, we estimated the upstream boundary for the water flow model using the

strong correlation between S_{radin} and Canada Stream discharge during 15 hours of clear skies at the beginning of the simulation ($R^2 = 0.92$, $p < 0.01$). When this correlation is plotted with data from Huey Creek we see that it accurately describes the majority of the relationship between S_{radin} and Huey Creek discharge, and is not affected by the discharge insensitivity at high S_{radin} values. This relationship was used to create the 48 hr glacial melt input at the upstream boundary of the model.

Coupled surface-subsurface flow simulation

The full model simulates Huey Creek's hydrograph by routing water down the channel and varying storage and exchange based on discharge and subsurface flow in the anabranching reach. High discharges increase storage through two mechanisms: 1) heightened stream stage creates a hydraulic gradient from the stream to the aquifer, and 2) excess water is routed into the anabranches when discharge at the upstream end of each of the three anabranches exceeds a given threshold. Once in the branches water may flow directly back into the main channel from the end of the branch, or it can infiltrate the subsurface and drain to the water table. As discharge and subsequently stream stage decrease, a hydraulic gradient promotes drainage of water from the aquifer back into the stream channel.

Calibration and Sensitivity

Plots of simulated and observed hydrographs and simulated versus observed discharge for the full model and intermediate scenarios are displayed in Figure 6, with model statistics summarized in Table 3. The full model (Figure 6A) leads to the minimum RMSE, a slope near 1.00, and the highest R-squared. Channel roughness, hydraulic conductivity, the anabranch threshold, and evaporation were adjusted to

Table 3: Statistical Parameters for the 3 model scenarios. Part A displays the decrease in model fit as individual components of the full model are removed. Part B indicates the effect of adjusting hydraulic conductivity and the discharge at which anabranches begin forming from their values in the full model, 10 m/hr and 65 m^3/hr, respectively.

	Root Mean Square Error (m^3/hr)	**Simulated vs. Observed R^2**	**Simulated vs. Observed Slope**	**Simulated vs. Observed Intercept**
---------- A. Comparing Model Components ----------				
Kinematic Wave, Subsurface Flow, Anabranching, and Evaporation	10.5	0.86	1.00	5.79
No Anabranching	11.6	0.85	1.01	2.28
No Evaporation	12.3	0.80	1.07	1.83
Kinematic Wave Only	14.8	0.80	1.23	-4.69
---------- B. Model Sensitivity ----------				
Hydraulic Conductivity= 15 m/hr	12.5	0.79	0.89	10.7
Hydraulic Conductivity= 7 m/hr	10.9	0.85	1.04	3.44
Diversions if Q > 75 m^3/hr	11.6	0.85	1.07	3.78
Diversions if Q > 55 m^3/hr	10.3	0.85	0.93	7.61

achieve these results. The calibrated stream roughness values are consistent with Runkel et al.'s [1998] values for reaches modeled by both studies. Roughness is ten-fold greater in reach 1, which is by far the steepest reach of Huey Creek. Porosity, hydraulic conductivity, and specific yield were estimated based on the sandy-gravel soil, and then hydraulic conductivity was adjusted to reduce model error. The calibrated hydraulic conductivity value of 10 m/hr is slightly higher than values estimated from sediment studies [*Swanger and Marchant*, 2007], and consistent with subsurface travel times measured from tracer data [*Koch, et al.*, 2010]. The diversion threshold at which the anabranches begin filling was set to 65 m^3/hr, which is consistent with the truncated hydrograph peaks (shaded area in Figure 5A). The RMSE was minimized when evaporation was set to 2.58E-4 m/hr, a value consistent with measurements made in the McMurdo Dry Valleys using batch pan experiments (2.6E-4 m/hr [*Gooseff, et al.*, 2003; *Koch, et al.*, 2010]), and slightly greater than the range of values calculated from thermal budgets (1.00 – 2.16E-4 m/hr [*Cozzetto, et al.*, 2006]). The full simulation was most sensitive to hydraulic conductivity (K) and the minimum discharge at which the anabranches filled (Q_{div}). Manipulating K by a factor of 1.5 had large effects on the model fit (Table 3): a lower K resulted in high simulated discharges that varied little from the inflow hydrograph and a higher K increased low discharges and decreased sensitivity to the shape of the input. Maximum simulated discharge was sensitive to Q_{div}, with the lowest RMSE when Q_{div} is equal to 65 m^3/hr.

The effect of removing anabranching, subsurface flow, and the kinematic wave from the full model are presented in Figures 6B to 6D and Table 3. Figure 6B displays the effect of removing anabranching at high flows. This results in less water moving

from the stream to storage in the anabranches and the subsurface. With less water in storage, the simulation overestimates high flows. Figure 6C displays the effect of removing subsurface flow in the anabranching reach. This results in underestimating low flows, because there is no water stored in the subsurface to recharge the stream during periods of low glacial melt. Subsurface flow raises the minimum discharge, and smoothes changes that occur at low discharge, while having no effect on high discharge. Raising the minimum discharges also improves the slope and intercept of the simulated versus observed correlation. Figure 6D compares the modeled glacial melt hydrograph to the observed hydrograph at the bottom of the reach. The difference between 6C and 6D is caused by incorporating the KWA, which improves the timing of rising and falling hydrograph limbs. The KWA shifts the hydrograph by three hours, which is consistent with the 3.25 hr lag estimated from incoming solar radiation – Huey Creek discharge correlation (Figure 5B). Incorporating the KWA results in little improvement in the maximum and minimum discharges.

Anabranching, subsurface flow, and the kinematic wave factors affect the model in unique ways (ie. they are non-correlated), which means that one cannot be used to replace the others. Therefore, removing individual factors always decreases the model fit, and re-calibration can not improve the RMSE unless physical model parameters were adjusted to well outside the range of realistic values. In most cases, such adjustments led to non-convergence of the model.

The effects of unsteady flow on storage and exchange are plotted in Figure 7. Storage area varied from 2.19 to 3.55 m^3/m of water. The flux of water through the storage zone (q_s) was defined as positive when water was moving from the stream to

storage, and varied from of -0.11 to 0.19 m^3/hr/m (Figure 7C). Under unsteady flow conditions 7 % of the daily discharge moved through the anabranch storage zone.

Hydraulic head contours are plotted for large and small aquifer storage conditions at t = 16 and t = 39 hr, respectively (Figure 8A). The grey shaded area represents the change in head and subsequent change in storage associated with unsteady flow. Because water moves perpendicular to head contours, these lines also indicate the shift in flowpaths between rising and receding hydrographs. At t = 16 hr, stream flow is rising, and the storage is reaching its maximum. This is demonstrated by the straighter head contours that form the upstream boundary of the gray polygons. At t = 39 hr, storage is minimal, discharge is rising, and the anabranches are dry. This situation is represented by the angular head contours that form the downstream boundary of the gray polygons in Figure 8A. The sharp angle between the head contours and the channels (interior black lines) indicates flux of water from the channel into the subsurface during this period of rising hydrograph. The greatest head variability and subsequent change in storage along the stream channel occurs in the upper two thirds of the anabranching reach. There is also a large change in head associated with the longest anabranch. Figure 8B displays hydraulic head in the aquifer associated with a steady discharge and empty anabranches. Under steady flow conditions, the right section of the domain (the area without head contours) is completely dry. The aquifer storage will vary depending on the discharge used for the steady state simulation, but regardless of steady discharge magnitude, there is no longer significant exchange between the stream and subsurface.

Nitrate loss in the anabranching reach was highly dependent on the storage zone residence time. In the 12 hr that nitrate resided in the anabranches and aquifer, 100 % of

the nitrate was denitrified. In the shorter, rapidly-exchanging hyporheic pathways, only 12 % of the initial nitrate was lost. Because 7% of the total daily discharge flows through the longer anabranching storage zone, we believe that this storage accounts for a loss of at least 7% of the daily nitrate load. This is a conservative estimate, which will be considered further in the discussion.

Discussion

Unsteady flow is a fundamental aspect of most streams. Unsteady conditions are caused by diel cycles in evapotranspiration in natural systems and by discharge requirements of streams dammed for hydroelectric power generation. Unsteady flow occurs on seasonal time scales due to precipitation events, dam releases, snowmelt, and agricultural diversions. Our coupled surface / groundwater flow model demonstrates the effects of unsteady flow and subsequent temporal variability in storage and exchange in Huey Creek. Anabranches provide a simple conceptual and observable feature that is responsible for the large temporal change in exchange between the channel and storage pools. We expect that similar unsteady exchange occurs in many channelized streams, with variable stream stage providing the dominant mechanism of exchange.

Despite a limited data set and minimal calibration, our model reveals the benefit of considering surface / groundwater interactions to explain discharge, storage, and exchange under unsteady flow conditions. Our results have been presented using common TSM parameters to underscore how unsteady flow may affect the utility and analysis of stream tracer injection results. The simplest way to facilitate quantification of hyporheic dynamics is to avoid conducting tracer tests when unsteady conditions exist.

This is often impossible, given the rapid timescales and unpredictability of flood events. Large changes in flow regime are especially likely in the small streams that are best suited for tracer and biogeochemical studies. Furthermore, the biogeochemical processes that many tracer experiments are designed to study often demonstrate relevant responses to unsteady conditions caused by flooding [*Holmes, et al.*, 1998], groundwater inflows [*Harvey, et al.*, 1996; *Wondzell and Swanson*, 1996; *Wroblicky, et al.*, 1998], and diel cycles [*Koch, et al.*, 2010].

Hydrologic Implications of Unsteady Streamflow

Figure 9 compares stream/subsurface storage and exchange rates from this study to other studies conducted in the MDV. Our results are compared to Runkel et al.'s [1998] study, which was also performed in Huey Creek, albeit during a much higher discharge regime (ranging from approx. 180 to 414 m^3/hr). While our model calculates similarly high storage areas, their maximum storage was measured in a downstream reach not considered by our model. Our work determines that mean storage in the anabranching reach is 21 times higher than values reported by Runkel et al [1998] for a similar location in the stream. Exchange rates calculated in this study are consistent with values reported from other tracers in the Dry Valleys, but notably lower than values reported by Runkel et al [1998] in Huey Creek. Because our results were derived from a transient water flow simulation rather than a temporally-static TSM, we witness a range of exchange rates that can occur in a single reach subject to unsteady flow.

There are several reasons for the discrepancy between reported storage and exchange rates in the anabranching reach: 1) The two studies do not have consistent reach lengths and locations. Because the focus of Runkel et al [1998] was not on the

anabranching reach, their parameters lump storage in the anabranching reach with some length of reach upstream of the anabranches. 2) Results from Koch et al. [2010] suggest that the anabranching zone is not perfectly mixed by each flood pulse, which decreases the efficacy of tracer methods in accurately quantifying storage and exchange in this reach. In fact, Runkel's study recovered effectively 100% of the injected tracer mass over the span of several hours, suggesting that the tracer did not enter longer residence time flowpaths in the anabranching reach. 3) Huey Creek discharge during Runkel et al.'s tracer was well above the anabranching threshold determined by our study. Furthermore, peak flows in Huey Creek often significantly exceed the anabranch threshold (January 9th and 12th, 2006 floods in Figure 5A), suggesting that storage potential and exchange in the anabranching reach decrease when discharge exceeds the 65 m^3/hr threshold for several hours, because the storage volume is already full. Once this area is fully saturated, as we suspect it was during the Runkel et al. [1998] tracer, additional tracer-labeled water would be routed downstream without entering the longer storage flowpaths, leading to lower estimates of tracer-determined storage areas.

Another complication of unsteady flow is the inability of a single exchange rate to express stream/storage interactions. In TSM terms, "exchange rate" refers to a constant value that describes the transfer of water and solutes between the stream and a storage zone. This rate acts to simultaneously transfer mass from the stream to storage and vice versa, thereby conserving the total mass within these two zones. Results from this work show that unsteady flow leads to variability in storage zone size, and in the magnitude, location, and direction of exchange (Figures 7 and 8). We would expect similar results in

channelized streams, and specifically from any system where storage and exchange in the subsurface are due to hydraulic gradients caused by a changing stream stage.

Biogeochemical Implications of Unsteady Streamflow

We hypothesize that ecosystems will thrive downstream of branches and braids in Huey Creek and in similar streams. In Huey Creek, anabranches provide suitable algal habitat because 1) decreased high flows lessen the chances that mats and microbes will be scoured from substrate, and 2) increased low flows improve the chance that water will be constantly available to support metabolic processes. Anabranches and pools that form in many MDV streams appear at the shallowest slopes, which provide a zone of warmer, quiescent water where algal mats are likely to thrive.

Unsteady streamflow also affects the storage and transport of nutrients and organic matter, and may therefore influence biogeochemical cycles. In Huey Creek, biogeochemical processes are dependent on the availability of carbon, which is flushed from the upper reaches at high discharges, and from the anabranch aquifer at low discharges [*Koch, et al.*, 2010]. Slow moving or stagnant waters that exist in the anabranches during the hydrograph recession may provide a location for autotrophs to photosynthesize, thereby adding carbon to the water before it enters the aquifer. Denitrification is an important mechanism of nitrate reduction in the MDVs [*Gooseff, et al.*, 2004; *Koch, et al.*, 2010; *McKnight, et al.*, 2004] and many temperate streams [*Fisher, et al.*, 1998; *Mulholland, et al.*, 2008]. Denitrification requires anaerobic conditions, which may occur in longer subsurface flowpaths or in anoxic microsites [*Parkin*, 1987]. We expect that the anabranching reach provides the highest potential for denitrification because of the long subsurface residence time and the carbon source,

which together may support heterotrophic microbial processes that can lead to anoxic conditions. Under a steady or high discharge regime (ie. such as witnessed by Runkel et al [1998]), lower exchange rates would preclude the exchange of oxygen, organic matter, and nutrients between surface and subsurface waters, and subsequently decrease the biogeochemical activity.

We considered the potential for denitrification in the anabranching reach by comparing nitrate loss that can be expected given first order reaction in the long subsurface flowpaths and the short hyporheic flowpaths. Our calculations conservatively estimate a 7 % decrease in the daily stream load due to the anabranches and subsurface flow. This loss is likely larger due to the two-fold increase in nitrate which accompanies rising discharge [*Koch, et al.*, 2010]. Some of this high-concentration pulse will infiltrate the aquifer through the anabranches, thereby increasing the nitrate available for reduction in the longer subsurface flowpaths. Also, our calculations do not consider carbon- or transport- limitations, both of which are likely to decrease the reaction potential in the rapid hyporheic flowpaths relative to the anabranch aquifer.

Recent work has identified the hyporheic zone as a necessary element in river restoration [*Hester and Gooseff*, 2010], and natural and engineered branches and braids may provide a means of restoring and bolstering hyporheic zones and subsequent ecosystem benefits. Because stream branches and braids often stem from unsteady flow regimes, our work supports studies that have recognized the importance of flooding, and suggests that in addition to delivering sediments to ecosystems, floods may provide benefits by spurring stream hyporheic dynamics.

Model Limitations

Our model was created as a way to conceptualize the various processes responsible for the quantity and timing of water delivery at the downstream end of the Huey Creek; it is not intended to be a well-calibrated groundwater flow model with exact porous medium parameters. The model's ability to accurately simulate water flow in Huey Creek is limited relative to the actual system for several reasons.

Our inflow hydrograph is based on the assumption that kinematic wave routing and storage are negligible in Canada Stream relative to Huey. This assumption allows us to estimate Huey's inflow hydrograph by assuming that Canada Stream discharge at the gaging station is representative of the amount of glacial melt caused by incoming solar radiation. We believe that such an assumption is valid, based on Huey Creek's much larger stream length (approx. 3-fold greater) and elevation change between the stream source and outlet (approx. 3.5-fold greater).

The high Manning's roughness in the uppermost reach stems from our limited knowledge of this long reach. Our roughness values for all other reaches are similar to those estimated by Runkel et al. [1998]. However, in the highest reach, which was not considered by Runkel, we estimate roughness five-fold greater than their highest calculation. This value is related to the very high stream slope, which correlates to chaotic water falls through coarse materials. This value may be overestimated because our model ignores the concavity of the channel slope, which therefore underestimates channel length and subsequently the friction affecting the falling water. Improved representation of this reach within our model may improve the shape of our modeled hydrograph, but would likely also increase the lag between the simulated and observed flood pulse, thereby decreasing our model accuracy.

The remainder of our major model limitations relate to our underestimation of water storage in the surface and subsurface:

1) *Simplified stream geometry:* Our model only considers three anabranches. These modeled branches are long relative to many of the other branches, and therefore have a significant effect on water storage. However, as can be seen in Figure 2, there are many shorter branches that fill during high flows. We expect that modeling these branches would increase water storage only minimally, because they are shorter and do not carry water far from the stream relative to the modeled branches.

2) *No storage in non-anabranching reaches:* It is likely that some amount of storage and exchange occurs in every reach of Huey Creek. Our assumption that the anabranching reach is the dominant location of significant storage and exchange is based on its shallow stream slope, which promotes ponding and seepage. The importance of slope break is supported by data in Runkel et al. [1998], which shows that the largest storage zone occurs in the reach with the shallowest slope. Data from Runkel et al. [1998] also attribute the highest rates of exchange and flux through the storage zone to the reach containing anabranches. We suggest that this large flux is due to high discharge and subsequent high water / sediment contact in the anabranching reach. Wondzell [2006] provides another example of a tracer study conducted in a stream with a steep slope, which highlights the importance of a few large slope breaks relative to multiple smaller breaks in promoting hyporheic storage and exchange.

Because of its steepness and length, the uppermost reach is another potential location of significant storage and exchange. We evaluated this potential using data from Runkel [1998], which shows that while there is a weak trend of increasing flux through

the storage zone with increasing slope, the flux through the storage zone in the anabranching reach is significantly larger. Furthermore, MDV streams constantly hover around freezing temperatures, and it is likely that sediments in the uppermost reach are minimally thawed relative to the anabranching reach sediments. Therefore, we suggest that water lost from the channel during its chaotic descent through pools and falls is more likely to splash on to the surrounding sediments and evaporate/sublimate than to infiltrate and return to the stream. Subsequently, the uppermost reach would likely provide a mechanism of loss rather than transient storage.

3) *Unrealistic uniform aquifer thickness:* We defined the aquifer depth as 0.5 m. In actuality, the aquifer depth is dictated by a thaw bulb under the stream [*Brosten, et al.*, 2006; *Zarnetske, et al.*, 2007]. In the anabranching reach, these thaw bulbs may exist in a complicated pattern related to the temporally-variable surface streams. Such a detailed representation of the ice surface is beyond the scope of this model, and our simplified representation leads to some uncertainty in our calculations of storage volume and exchange rates.

These model limitations negatively affect our ability to simulate the Huey Creek hydrograph. Including more anabranches and storage in other reaches would increase the overall storage potential of our system, and would positively influence our model results by decreasing the maximum simulated flows even further. While additional complexity could be added to this model, the stream morphology and storage properties are sufficiently represented for the purpose of comparing the multiple effects of unsteady flow.

Conclusion

Huey Creek is characterized by unsteady flow on a diel timescale. The causes and effects of unsteady flow were examined by simulating water movement using a coupled surface water routing and groundwater flow model. Simulating anabranch diversions proved necessary in truncating high flows and ensuring that simulations did not exceed the observed discharge. Physically, anabranches divert water out of the main channel and into slower-moving pools, promoting infiltration into the subsurface. Subsurface flow through a high conductivity medium was necessary to reproduce the minimum discharge observed in Huey Creek. This work demonstrates how unsteady flow may lead to temporally variable water storage, and exchange rates that vary in magnitude and location.

Considering the effects of unsteady flow is paramount to correctly quantifying solute and tracer fluxes in many hydrologic and ecosystem studies. Unsteady flow is ubiquitous in streams and can be rigorously modeled using combined kinematic wave routing and subsurface groundwater flow models. Furthermore, unsteady flow may create the biologic hotspots and hot moments that many tracers are designed to study. Without rigorously considering the surface / groundwater interactions caused by unsteady flow, one cannot hope to correctly interpret or model such biogeochemical data. By quantifying the surface – subsurface water interactions that relate unsteady flow to hyporheic dynamics this work attests to the ecosystem benefits of flooding, and indicates that braiding and anabranches are worth protecting and creating as part of river restoration programs.

Acknowledgements

Thanks to Raytheon Polar Services and PHI helicopters for invaluable field support, and Seth White of UNAVCO for the GPS Survey of Huey Creek. Rich Niswonger provided guidance on the use of SFR2. Thanks to three anonymous reviewers for their comments which significantly improved this manuscript. This work was supported by NSF OPP-9810219.

References

Boano, F., et al. (2007), Bedform-induced hyporheic exchange with unsteady flows, *Advances in Water Resources*, *30*, 148-156.

Brosten, T. R., et al. (2006), Profiles of temporal thaw depths beneath two arctic stream types using ground-penetrating radar, *Permafrost and Periglacial Processes*, *17*, 341-355.

Burkins, M. B., et al. (2001), Organic carbon cycling in Taylor Valley, Antarctica: quantifying soil reservoirs and soil respiration, *Global Change Biology*, *7*, 113-125.

Cardenas, M. B., et al. (2004), Impact of heterogeneity, bed forms, and stream curvature on subchannel hyporheic exchange, *Water Resources Research*, *40*.

Choi, J., et al. (2000), Characterizing multiple timescales of stream and storage zone interaction that affect solute fate and transport in streams, *Water Resources Research*, *36*, 1511-1518.

Conovitz, P. A., et al. (1998), Hydrologic processes influencing streamflow variation in Fryxell Basin, Antarctica., in *Ecosystem dynamics in a polar desert: The McMurdo Dry Valleys*, edited, pp. 93-108, American Geophysical Union, Washington, DC.

Cozzetto, K., et al. (2006), Experimental investigations into processes controlling stream and hyporheic temperatures, Fryxell Basin, Antarctica, *Advances in Water Resources*, *29*, 130-153.

Doran, P. T., et al. (2002), Valley floor climate observations from the McMurdo dry valleys, Antarctica, 1986-2000, *Journal of Geophysical Research-Atmospheres*, *107*.

Fisher, S. G., et al. (1998), Material spiraling in stream corridors: A telescoping ecosystem model, *Ecosystems*, *1*, 19-34.

Fountain, A. G., et al. (1999), Physical controls on the Taylor Valley ecosystem, Antarctica, *Bioscience*, *49*, 961-971.

Gooseff, M. N., et al. (2006), A modeling study of hyporheic exchange pattern and the sequence, size, and spacing of stream bedforms in mountain stream networks, Oregon, USA (Retraction of vol 19, pg 2915, 2005), *Hydrological Processes*, *20*, 2441-+.

Gooseff, M. N., et al. (2007), Relating transient storage to channel complexity in streams of varying land use in Jackson Hole, Wyoming, *Water Resources Research*, *43*.

Gooseff, M. N., et al. (2003), Determining long time-scale hyporheic zone flow paths in Antarctic streams, *Hydrological Processes*, *17*, 1691-1710.

Gooseff, M. N., et al. (2004), Denitrification and hydrologic transient storage in a glacial meltwater stream, McMurdo Dry Valleys, Antarctica, *Limnology and Oceanography*, *49*, 1884-1895.

Grimm, N. B., and S. G. Fisher (1984), Exchange between Interstitial and Surface-Water - Implications for Stream Metabolism and Nutrient Cycling, *Hydrobiologia*, *111*, 219-228.

Haggerty, R., et al. (2000), On the late-time behavior of tracer test breakthrough curves, *Water Resources Research*, *36*, 3467-3479.

Harbaugh, A. W. (2005), MODFLOW-2005, The U.S. Geological Survey modular ground-water model--the Ground-Water Flow Process, *U.S. Geological Survey Techniques and Methods 6-A16*.

Harvey, J. W., and K. E. Bencala (1993), The Effect of Streambed Topography on Surface-Subsurface Water Exchange in Mountain Catchments, *Water Resources Research*, *29*, 89-98.

Harvey, J. W., et al. (1996), Evaluating the reliability of the stream tracer approach to characterize stream-subsurface water exchange, *Water Resources Research*, *32*, 2441-2451.

Hester, E. T., and M. N. Gooseff (2010), Moving beyond the banks: Hyporheic restoration is fundamental to restoring ecological services and functions of streams, *Environmental Science and Technology*, *44*, 1521-1525.

Holmes, R. M., et al. (1998), The impact of flash floods on microbial distribution and biogeochemistry in the parafluvial zone of a desert stream, *Freshwater Biology*, *40*, 641-654.

Holmes, R. M., et al. (1996), Denitrification in a nitrogen-limited stream ecosystem, *Biogeochemistry*, *33*, 125-146.

Jones, J. B., et al. (1995a), Nitrification in the Hyporheic Zone of a Desert Stream Ecosystem, *Journal of the North American Benthological Society*, *14*, 249-258.

Jones, J. B., et al. (1995b), Vertical Hydrologic Exchange and Ecosystem Metabolism in a Sonoran Desert Stream, *Ecology*, *76*, 942-952.

Joslin, J. C. (2005), Determining the role of chemical weathering reactions and hyporheic exchange on silicate concentrations in Dry Valley streams, Antarctica, University of Colorado, Boulder, CO.

Junk, W. J., et al. (1989), The Flood Pulse Concept in River-Floodplain Systems, paper presented at Proceedings of the International Large River Symposium, Can. Spec. Publ. Fish. Aquat. Sci.

Kasahara, T., and A. R. Hill (2006), Hyporheic exchange flows induced by constructed riffles and steps in lowland streams in southern Ontario, Canada, *Hydrological Processes*, *20*, 4287-4305.

Koch, J. C., et al. (2010), Effect of unsteady flow on nitrate loss in an oligotrophic, glacial meltwater stream, *Journal of Geophysical Research-Biogeosciences*, *115*.

Lautz, L. K., and D. I. Siegel (2006), Modeling surface and ground water mixing in the hyporheic zone using MODFLOW and MT3D, *Advances in Water Resources*, *29*, 1618-1633.

Lautz, L. K., et al. (2006), Impact of debris dams on hyporheic interaction along a semi-arid stream, *Hydrological Processes*, *20*, 183-196.

McKnight, D. M., et al. (1999), Dry valley streams in Antarctica: Ecosystems waiting for water, *Bioscience*, *49*, 985-995.

McKnight, D. M., et al. (2004), Inorganic N and P dynamics of Antarctic glacial meltwater streams as controlled by hyporheic exchange and benthic autotrophic communities, *Journal of the North American Benthological Society*, *23*, 171-188.

Mulholland, P. J., et al. (2008), Stream denitrification across biomes and its response to anthropogenic nitrate loading, *Nature*, *452*, 202-U246.

Nanson, G. C., and A. D. Knighton (1996), Anabranching rivers: Their cause, character and classification, *Earth Surface Processes and Landforms*, *21*, 217-239.

Niswonger, R. G., and D. E. Prudic (2005), Documentation of the Streamflow-Routing (SFR2) Package to include unsaturated flow beneath streams - A modification to SFR1, *U.S. Geological Survey Techniques and Methods 6-A13*.

Niswonger, R. G., et al. (2008), Method for estimating spatially variable seepage loss and hydraulic conductivity in intermittent and ephemeral streams, *Water Resources Research*, *44*.

Parkin, T. B. (1987), Soil Microsites as a Source of Denitrification Variability, *Soil Science Society of America Journal*, *51*, 1194-1199.

Peterson, B. J., et al. (2001), Control of nitrogen export from watersheds by headwater streams, *Science*, *292*, 86-90.

Runkel, R. L. (1998), One-dimensional tranpsort with inflow and storage (OTIS): a solute transport model for streams and rivers, U.S. Geological Survey, Denver, CO.

Runkel, R. L., et al. (1998), Analysis of transient storage subject to unsteady flow: diel flow variation in an Antarctic stream, *Journal of the North American Benthological Society*, *17*, 143-154.

Storey, R. G., et al. (2003), Factors controlling riffle-scale hyporheic exchange flows and their seasonal changes in a gaining stream: A three-dimensional groundwater flow model, *Water Resources Research*, *39*.

Swanger, K. M., and D. R. Marchant (2007), Sensitivity of ice-cemented Antarctic soils to greenhouse-induced thawing: Are terrestrial archives at risk?, *Earth and Planetary Science Letters*, *259*, 347-359.

Tonina, D., and J. M. Buffington (2007), Hyporheic exchange in gravel bed rivers with pool-riffle morphology: Laboratory experiments and three-dimensional modeling, *Water Resources Research*, *43*.

Wondzell, S. M. (2006), Effect of morphology and discharge on hyporheic exchange flows in two small streams in the Cascade Mountains of Oregon, USA, *Hydrological Processes*, *20*, 267-287.

Wondzell, S. M., and F. J. Swanson (1996), Seasonal and storm dynamics of the hyporheic zone of a 4th-order mountain stream .1. Hydrologic processes, *Journal of the North American Benthological Society*, *15*, 3-19.

Woolhiser, D. A. (1974), Unsteady free surface flow problems., in *Proc. of Institute on Unsteady Flow in Open Channels*, edited, pp. 195-213, Colorado State University, Fort Collins, CO.

Wroblicky, G. J., et al. (1998), Seasonal variation in surface-subsurface water exchange and lateral hyporheic area of two stream-aquifer systems, *Water Resources Research*, *34*, 317-328.

Zarnetske, J. P., et al. (2007), Transient storage as a function of geomorphology, discharge, and permafrost active layer conditions in Arctic tundra streams, *Water Resources Research*, *43*.

Figure 1: Location of Huey Creek and Canada Stream within the Lake Fryxell Basin. The inset shows the relative location of the McMurdo Dry Valleys in Antarctica.

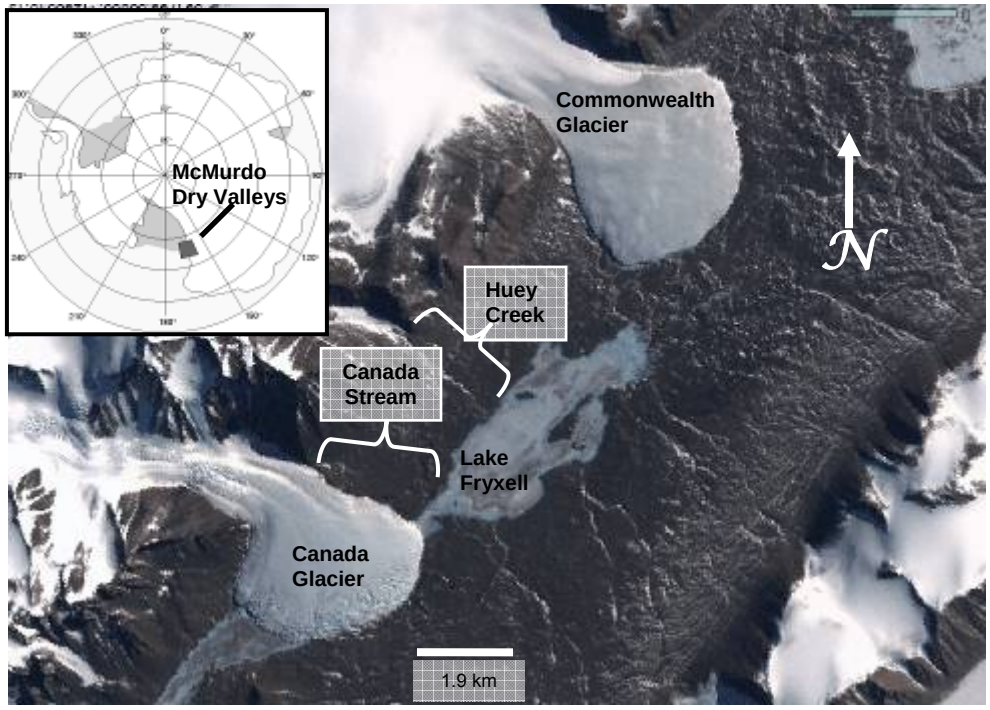

Figure 2: The anabranching reach of Huey Creek, looking upstream. A radio is in the foreground for scale. The stream channel meanders from the center background to the left foreground. Note anabranches leaving the frame on the right side, and infiltrating in the right foreground.

Figure 3: Side view of the stream reaches studied in Koch et al. 2010. Note that the shallowest slope occurs in the anabranching reach, with a knickpoint where the stream again becomes channelized (just upstream of location C).

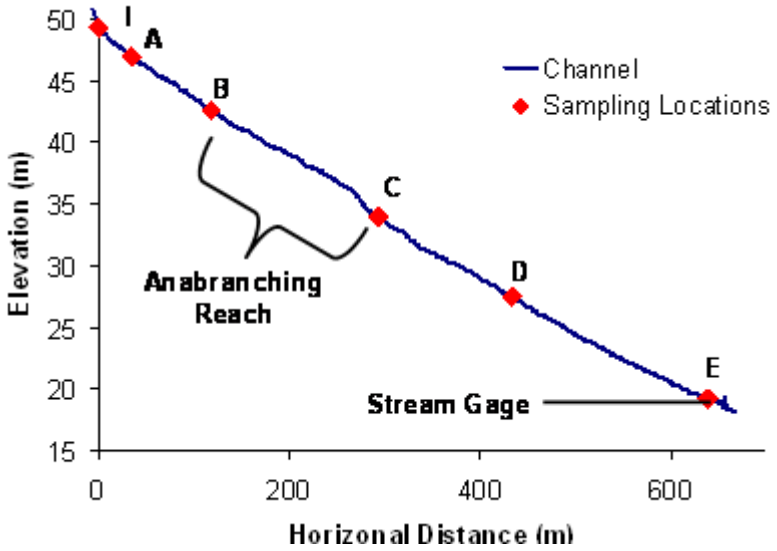

A) **Figure 4:** MODFLOW model domains: A) The entire model, and B) the anabranching reach. Subsurface flow is only allowed inside the anabranching reach model domain (exterior black line in B). Interior black lines represent the channel (solid) and anabranch (dashed) locations. Arrows indicate the direction of streamflow.

A) B)

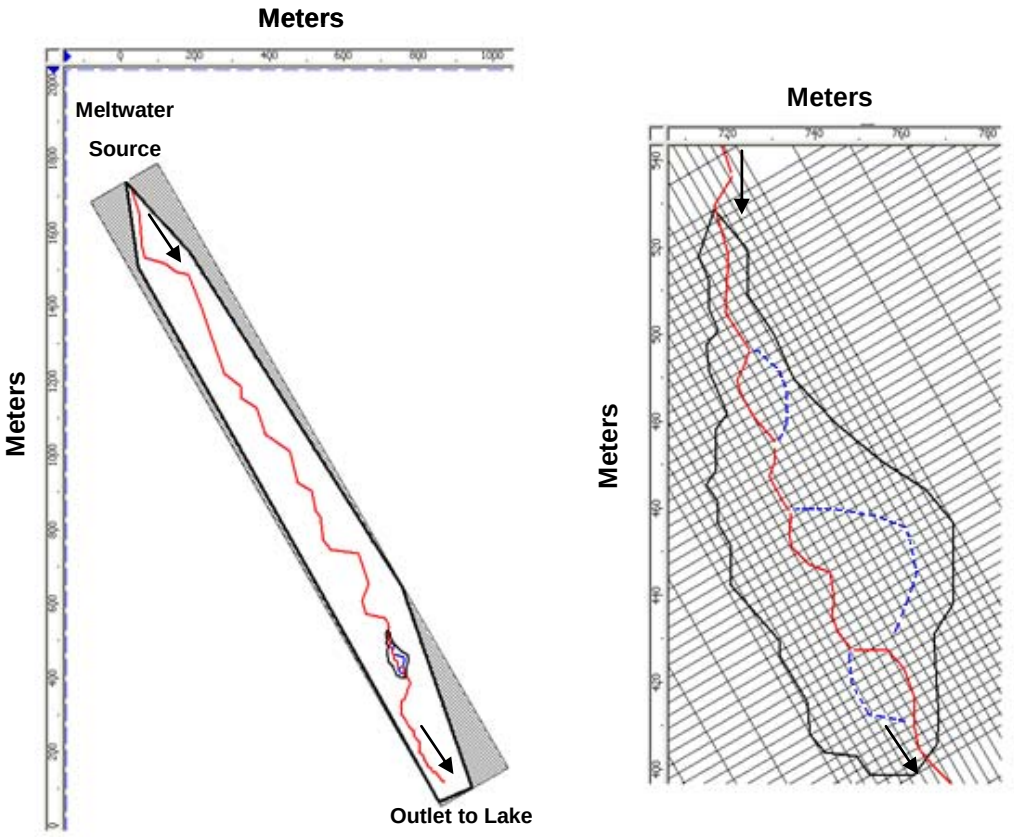

Figure 5: (A) Huey Creek and scaled Canada Stream hydrographs over the week of the field campaign in January, 2006. Canada discharge was scaled by 3.89, the ratio of glacial melt source areas for the two streams. The grey bar indicates the range at which Huey Creek discharge is truncated. (B) Regressions of incoming solar radiation and discharge in Canada Stream and Huey Creek from the beginning of the study period 1/9/06 at 19:00, until solar radiation decreased due to cloud cover on 1/10/06 at 13:00. The regression line was determined from the relationship between incoming solar radiation determined from Canada Stream.

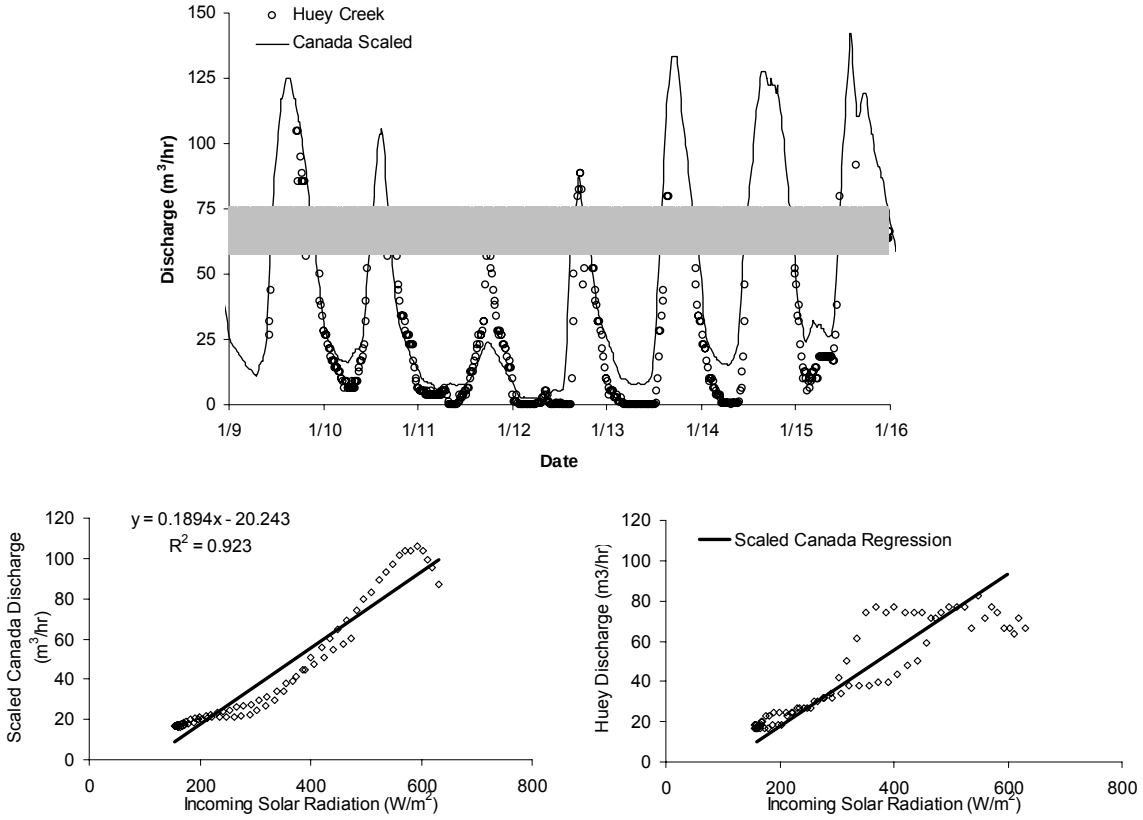

Figure 6: Simulated and observed discharges for (A) the full model; B) kinematic wave routing and subsurface flow, but no anabranching; C) kinematic wave routing, but no subsurface flow, and no anabranching. D) displays the difference between observations and the upstream boundary condition for each simulation.

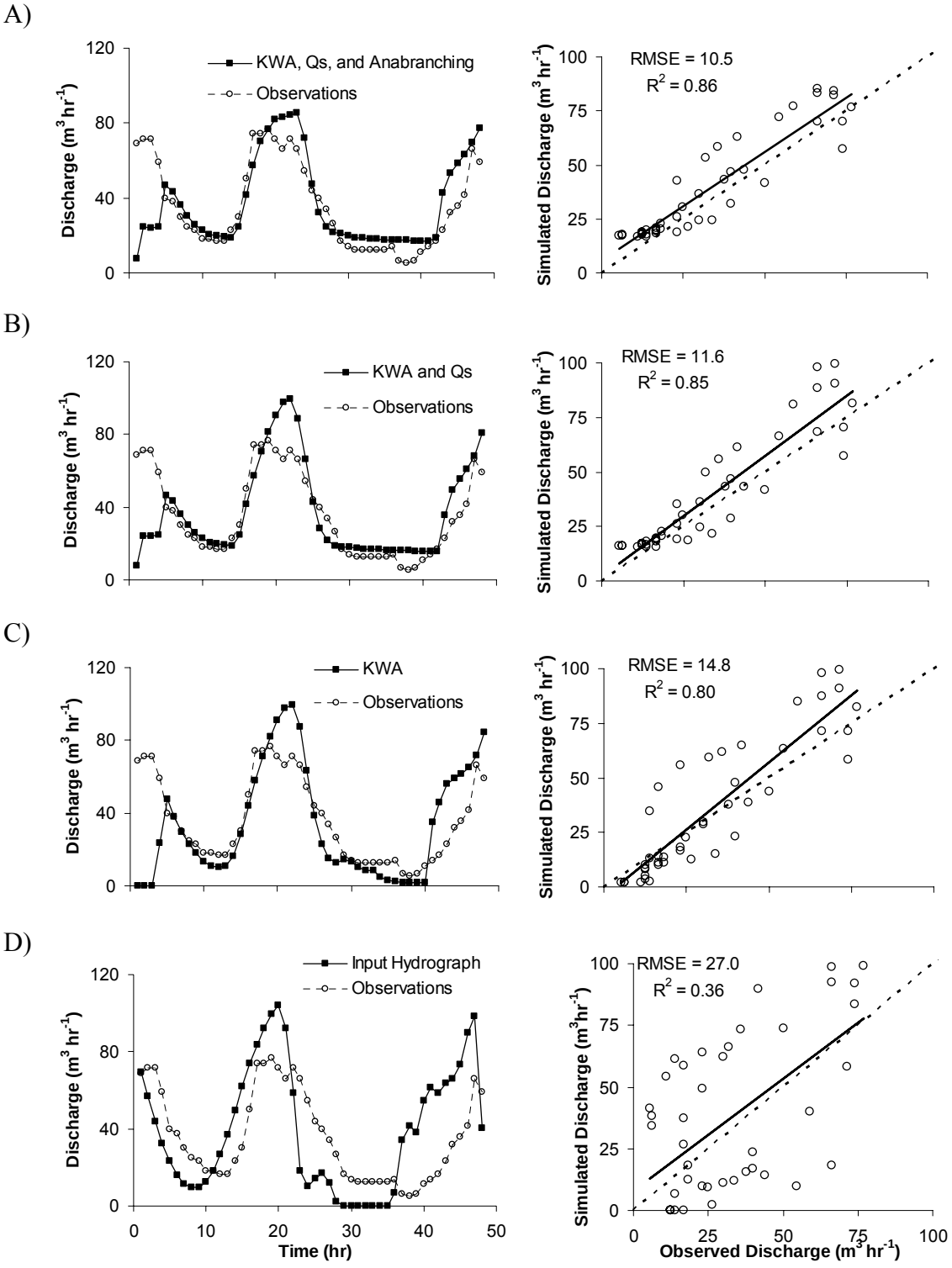

Figure 7: The input hydrograph (A), water storage (B), and exchange (C) between the stream and aquifer over 44 hr of the simulation. Timesteps one through four are omitted because they are influenced by the initial conditions.

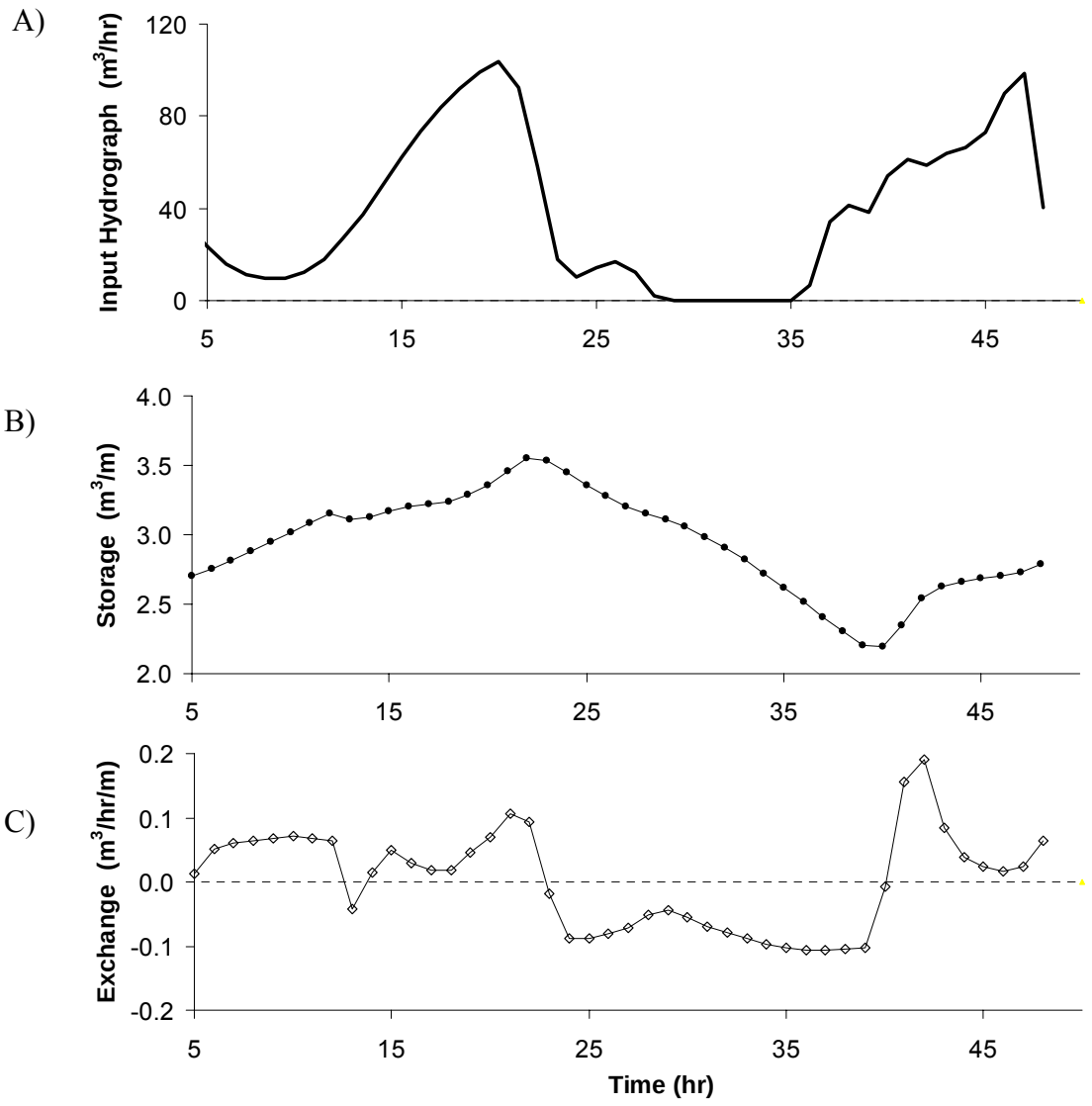

Figure 8: Head contours (m) in the anabranching reach. Horizontal and vertical axes display the length and width, respectively, of the anabranching reach. The solid black line around the perimeter of the contours is a no flow boundary. Interior black lines represent the channel (solid) and anabranch (dashed) locations. Shaded grey areas in A) represent the change in water table elevation between rising and receding hydrographs. B) indicates the water table elevation given a steady discharge or 50 m^3/hr. The edge of the contours are well inside the domain boundary, indicating that much of the region does not become saturated when the anabranches remain dry.

A) B)

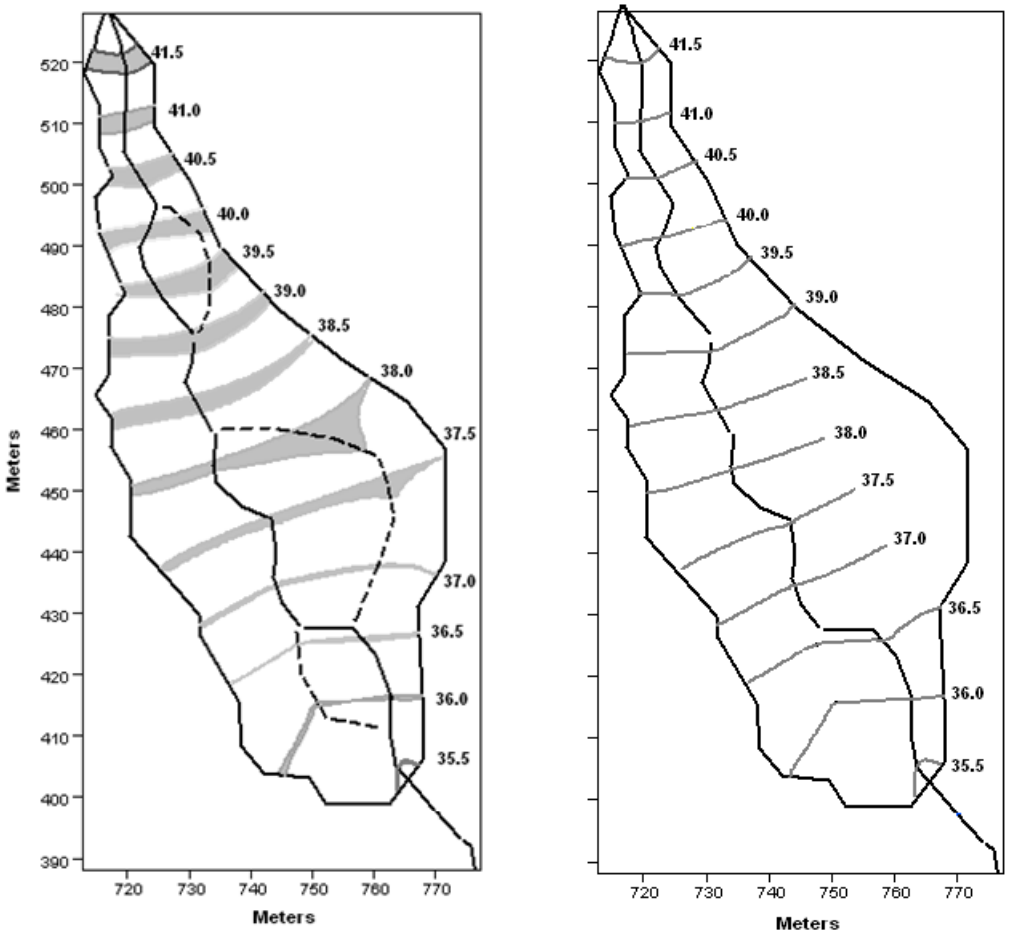

Figure 9: Hyporheic parameters calculated during this study relative to other studies conducted in individual reaches of McMurdo Dry Valley streams including Huey Creek, Von Guerard Stream, and Green Creek. Huey is separated into two columns to highlight differences inherent in calculating parameters from a groundwater/surface water flow model (GW/SW) and from a transient storage model (TSM). Bars for "This Study" represent the total range of temporally variable values within the anabranching reach of Huey Creek that occurred due to unsteady flow conditions.

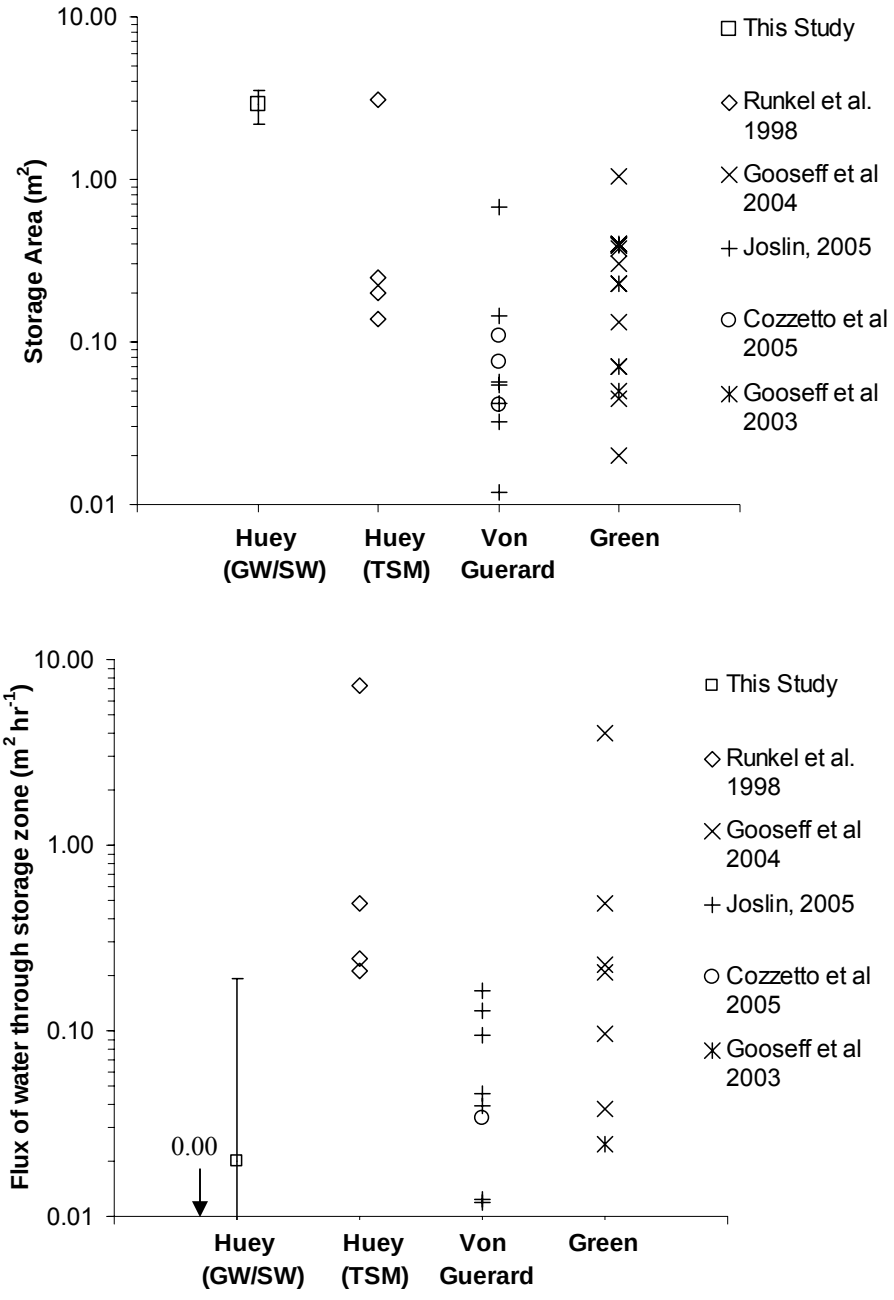

CHAPTER 3

Effect of unsteady flow on nitrate loss in an oligotrophic, glacial meltwater stream

Joshua C. Koch, INSTAAR, CU

Diane M. McKnight, INSTAAR, CU

Jenny L. Baeseman, IARC, University of Alaska, Fairbanks

Abstract

The McMurdo Dry Valleys of Antarctica are among the coldest, driest ecosystems on Earth. During the austral summer, glacial meltwater streams support cyanobacterial mat communities in some streams, but they are not ubiquitous. We conducted a nitrate (NO_3^-) enrichment tracer injection in Huey Creek, to quantify NO_3^- loss in a Dry Valley stream where algal mats would not obscure hyporheic microbial processes. Unsteady streamflow led to diel variability in the tracer concentration and in surface/subsurface water and solute exchange. Subsequently, concentrations of NO_3^-, nitrite (NO_2^-), ammonium (NH_4^+), and dissolved organic carbon (DOC) varied significantly during the injection, with a net loss of NO_3^-, NO_2^- , and DOC, and production of nitrous oxide. These mass changes within a reach were often coincident with high streamflows. Reactivity also coincided with the highest DOC concentrations, suggesting that DOC is the primary limitation to heterotrophic microbial activity in the stream. Together, streamflow and DOC availability create the hotspots and hot moments that dominate NO_3^- reactivity and removal in this polar desert ecosystem. The combination of spatially and

temporally variable hyporheic dynamics and solute availability underscore the limitations of common nutrient uptake metrics and transient storage models when unsteady flow conditions exist.

Introduction

Recent studies in stream ecosystem dynamics have demonstrated the importance of spatial and temporal variability of biogeochemical activity [*Harms and Grimm*, 2008; *McClain, et al.*, 2003]. Hot spots and hot moments are the locations and periods in which a number of variables come together to allow elevated rates of biogeochemical activity. In semi-arid riparian systems, hot spots and hot moments are crucial to the cycling of carbon (C) and nitrogen (N). Such events are often tied to hydrology and the short timescales on which rainstorms, ephemeral inflows, and flooding events occur. Unsteady flow can influence exchange rates of water and solutes across the sediment/water interface [*Harvey, et al.*, 1996], which affects the distribution of hotspots and/or hot moments in lotic ecosystems [*Holmes, et al.*, 1998; *Jones, et al.*, 1995b; *Valett, et al.*, 2005]. In this paper we expand the hotspot/hot moment concept to include semi-arid streams in polar deserts.

Hotspots and hot moments in streams are particularly important in the hyporheic zone, an area proximal to the stream in which surface and subsurface waters mix, resulting in a region of strong physical gradients in light, velocity, and temperature, and in chemical gradients of oxygen content and subsequently redox potential. Hyporheic storage size and exchange rates can be spatially variable, due to variability in the relative fluxes of groundwater return flows and fine-scale vertical hydraulic gradients in the stream bottom [*Harvey and Bencala*, 1993]. The resultant flux of water and solutes across the boundary between the stream and subsurface create

a dynamic setting in which chemical reactants and products may be delivered and removed from reaction sites. For this reason, storage and exchange of hyporheic waters often strongly influence rates of biogeochemical processes [*Brunke and Gonser*, 1997; *Dahm, et al.*, 1998; *Dent, et al.*, 2007; *Gooseff, et al.*, 2004b; *McKnight, et al.*, 2004; *Miller, et al.*, 2006].

The McMurdo Dry Valleys of Antarctica are conducive to measuring hyporheic parameters via tracer studies due to low stream flows, a lack of regional groundwater flow, absence of terrestrial vegetation, high hydraulic conductivity, and no human impacts. Tracer experiments have been conducted in this environment to study the potential for subsurface storage [*Gooseff, et al.*, 2003; *Runkel, et al.*, 1998], to elucidate sources and sinks of solutes and nutrients [*Gooseff, et al.*, 2002; *Joslin*, 2005; *McKnight, et al.*, 2004], and to assess the retention and processing of NO_3^- by cyanobacterial mats [*Gooseff, et al.*, 2004b; *McKnight, et al.*, 2004].

Nitrogen utilization is of particular interest in the McMurdo Dry Valleys for many reasons. Due to atmospheric production of NO3- by auroral activity and the absence of vegetation, the McMurdo Dry Valleys are naturally N – saturated, with high concentrations of NO_3^- on valley surfaces [Green 1988] and in stream waters and the hyporheic zone [McKnight 2004]. Understanding ecosystem response to the high N loading in this system may provide insights into the many regions experiencing similar anthropogenic N loading. McKnight [2004] showed that NO_3^- concentrations are higher in Dry Valley streams without mats, resulting in greater NO_3^- delivery to the lake ecosystems from streams such as Huey Creek. Reduced N species are detected in matless streams [McKnight 2004], suggesting that some amount of NO3- loss may occur even in the absence of cyanobacterial mats.

The goal of this study was to quantify the relative importance of several N redox pathways in a Dry Valley stream devoid of microbial mats, where periphyton uptake would not

obscure hyporheic microbial processes. An injection of greater than 24 hr was performed in order to witness the potential effects of diel flow variability on hyporheic dynamics and microbial activity. This is the first nutrient enrichment tracer experiment in an Antarctic stream without microbial mats and may provide new insights into microbial activity in one of the harshest environments on the planet.

Site Description

While ninety-eight percent of Antarctica is covered by ice sheets, the McMurdo Dry Valleys are representative of the ice-free desert oases on the coasts of the continent. The valleys are relatively free of snow and ice, receiving an average of less than ten centimeters of precipitation annually as snow [*Doran, et al.*, 2002]. Snow collects in depressions and entrenched stream channels during the winter months, and melts at lower elevations during the austral summer. Ninety-five percent of the valley surfaces are composed of arid soils [*Burkins, et al.*, 2001] derived from tills composed of granites, sandstones, dolerites, and meta-sedimentary rocks. There is no terrestrial vegetation, except for mosses near some stream channels and in wetted areas surrounding lakes and ponds. A half meter below the surface the ground is permanently frozen. Streams typically flow for up to 12 weeks in the austral summer [*McKnight, et al.*, 1999], during which time the sun is above the horizon 24 hr a day. Water is derived from glacial melt [*Fountain, et al.*, 1999] and follows established channels into perennially ice-covered lakes on the valley floors. Stream solutes are weathered and leached from sediments in the hyporheic zones [*Gooseff, et al.*, 2002; *Green, et al.*, 1988]. Streamflow fluctuates on a daily timescale with pulses of high flow generated when the sun shines directly on glacier surfaces [*Conovitz, et al.*, 1998]. The parafluvial zone is defined as the wetted perimeter around streams and is visually evident in the Dry Valleys, due to the lack of vegetation

and soils. Water is evaporated from the stream and parafluvial zone [*Cozzetto, et al.*, 2006; *Gooseff, et al.*, 2003]. Evaporation concentrates and precipitates dissolved solutes, leading to salt accumulation on the streambank that mark the furthest lateral extent of the parafluvial zone. These dynamics result in large streamflow and aqueous solute concentration fluctuations on a diel timescale.

Dry Valley streams are useful model systems to study interactions between microbial communities and nutrients, specifically N. Sources of N to the stream include atmospheric deposition, and leaching of N from hyporheic and parafluvial sediments. Many Dry Valley streams contain microbial mats composed primarily of filamentous cyanobacteria and diatoms. Streams with cyanobacterial mats have lower concentrations of NO_3^- relative to mat-less streams, subsequently delivering smaller N yields to the lake ecosystems [*McKnight, et al.*, 2004]. Once in the stream, N storage in interstitial water in the cyanobacterial mats and the subsurface, assimilation by cyanobacterial mats and microbes, and loss of N during biogeochemical reactions to gaseous species such as N_2O and N_2. Stream-scale experimental studies indicate that decreased NO_3^- concentrations in streams with cyanobacterial mats result from uptake and denitrification within the cyanobacterial mats [*Gooseff, et al.*, 2004b]. A NO_3^- injection in an mat-rich stream resulted in an approximate 20% loss of NO_3^- attributable to dissimilatory reduction [*McKnight, et al.*, 2004]. Whereas most of this activity occurred while water was stored within the cyanobacterial mats, 7-16 % of NO_3^- uptake was due to microbial processes in the hyporheic zone. A NO_2^- pulse accompanied this NO_3^- injection. Gooseff [*Gooseff, et al.*, 2004b] inferred that denitrification was occurring, but not proceeding to completion due to either transport or reductase limitation.

Huey Creek is a stream in the McMurdo Dry Valleys with a steep slope. This stream is characterized by a shallow channel with a narrow floodplain that is incised below the valley fill level. A previous tracer injection performed on Huey Creek quantified hyporheic exchange rates ranging from 4.67 E^{-4} to 1.62 E^{-2} s^{-1}, which are high relative to many small streams, and storage zone areas ranging from 0.8 to 3.07 m^2 [*Runkel, et al.*, 1998]. There is a 182 m stream reach that is characterized by a shallow stream slope. During the daily high flow period this reach is dominated by anabranches, which are defined as multiple channels separated by semi-permanent alluvial islands [*Nanson and Knighton*, 1996]. These branches dry when the daily flood pulse recedes. Anabranch formation often occurs in streams with flood-dominated flow regimes, and likely occurs at this location in Huey Creek due to the decrease in stream slope within this reach. The anabranches in Huey Creek are decimeters wide, non-migratory braids, separated by gravel bars that route water laterally away from the main channel. The length of the anabranches ranges from meters to tens of meters. Water and solute storage in the surface and subsurface of the anabranching reach may have important implications for the timing and location of microbial activity in this system. While no mats were seen during our injection, sparse populations of microbial mats have been observed in distal anabranches of Huey Creek in previous studies [*Alger, et al.*, 1997]. These mats appeared predominantly in the far-lateral anabranches. Their absence in other stream reaches of Huey Creek may be related to the steep stream slope, which results in high water velocities, turbulent flow, an unstable sandy substrate, and overall an environment too harsh to support perennial cyanobacterial mats [*Alger, et al.*, 1997; *Esposito, et al.*, 2006].

Methods

Sample Collection

NaCl, LiCl, and $NaNO_3$ were injected into Huey Creek for 31 hours. Solute injection began at 7 pm on 9 January 2006 (t = 0 hr) on the tail of the daily flood pulse, and ended at 2 am on 11 January 2006 (t = 31 hr). A multiple day injection in Huey Creek was employed to capture diel variability in flow – and the subsequent potential variability in solute storage and biological activity. The injection site was located in a steep, narrow reach, which facilitated mixing of the tracer in the stream. Above this point the stream flowed beneath remnant winter snowdrifts for much of its length. Five sampling sites that reflected clear changes in the dominant stream morphology were selected to collect water chemistry. These five sites (Figure 1) were labeled A through E, and are 16, 123, 305, 451, and 665 m downstream of the injection, respectively, as determined by a GPS survey. Samples were also collected directly above the injection, at a site labeled Site I. Reaches 1, 2, 3, and 4 were defined as the length of stream bounded by site A and B, B and C, C and D, and D and E, respectively. Reach 2, between sites B and C, displayed significant anabranching during high flows. Stream stage in Huey Creek was measured at a gaging station located just downstream of site E. Stage was recorded every 15 minutes by a pressure transducer and converted to discharge using a stage-discharge relationship developed at the gaging station [*Von Guerard, et al.*, 1995].

Anion, cation, and nutrient samples were collected at each site every 5 minutes during the first and last hours of the injection, and once every hour during the 31 hours of steady injection. Samples were collected every 2 hr at site I, just above the injection pump, to monitor background stream chemistry. After the injection, samples were collected at t = 33, 34, 35, 36, 38, 40, 44,

48, 52, and 56 hrs. DOC and N_2O samples were collected at sites I, B, D, and E at t = 0, 0.5, 1, 2, 6, 12, 18, 24, 36, 48, and 52 hrs. All sites were sampled twice during the hour preceding the start of the tracer injection. Stream samples were collected using Geopump peristaltic pumps, and filtered through a 147 mm diameter 0.45 μm filter. The filters were rinsed with stream water immediately before sample collection to minimize carryover from the previous sample. Samples for nutrient analysis were frozen using liquid N within 4 hr of collection and remained frozen until analysis. All other samples were stored in the dark at 4 ºC or less in the field and at the Crary Lab at McMurdo Station. Anions were analyzed on a Metrohm 761 Compact Ion Chromatograph and NH_4^+ on an OI Analytical Flow Solution IV Spectrophotometric Analyzer at the Kiowa Laboratory at INSTAAR's Mountain Research Station. Precision for Cl^-, NO_2^-, NO_3^-, and NH_4^+ was 1.98, 0.60, 0.81, and 0.55 %RSD, respectively, with detection limits of 0.14, 0.05, 0.02, and 0.13 μM, respectively. Li^+ was analyzed at INSTAAR using a Perkin Elmer Flame Atomic Adsorption Spectrometer, with precision estimated at 2.00% RSD and a detection limit of 2.9 μM. DOC was analyzed at the Crary Lab in McMurdo station on a Shimadzu TOC-V CPN Total Organic Carbon Analyzer, with a precision estimated at 1.34 %RSD and a detection limit of 8.26 μM. N_2O was measured on an HNU Systems Gas Chromatograph 301 fitted with a ^{63}Ni, electron capture detector, with a precision estimated at 3.61 %RSD and a detection limit of 1.5 nM.

Data Analysis

A mass balance approach was used to quantify water flow and reactive species concentration in the anabranching reach, between sites B and C. This reach was unique in its hydrology and subsequently its ecosystem potential, requiring a method to quantify the

significant subsurface flow and solute transport. When conservative solute variability indicated mixing of stream and subsurface waters, return flows were calculated using:

$$Q_C = Q_{RF} + Q_B \quad (1)$$

and

$$Q_C * C_C = Q_{RF} * C_{RF} + Q_B * C_B \quad (2)$$

, where Q represents flow in liters per second, and C is concentration in micromoles per liter. Subscripts denote the measurement location, where B and C represent sampling sites B and C respectively, and RF is the subsurface return flow. Q_C was estimated as flow measured at the stream gage below site E. Solute concentrations were measured at sites B and C and estimated for C_{RF} as the streamwater concentration at site B during the hours the anabranches were actively recharging the subsurface. Q_{RF} and Q_B were calculated by solving equations 1 and 2 simultaneously using Cl^- concentrations. Once all three flow terms were known, subsurface production/loss of N species and DOC was calculated as the difference between the observed and calculated values of return flow mass ($C_{RF} * Q_{RF}$).

We assumed that streamflows were steady between sites above and below the anabranches for all times. Therefore, flow at Site B (Q_B) was assumed equal to flow at Sites I and A. Similarly, flow at Site C (Q_C) was assumed equal to flow at Sites D and E. The average return flow for both low flow periods was divided by the return flow interval to determine an hourly difference in flow between Sites B and C. This value was subtracted from Q_A and Q_B during the low flow periods, and added to Q_A and Q_B during the preceding high flow periods.

Areal Uptake (U) is a metric defined by the Stream Solute Workshop [1990] that relates nutrient availability and demand by considering the rate of solute utilization given the physical stream properties velocity and depth. Proper use of this metric requires steady state conditions of streamflow, solute concentrations, and hyporheic dynamics, and was calculated during the quasi-stable low flow periods (Q < 15 L/s) for reactive species. Reach 4 was chosen for U calculation because: 1) DOC was measured at the upstream and downstream sampling sites, 2) this reach is downstream of the anabranches and thus influenced by return flow chemistry, and 3) it is not a gaining reach at low flow. Uptake was calculated according to:

$$U = u * h \ / x * [ln(C_o) - ln(C_x * Q_x / Q_o)] * C_x \qquad (3)$$

, where u is the streamwater velocity, h is the depth of the water, x is the distance between two sampling sites, C is solute concentration in moles per liter, Q is streamflow in liters per second, x is a downstream sampling site, and o is an upstream sampling site.

Mass change (ΔM) was calculated at all times and sites for conservative and reactive constituents according to:

$$\Delta M = Q_x * C_x - Q_o * C_o \qquad (4)$$

, where ΔM is mass of solute produced or lost in each reach in mols/hr. Total mass production/loss during the injection was calculated using equation 4, with results summed from t = 0 through 32 hr. Error for each calculation was determined by considering laboratory analyses uncertainty, and an estimated flow measurement error of 5%.

Results

Discharge and background solute concentrations during the injection are displayed in Figure 2. Flow varied between 3.5 and 25.5 L/s, with maxima at t = 4 and 21 hr and minima at t = 14 and 32 hr. Anabranches were active in Reach 2 during the two high flow periods of the injection (Figure 3). Many of the anabranches were only meters long and remained hydrologically connected to the stream. However, others routed water far from the main channel where they became stagnant and eventually dried. Presumably, this water infiltrated the subsurface. In addition to the diel flow pattern, there was also a trend of decreasing streamflow related to decreasing temperatures and overcast skies during the second day of the injection. Background concentrations of Cl^- and NO_3^- fluctuated with both the diel and longer-term trends in streamflow, with an overall increase in concentration of about 50%.

Solute injection increased Cl^- and NO_3^- from background concentrations of 358 and 11.5 μM to average concentrations of 515 and 52 μM, respectively (Figure 4). Lithium was initially undetectable, and increased to an average of 29 μM during the injection. Injected solute concentrations were variable during the injection, and displayed travel times between sites A and E of approximately 30 min. Chloride and Li^+ concentrations only neared steady state during low stream flow periods, between t = 5 and 16 hr, and between t = 24 and 31 hr. Li^+ concentrations varied with flow, and also decreased in magnitude from site A to site E. Nitrate concentrations decreased between tracer time t = 5 and 20 hr and increased from t = 20 hr until the end of the injection. Sodium concentrations varied similarly to Cl^- values, and therefore will not be discussed in this paper.

Reach 2 displayed substantial anabranching during the tracer injection, and displayed trends in conservative and reactive solutes dissimilar from trends in the other reaches. There was

a significant decrease in Cl^- and Li^+ concentrations in this reach during two low flow periods, from t = 5 to 16 hr and t = 26 to 31 hr (Figure 6). The dilution lasted for 6 hours during the first low flow period. During the second flood recession dilution is less clear due to 1) a large concentration spike at Site C at t = 29 hr and 2) cessation of the injection at t = 31 hr. Using Cl^- as the conservative tracer, average subsurface return flows for the first and second low flow periods were calculated using Equations 1 and 2 as 1.90 and 3.15 L/s. Return flows accounted for 27 and 38% of the total streamflow during the two low flow periods, respectively.

Non-injected reactive N-species displayed a range of responses during the injection. NO_2^- concentrations were significantly higher at site A relative to the downstream sites from t = 0.5 to 6 hr, and concentrations were highly variable at Site C. NH_4^+ displayed large spikes in concentration that typically lasted only one to two hours, occurring at sites B, C, and D at different times, and often occurred during high and receding streamflows. Mean N_2O concentrations increased with distance from the injection, and displayed the highest concentrations at all measured sites during high and receding streamflows.

DOC concentrations were temporally and spatially variable (Figure 6). The highest DOC concentrations were 240 and 755 μM, and were measured at Site I at t = 1 and 2 hr respectively. Mean concentrations decreased downstream of this pulse at Site I. At Site D, DOC concentrations were significantly higher than other sites during low flow periods, and not statistically different from other sites during high flow periods. Even with the pulses of DOC at Site D at low flows, DOC concentrations at Site E were never significantly different from the minimum detection limit.

Areal uptake calculated in Reach 4 was variable between species and between return flows (Figure 7). Nitrate uptake was variable, with greater uptake during the second return flow.

Nitrite was taken up during the first return flow and produced during the second return flow. Ammonium rates were variable, with the greatest production during the second return flow. Nitrous oxide was produced at similar rates during both periods. DOC was taken up, with a greater loss during the second return flow.

Total changes in injected solute mass during the tracer are summarized in Figure 8. There was no significant difference in the Cl^- mass passing sites A and E during the injection. In contrast, Li^+ recovery at site E was only 47% (+/- 3.8) of that measured at site A, with 74% of this loss occurring in the anabranching reach. NO_3^- recovery was 86% (+/- 4.0), which corresponds to a total loss of 10.6 mol. Relative to NO_3^-, other N species mass changes were small (Table 1). NO_2^- remained a small portion of total dissolved nitrogen (TDN) at all sites. NH_4^+ mass was 3.8 times greater at site B than at site A, and decreased significantly with distance downstream between sites B and E.

Maximum, minimum, and mean mass changes were calculated for each biogeochemically active species measured during the injection using Equation 4. These results were calculated hourly for NO_3^-, NO_2^-, and NH_4^+ (Table 2) and less frequently for N_2O and DOC (Table 3). Figure 9 displays these changes on a per-hour basis, and also includes Cl^- and Li^+ mass changes. In general, the "All Reaches" column of Figure 9a and 9b shows that Cl^- and NH_4^+ mass was constant, Li^+, NO_3^-, NO_2^-, and DOC were lost, and N_2O was produced. Reactivity was focused around high flow periods. Cl^- mass changed only slightly between sites A and E, with the largest instances of production/loss in Reach 2, the anabranching reach. Li^+ loss occurred mainly on the regression limb of the daily flow pulse, and occurred predominantly in the Reach 2. NO_3^- was produced and lost in all reaches, with the greatest loss during high flow periods in Reach 1 and 2. NO_2^- was lost predominantly in Reach 1. The greatest NO_2^- loss occurred during the first high

Table 1: Nitrogen species mass in moles at Sites A, B, C, and E. N_2O was not sampled at Sites A and C. Values in parentheses represent the maximum error range. TDN was calculated as the sum of all measured species

	Site A	Site B	Site C	Site E
Nitrate	74 (1.5)	70 (1.4)	66 (1.3)	64 (1.3)
Nitrite	0.23 (0.0021)	0.08 (0.0020)	0.11 (0.0013)	0.06 (0.0051)
Ammonium	0.16 (0.0032)	0.63 (0.0012)	0.27 (0.0053)	0.12 (0.0024)
N_2O	NA	0.026 (0.00045)	NA	0.034 (0.00058)
TDN	74 (1.5)	70 (1.4)	67 (1.3)	64 (1.3)

Table 2a: Hourly average, maximum and minimum production (positive) and loss (negative) rates of mass change for reactive species measured each hour during the 32 hours in which tracer mass was stored in the experimental reaches. Values in parentheses represent the maximum error range.

	Nitrate (mol/hr)	Nitrite (mol/hr)	Ammonium (mol/hr)
	Reach 1 (A-B)		
Average	-0.12	-0.0038	0.012
	(0.22)	(0.00067)	(0.0018)
Maximum	1.1	0.0028	0.25
	(0.093)	(0.00032)	(0.00062)
Minimum	-3.60	-0.034	-0.10
	(0.98)	(0.0041)	(0.0019)
	Reach 2 (B-C)		
Average	-0.082	0.00058	-0.0094
	(0.21)	(0.00023)	(0.0018)
Maximum	1.3	0.014	0.067
	(0.56)	(0.00043)	(0.00023)
Minimum	-2.5	-0.0050	-0.24
	(0.89)	(0.000075)	(0.028)
	Reach 3 & 4 (C-E)		
Average	-0.073	-0.0013	-0.0039
	(0.19)	(0.00016)	(0.00034)
Maximum	1.4	0.0022	0.018
	(0.21)	(0.00024)	(0.0026)
Minimum	-1.0	-0.013	-0.068
	(0.60)	(0.00018)	(0.0077)
	All Reaches (A-E)		
Average	-0.27	-0.0045	-0.0011
	(0.22)	(0.00067)	(0.0018)
Maximum	2.44	0.00063	0.0094
	(0.21)	(0.00032)	(0.0026)
Minimum	-3.32	-0.035	-0.096
	(0.98)	(0.0041)	(0.0077)

Table 2b: Hourly average, maximum and minimum production (positive) and loss (negative) rates of mass change for N_2O and DOC, respectively during the 32 hours in which tracer mass was stored in the experimental reaches. Values in parentheses represent the maximum error range. Samples for these two species were collected at hours 0, 0.5, 1, 2, 6, 12, 18, 24, and 30 hours.

	N_2O (mmol/hr)	**DOC (Kmol/hr)**
Reach Upstream & 1 (I - B)		
Average	-0.0041	-1.3
	(0.15)	(0.10)
Maximum	0.21	0.42
	(0.12)	(0.032)
Minimum	-0.44	-7.6
	(0.26)	(0.80)
Reach 2 & 3 (B - D)		
Average	0.27	-0.0040
	(0.18)	(0.040)
Maximum	0.61	0.47
	(0.26)	(0.076)
Minimum	0.056	-0.50
	(0.28)	(0.019)
Reach 4 (D - E)		
Average	0.16	-0.16
	(0.20)	(0.022)
Maximum	0.36	0.47
	(0.25)	(0.047)
Minimum	-0.0043	-0.77
	(0.077)	(0.031)
All Reaches (I - E)		
Average	0.50	-1.5
	(0.32)	(0.16)
Maximum	1.0	0.0060
	(0.084)	(0.011)
Minimum	0.052	-7.4
	(0.0071)	(0.80)

Table 3: Reactive species mass production (positive) and loss (negative) in return flows from the anabranches. Values represent the difference between the expected and calculated mass. Maximum errors from chemical analyses are shown in parentheses. Values that were not significantly different from 0 at a 95% confidence interval are not reported.

Time (hr)	Return Flow #1 5 – 16	Return Flow #2 24 - 31
Nitrate (µmol)		-31 (7.9)
Nitrite (µmol)	0.031 (0.0063)	-0.19 (0.0074)
Ammonium (µmol)	0.28 (0.030)	0.11 (0.014)
Nitrous Oxide (µmol)	0.045 (0.021)	0.049 (0.023)
DOC (mol)	195 (11)	447 (12)

flow period, with a second period of loss during the second high flow. Discrete pulses of NO_2^- were produced in Reach 2 during the second high flow period, and lost in Reach 3. Ammonium pulses were produced in Reach 1 during the second high flow, and lost in reach 2. N_2O production was greatest in Reaches 2 and 3, and mainly occurred during high flow periods. DOC loss was greatest in the upstream reaches during the first flood pulse.

Mass change calculations (Figure 9) show that the greatest rates of NO_3^-, NO_2^-, N_2O, and DOC loss occurred during the initial hours of the experiment. The greatest NO_3^- loss occurs in Reach 1 at t = 1 hr, while NO_2^- loss is greatest at t = 3 to 4 hr, with significant loss through t = 7 hr. These losses coincide with the highest streamflow and highest concentration of DOC measured over the sampling interval. This period of high activity corresponded to DOC decreasing from 240 to 57 μM and from 755 to 26 μM at t = 1 and 2 hr, respectively between sites I and B. Extended periods of NO_3^- and NO_2^- loss also occur at early times between reaches C and E, coincident with elevated DOC. NO_3^- and NO_2^- loss rates and DOC concentrations are smaller during the second high flow period, but still occur to some extent at both locations.

N-species and DOC in the return flows were calculated from equations 1 and 2 (Table 4). Differences between the calculated and observed reactive species indicate variations in N species and DOC mass change in the subsurface of the anabranching reach between the two low flow periods when return flow occurred. The first return flow displayed production of NO_2^-, NH_4^+, N_2O, and DOC. The second return flow displayed uptake of NO_3^- and NO_2^-, decreased production of NH_4^+, and increased production of N_2O and DOC.

Discussion

Parsing Hydrology and Chemistry

Dynamic variations in N species over the length of the 31 hr Huey Creek NO_3^- enrichment injection provide evidence of microbial activity. However, extreme variability of both reactive and conservative breakthrough curves (Figure 4) highlight the necessity of considering the influence of unsteady stream flow in order to understand the importance of hot spots and hot moments in this oligotrophic stream ecosystem. Conservative solutes are chemically inert; therefore changes in such constituents are indicative of hydrologic changes in the system (high vs. low flows, lateral inflows, etc). Changes in reactive solutes result from both hydrology and chemical reactivity. By comparing the conservative and reactive solute records we attempt to parse effects of microbial activity from the overall variability in the tracer data.

Several solutes appeared nonreactive in Huey Creek during the injection. In-stream concentrations of injected Cl^-, and background solutes PO_4^- and SO_4^{2-} (not shown) varied similarly in time and space. Such covariance is indicative of changes in hydrology, which acts to dilute or concentrate solutes in the stream. While Li^+ acted conservatively during low flows, there was significant loss of Li^+ during high flow periods, especially in the anabranching reach (Figure 9a). Similar loss of Li^+ has been witnessed in previous injections in a Dry Valley stream and attributed to sorption and/or cation exchange [*Gooseff, et al.*, 2004a]. The large loss in Li^+ during the Huey Creek injection was likely a result of similar processes, and occurred predominantly in the anabranching reach and during high flows due to the heightened interaction between water and sediments. This evidence highlights this reach and high flow periods as potentially biogeochemically active and therefore important foci of our current study.

Anabranch Hydrology

Evidence from breakthrough curves and mass change calculations suggest that subsurface storage and exchange in the anabranching reach is significant and temporally variable. Water and solute exchange is the result of unsteady flow and subsequent anabranching and subsurface storage. Observations suggests that during high flows, which occurred between t = 0 to 4 hr and t = 17 to 23 hr, water was exchanged from the channel to the anabranches and into the subsurface. The loss of water from the stream to the anabranches and subsurface is most clearly witnessed in Cl^- mass loss in reach 2 during the second high flow period (Figure 9a). Decreased Cl^- concentrations between sites B and C (Figure 5) during low flow periods provide evidence that a mixture of clean, and tracer-labeled water returned to the stream once the flood pulse receded, creating a hot moment in terms of stream-hyporheic zone interactions.

Cl^- dilution was a result of "clean", tracer-less water moving from the subsurface into the stream and lasted for 6 hours during the first low flow period. Cessation of the clean water pulse was concurrent with a NO_2^- pulse at t = 16 hr, which signaled 1) the arrival of the injected tracer at the end of the subsurface flowpath, and 2) incomplete reduction of the NO_3^- injection in the subsurface. During the second flood recession there was another instance of diluted concentrations and increased NO_2^- concentrations at site C. These changes signaled a second subsurface return flow. While our mass balance calculations show that this second return flow is entering the stream, the dilution is less visually apparent in Figure 5, because all of the water entering the subsurface during the second high flow was tracer-labeled. Further evidence of the second return flow is provided by higher Cl^- at Site C relative to Site B after cessation of the injection. This increase occurred because the return flow water measured at Site C was a

mixture of the tracer-labeled water exiting the anabranches and the unlabeled stream water from Site B.

Anabranch Biogeochemistry

The difference in anabranch water chemistry between the two return flows (Table 4) provides evidence of the effect of NO_3^-, our reactive tracer, on subsurface biogeochemistry. The first return flow likely contains a mixture of background and tracer-labeled water, and is therefore more closely related to background conditions than is the second return flow. The switch from NO_3^- and NO_2^- production during the first return flow and uptake during the second return flow suggests greater uptake of oxidized N species at later times. Less NH_4^+ and more N_2O and DOC are produced during the second return flow. These shifts may indicate a change in microbial activity as populations adjust to the elevated N availability. Alternatively, these shifts may be a function of the increased residence time of NO_3^- - rich pore water that remains in the subsurface for many hours after the first return flow and before flushing by the following high flow/infiltration event. The production of DOC in the anabranches is the cause of significantly higher concentrations measured at Site D at low flows (Figure 6), and likely also influences the calculated uptake rates (Figure 7).

Nitrogen Reactivity in Channelized Reaches

Reactivity in the channelized reaches of Huey Creek is highly variable in time and space. Production or loss in any given reach often results in mass change in subsequent reaches, creating chain reactions as limiting nutrients are cycled downstream.

Ammonium production in Reach 1 and rapid loss in Reach 2 during the second high flow period (Figure 9a) provide evidence of microbial activity in Huey Creek. The source of the pulse is ambiguous; NH_4^+ production may be related to NO_3^- and NO_2^- reduction, or it may have been

generated by the exchange with Li^+ at sorption sites. Regardless of the source, the NH_4^+ pulse emanates from Reach 1 during high flows and is completely lost in Reach 2. This loss coincides with the highest NO_2^- production of the entire injection, N_2O production, and significant DOC loss. This reactivity provides evidence of N oxidation in the channel of Huey Creek.

The direct correlation between N reduction and high streamflows in channelized reaches suggests the cycle of wetting and drying of stream banks may be an important control on hyporheic redox conditions. N cycling in larger river systems has been related to water table elevations, which determine whether soils are aerobic, anoxic, or anaerobic, and subsequently whether nitrification or denitrification dominates (Hefting et al 2004). In the channelized reaches of Huey Creek, changes in N species mass are not associated with Cl^- mass changes (Figure 9), suggesting that biogeochemical processes are not related to large changes in solute storage. Instead, N species reactivity and oxidation state may be primarily controlled by exchange between oxidized surface water and sub/anoxic sediments in the hyporheic zone. High stream flows have previously been linked to decreased hyporheic exchange [*Harvey, et al.*, 1996]. In Huey Creek, high streamflow may similarly retard hyporheic flushing, thereby allowing the subsurface conditions to become anoxic, and increasing contact time between NO_3^- and reaction sites. Anoxic conditions have been inferred from denitrifying activity in other Dry Valley streams [*Gooseff, et al.*, 2004b]. As streamflow decreases, exchange rates may increase, bringing reduced N (ie. NH_4^+ in reach 1 @ t = 17 and 20) back in contact with oxygenated surface waters. This scenario would explain the NH4+ peaks that emanate from reach 1 at low flows. This model is useful in understanding N dynamics in Huey Creek, and testifies to the temporal and spatial variability in N storage and cycling that can be caused by unsteady flow conditions (Figure 10).

Reactive species mass change also occurs in Reach 4, as inferred from uptake calculations (Figure 7). This is one of only a few instances of reactivity during low flows periods, and is likely dependent on the DOC – rich return flows from the anbranching reach. Variability in uptake lengths may stem from several causes. During the first return flow, the switch from a tracerless, to a labeled return flow could affect microbial processes and subsequently the reactive species inputs to Reach 4. Furthermore, even at low flows, streamflow is not completely steady, which likely affects the calculated uptake. Changes in uptake rates may be related to variability in the N-species and DOC mass in the return flows (Table 4), or may be associated with some lag in microbial reaction time, in which populations adjust their activity to most efficiently utilize the elevated N species and DOC concentrations.

Dissolved Organic Carbon

The coincidence of high DOC concentrations and reactive species loss suggests that Huey Creek is significantly C limited and that C availability creates hotspots and hot moments of microbial activity. DOC represents an important energy source for microbes, and is in short supply in Huey Creek relative to Dry Valley streams with significant cyanobacterial mat material. High DOC mass from an unknown source was measured at site I in the early, high flow hours of the injection. DOC concentrations decreased significantly in Reach 1, accompanied by the highest rates of NO_3^-, NO_2^-, and N_2O loss for the entire experiment. This pulse continues downstream, leading to NO_3^- and NO_2^- loss between sites C and E as well.

The anabranching reach is another significant source of DOC as evidenced by DOC pulses measured at Site D during subsurface return flows (Figures 4 and 6), and DOC production calculated from the anabranch reach mass balance (Table 4). Mass balance calculations also suggest that return flows from the anabranches experienced significant reduction of NO_3^- and

NO_2^- (Table 4). DOC pulses that exit the anabranches are first measured at site D and decrease below the minimum detection limit by site E (Figure 6). This decrease testifies to the rapid utilization of DOC in Huey Creek.

While the importance of DOC to ecosystem function in Huey Creek is clear, its source is less so. Microbial mat growth in Dry Valley streams is often limited by high water velocity, unsteady streamflow and unstable substrates [*Alger, et al.*, 1997]. In previous years cyanobacterial mats have been found growing in the anabranching reach of Huey Creek [*Alger, et al.*, 1997], where low water velocities and stagnant pools dominate. In lieu of visible mats in the anabranching reach during our injection, a more likely DOC source may be leaching of dead or dormant mat material that has been buried in the anabranch sediments from previous periods of high cyanobacterial mat growth. Infiltrating water may transport senescent material from this source through the anabranches, allowing NO_3^- reduction to occur in the subsurface, and creating a DOC pulse as water returns to the stream channel hours later.

The source of DOC measured at site I is similarly unclear. The stream slope steepens above the tracer reach, precluding the possibility of anabranching upstream. Furthermore, the DOC pulse at site I occurred at high flows, while the DOC pulse from the anabranching reach emanated at low flows. It is possible that the source of the DOC is the icefield from which Huey Creek originates. During periods of significant melt, supra-glacial streams may flush material from cryoconite holes and other DOC-rich glacial features [*Fortner, et al.*, 2005; *Fountain, et al.*, 2007; *Porazinska, et al.*, 2004], providing a critical C source to Huey Creek.

Implications of Unsteady Flow

The unsteady flow regime that produces hotspots and hot moments of biogeochemical activity in Huey Creek also precludes the use of transient storage modeling (TSMs) and limits

the use of common nutrient uptake metrics. Based on a previous conservative tracer experiment in Huey Creek, unsteady flow has been incorporated into TSMs by calculating the surface water kinematic wave [*Runkel, et al.*, 1998]. However, our results suggest the necessity of also considering the subsurface effect of the flood wave, which leads to spatial and temporal variability in subsurface storage and exchange rates. Coupling surface water flow, groundwater flow, solute transport, and biogeochemical reactivity is beyond the scope of this work, but is a worthy goal, because it would provide an integrated view of the hydrologic influences on stream ecosystems. Similarly, given Huey Creek's unsteady flow, variable hyporheic dynamics, and subsequent hotspots and hot moments in microbial activity, our system does not lend itself to meaningful application of areal uptake (U) and/or other similar metrics defined by the Stream Solute Workshop [1990]. While such metrics are useful for comparing disparate systems and extrapolating laboratory experiments, their calculation is highly dependent on steady-state streamflow, hyporheic exchange, and solute transport characteristics [*Runkel*, 2007]. Conditions during this injection were only stable at certain sites and times, precluding a thorough analysis using uptake metrics.

Conclusions

In Huey Creek, unsteady flow regulates microbial activity by controlling the interactions between water, sediments, and solutes and subsequently the location and duration of hotspots and hot moments. Li^+ loss results from sorption, and therefore Li^+ mass change may be used as a proxy for water/sediment interaction. This process is greatest at high flows and in the anabranching reach. Nitrate and NO_2^- loss are concurrent with high flows and Li^+ loss, suggesting that microbial activity is dependent on N transport reaching the parafluvial zone.

Unsteady flow also plays an important role by significantly increasing water and solute residence times within the anabranching reach. Shifts in reactive solute export from this reach implicate the anabranches as a hotspot of microbial activity. Furthermore, this reach is a DOC and reduced N source, and therefore water recharging the channel from the anabranches also delivers nutrients to reaction sites further downstream. Flushing from upstream/glacial sources may explain the large spikes in DOC at the beginning of our injection, which lead to the greatest hot moment of NO_3^- loss of the entire injection. Our results suggest that microbial activity in Huey Creek is dependent on DOC availability, and the solute transport facilitated by daily high flow periods. Moreover, without cyclical streamflow, the exchange of subsurface water in the anabranching reach would not occur, which might further limit microbial activity by limiting nutrient delivery and reactant removal. This shows that even though day/night light variability is minor in polar desert streams, diel variations in microbial activity may still occur.

Including the effects of unsteady flow on hyporheic storage and N cycling is an important step towards improving hydrologic and biogeochemical modeling of stream ecosystems. We have shown how a combination of solute and water mass balance calculations can be used to quantitatively evaluate the complicated biogeochemical signature of a system dominated by hotspots and hot moments of microbial activity. This dataset underscores the challenge inherent in analyzing stream data from harsh environments and unsteady flow regimes – characteristics common to many polar and arid environments.

Acknowledgements

We are indebted to two anonymous reviewers for their comments, which substantially improved this manuscript. We would like to thank Raytheon Polar Services and PHI helicopters for

invaluable field support, Chris Siebold and Amber Roche for laboratory analyses, Bess Ward for use of the gas chromatograph at Princeton University, Ken Bencala and Michael Gooseff for advice on previous drafts, and everyone who contributed time and talent to the seemingly endless bottle washing and 52 hour sample collection. This work was supported by NSF OPP-9810219 and the NSF Microbial Biology Postdoctoral Fellowship Program.

References

Alger, A.S., D.M. McKnight, S.A. Spaulding, C.M. Tate, G.H. Shupe, K.A. Welch, R. Edwards, E.D. Andrews, and H.R. House (1997), Ecological processes in a cold desert ecosystem: the abundance and species of algal mats in glacial meltwater streams in Taylor Valley, Antarctica, *Institute of Arctic and Alpine Research, Occasional Paper 51*, 108.

Brunke, M., and T. Gonser (1997), The ecological significance of exchange processes between rivers and groundwater, *Freshwater Biology*, *37* (1), 1-33.

Burkins, M.B., R.A. Virginia, and D.H. Wall (2001), Organic carbon cycling in Taylor Valley, Antarctica: quantifying soil reservoirs and soil respiration, *Global Change Biology*, *7* (1), 113-125.

Conovitz, P.A., D.M. Mcknight, L.H. MacDonald, A.G. Fountain, and H.R. House (1998), Hydrologic processes influencing streamflow variation in Fryxell Basin, Antarctica., in *Ecosystem dynamics in a polar desert: The McMurdo Dry Valleys*, pp. 93-108, American Geophysical Union, Washington, DC.

Cozzetto, K., D. McKnight, T. Nylen, and A. Fountain (2006), Experimental investigations into processes controlling stream and hyporheic temperatures, Fryxell Basin, Antarctica, *Advances in Water Resources*, *29* (2), 130-153.

Dahm, C.N., N.B. Grimm, P. Marmonier, H.M. Valett, and P. Vervier (1998), Nutrient dynamics at the interface between surface waters and groundwaters, *Freshwater Biology*, *40* (3), 427-451.

Dent, C.L., N.B. Grimm, E. Marti, J.W. Edmonds, J.C. Henry, and J.R. Welter (2007), Variability in surface-subsurface hydrologic interactions and implications for nutrient retention in an arid-land stream, *Journal of Geophysical Research-Biogeosciences*, *112* (G4).

Doran, P.T., C.P. McKay, G.D. Clow, G.L. Dana, A.G. Fountain, T. Nylen, and W.B. Lyons (2002), Valley floor climate observations from the McMurdo dry valleys, Antarctica, 1986-2000, *Journal of Geophysical Research-Atmospheres*, *107* (D24).

Esposito, R.M.M., S.L. Horn, D.M. McKnight, M.J. Cox, M.C. Grant, S.A. Spaulding, P.T. Doran, and K.D. Cozzetto (2006), Antarctic climate cooling and response of diatoms in glacial meltwater streams, *Geophysical Research Letters*, *33* (7).

Fortner, S.K., M. Tranter, A. Fountain, W.B. Lyons, and K.A. Welch (2005), The geochemistry of supraglacial streams of Canada Glacier, Taylor Valley (Antarctica), and their evolution into proglacial waters, *Aquatic Geochemistry*, *11* (4), 391-412.

Fountain, A.G., W.B. Lyons, M.B. Burkins, G.L. Dana, P.T. Doran, K.J. Lewis, D.M. McKnight, D.L. Moorhead, A.N. Parsons, J.C. Priscu, D.H. Wall, R.A. Wharton, and R.A. Virginia (1999), Physical controls on the Taylor Valley ecosystem, Antarctica, *Bioscience*, *49* (12), 961-971.

Fountain, A.G., M. Tranter, T.H. Nylen, K.J. Lewis, and D.R. Mueller (2007), Evolution of cryoconite holes and their contribution to meltwater runoff from glaciers in the McMurdo Dry Valleys, Antarctica (vol 50, pg 35, 2004), *Journal of Glaciology*, *53* (183), 723-723.

Gooseff, M.N., D.M. McKnight, W.B. Lyons, and A.E. Blum (2002), Weathering reactions and hyporheic exchange controls on stream water chemistry in a glacial meltwater stream in the McMurdo Dry Valleys, *Water Resources Research*, *38* (12).

Gooseff, M.N., D.M. McKnight, R.L. Runke, and B.H. Vaughn (2003), Determining long time-scale hyporheic zone flow paths in Antarctic streams, *Hydrological Processes*, *17* (9), 1691-1710.

Gooseff, M.N., D.M. McKnight, and R.L. Runkel (2004a), Reach-scale cation exchange controls on major ion chemistry of an Antarctic glacial meltwater stream, *Aquatic Geochemistry*, *10* (3-4), 221-238.

Gooseff, M.N., D.M. McKnight, R.L. Runkel, and J.H. Duff (2004b), Denitrification and hydrologic transient storage in a glacial meltwater stream, McMurdo Dry Valleys, Antarctica, *Limnology and Oceanography*, *49* (5), 1884-1895.

Green, W.J., M.P. Angle, and K.E. Chave (1988), The Geochemistry of Antarctic Streams and Their Role in the Evolution of 4 Lakes of the Mcmurdo Dry Valleys, *Geochimica Et Cosmochimica Acta*, *52* (5), 1265-1274.

Harms, T.K., and N.B. Grimm (2008), Hot spots and hot moments of carbon and nitrogen dynamics in a semiarid riparian zone, *Journal of Geophysical Research-Biogeosciences*, *113* (G1).

Harvey, J.W., and K.E. Bencala (1993), The Effect of Streambed Topography on Surface-Subsurface Water Exchange in Mountain Catchments, *Water Resources Research*, *29* (1), 89-98.

Harvey, J.W., B.J. Wagner, and K.E. Bencala (1996), Evaluating the reliability of the stream tracer approach to characterize stream-subsurface water exchange, *Water Resources Research*, *32* (8), 2441-2451.

Holmes, R.M., S.G. Fisher, N.B. Grimm, and B.J. Harper (1998), The impact of flash floods on microbial distribution and biogeochemistry in the parafluvial zone of a desert stream, *Freshwater Biology*, *40* (4), 641-654.

Jones, J.B., S.G. Fisher, and N.B. Grimm (1995), Vertical Hydrologic Exchange and Ecosystem Metabolism in a Sonoran Desert Stream, *Ecology*, *76* (3), 942-952.

Joslin, J. (2005), Determining the role of chemical weathering reactions and hyporheic exchange on silicate concentrations in Dry Valley streams, Antarctica, University of Colorado, Boulder, CO.

McClain, M.E., E.W. Boyer, C.L. Dent, S.E. Gergel, N.B. Grimm, P.M. Groffman, S.C. Hart, J.W. Harvey, C.A. Johnston, E. Mayorga, W.H. McDowell, and G. Pinay (2003), Biogeochemical hot spots and hot moments at the interface of terrestrial and aquatic ecosystems, *Ecosystems*, *6* (4), 301-312.

McKnight, D.M., D.K. Niyogi, A.S. Alger, A. Bomblies, P.A. Conovitz, and C.M. Tate (1999), Dry valley streams in Antarctica: Ecosystems waiting for water, *Bioscience*, *49* (12), 985-995.

McKnight, D.M., R.L. Runkel, C.M. Tate, J.H. Duff, and D.L. Moorhead (2004), Inorganic N and P dynamics of Antarctic glacial meltwater streams as controlled by hyporheic exchange and benthic autotrophic communities, *Journal of the North American Benthological Society*, *23* (2), 171-188.

Miller, M.P., D.M. McKnight, R.M. Cory, M.W. Williams, and R.L. Runkel (2006), Hyporheic exchange and fulvic acid redox reactions in an alpine stream/wetland ecosystem, Colorado front range, *Environmental Science & Technology*, *40* (19), 5943-5949.

Nanson, G.C., and A.D. Knighton (1996), Anabranching rivers: Their cause, character and classification, *Earth Surface Processes and Landforms*, *21* (3), 217-239.

Porazinska, D.L., A.G. Fountain, T.H. Nylen, M. Tranter, R.A. Virginia, and D.H. Wall (2004), The Biodiversity and biogeochemistry of cryoconite holes from McMurdo Dry Valley glaciers, Antarctica, *Arctic Antarctic and Alpine Research*, *36* (1), 84-91.

Runkel, R.L. (2007), Toward a transport-based analysis of nutrient spiraling and uptake in streams, *Limnology and Oceanography-Methods*, *5*, 50-62.

Runkel, R.L., D.M. McKnight, and E.D. Andrews (1998), Analysis of transient storage subject to unsteady flow: diel flow variation in an Antarctic stream, *Journal of the North American Benthological Society*, *17* (2), 143-154.

StreamSoluteWorkshop (1990), Concepts and Methods for Assessing Solute Dynamics in Stream Ecosystems, *Journal of the North American Benthological Society*, *9* (2), 95-119.

Valett, H.M., M.A. Baker, J.A. Morrice, C.S. Crawford, M.C. Molles, C.N. Dahm, D.L. Moyer, J.R. Thibault, and L.M. Ellis (2005), Biogeochemical and metabolic responses to the flood pulse in a semiarid floodplain, *Ecology*, *86* (1), 220-234.

Von Guerard, P., D.M. Mcknight, R.A. Harnish, J.W. Gartner, and E.D. Andrews (1995), Streamflow, water-temperature, and specific-conductance data for selected streams draining into Lake Fryxell, Lower Taylor Valley, Victoria Land, Antarctica, 1990-92, in *Open File Report 94-434*, U.S. Geological Survey, Denver, CO.

Figure 1: (A) The Lake Fryxell Basin. The inset shows the relative location of the McMurdo Dry Valleys in Antarctica.

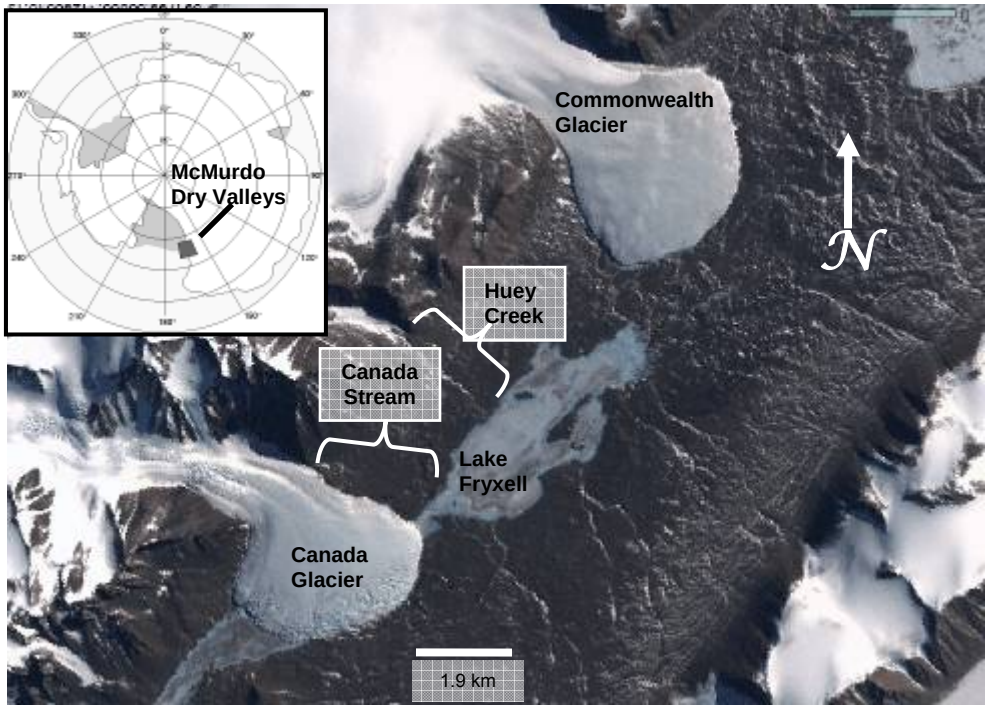

Figure 2: Huey Creek discharge over 60 hours, displaying three daily flood pulses. The tracer injection began at Time = 0 hours and ended at Time = 31 hours. Over this period there is a trend of decreasing flow related to declining weather conditions. Background concentrations of the primary injected solutes (measured above the injection at Site I) reacted to high flows and increased significantly during the tracer, between t = 16 and 18 hr.

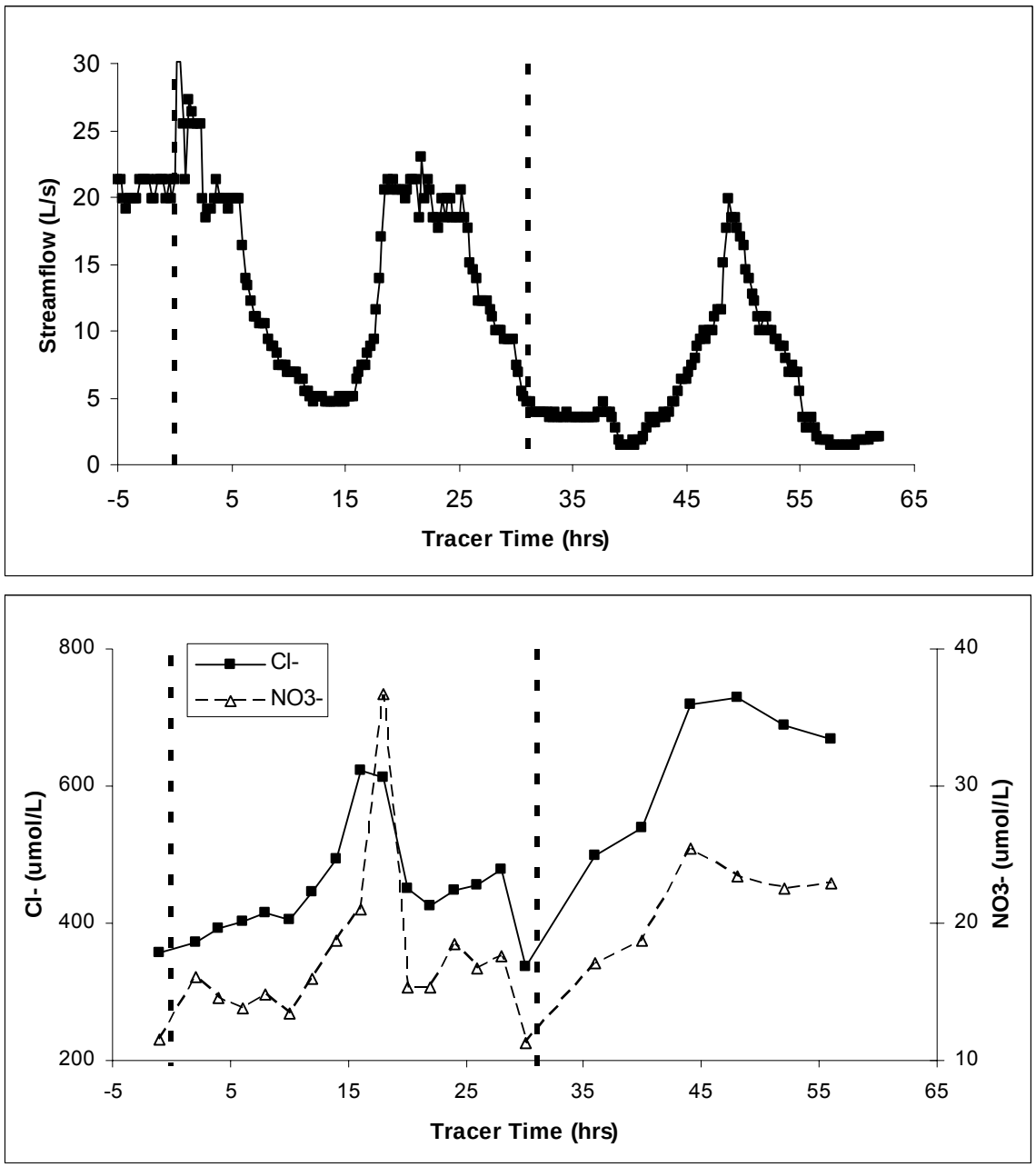

Figure 3: The anabranching reach of Huey Creek, looking upstream. Site B is located to the right of the large snowfield. A radio is in the foreground for scale. The stream channel meanders from the center background to the left foreground. Note anabranches leaving the frame on the right side, and infiltrating in the right foreground.

Figure 4: Breakthrough curves for the tracer injection. Injection of Cl^-, Li^+, and NO_3^- began at time = 0 hr and ended at time = 31 hr, as indicated by the dashed line. The large increase in Cl^- after the end of the injection results from increasing background Cl^- concentrations as streamflow decreased (shown in detail in Figure 2). DOC and N_2O were sampled at sites B, D, and E, and only at certain hours.

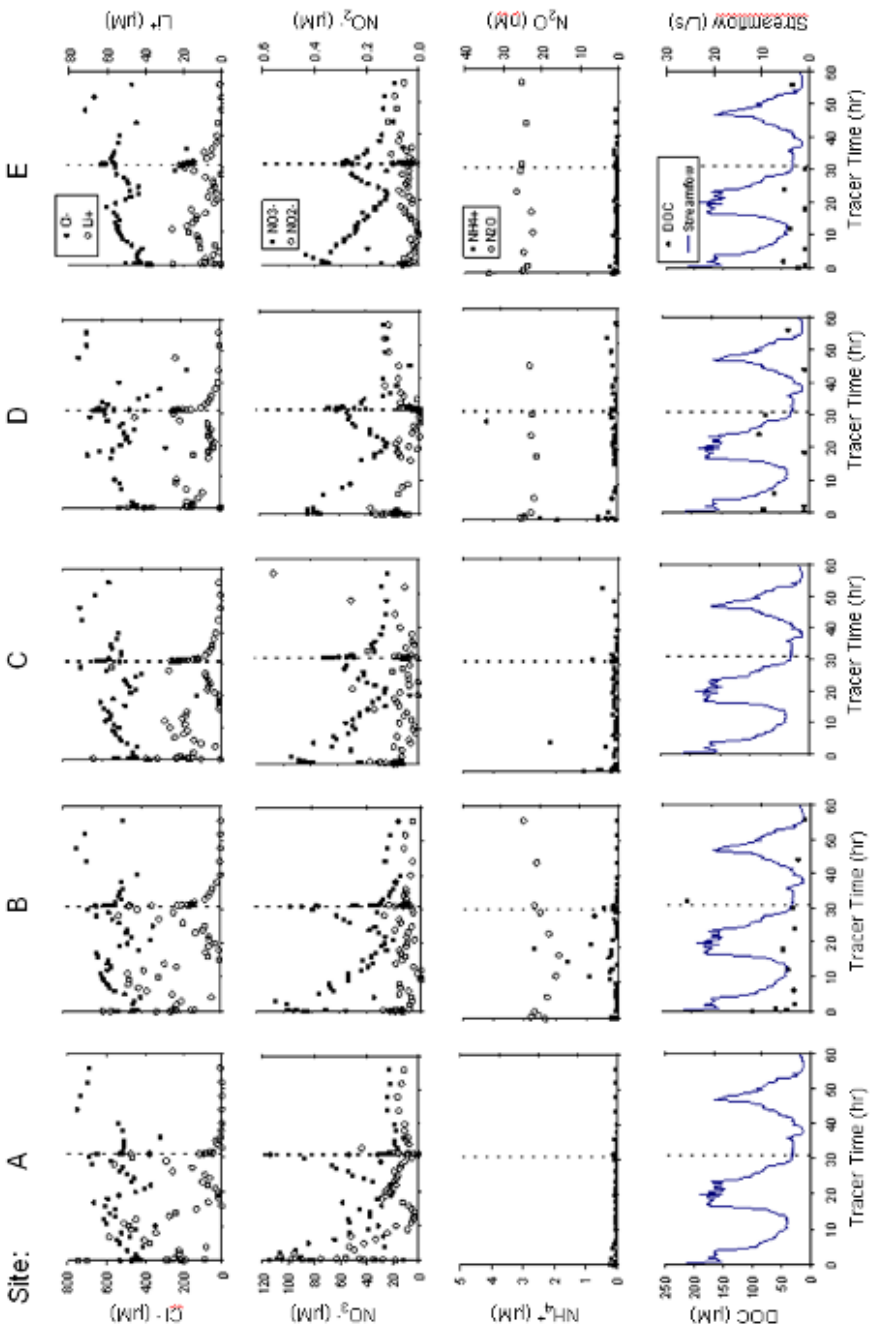

Figure 5: Chloride dilution between sites B and C occurred during the first low flow period (t = 5 – 16 hr), signaling an inflow of clean, tracerless water from the subsurface. This trend is less obvious during the second low flow period (t = 24 – 31 hr), because injected Cl^- entered the subsurface through anabranches during the previous high flow period. After cessation of the injection, the return flow is characterized by higher Cl^- at site C, because streamflow has returned to background Cl^- concentrations.

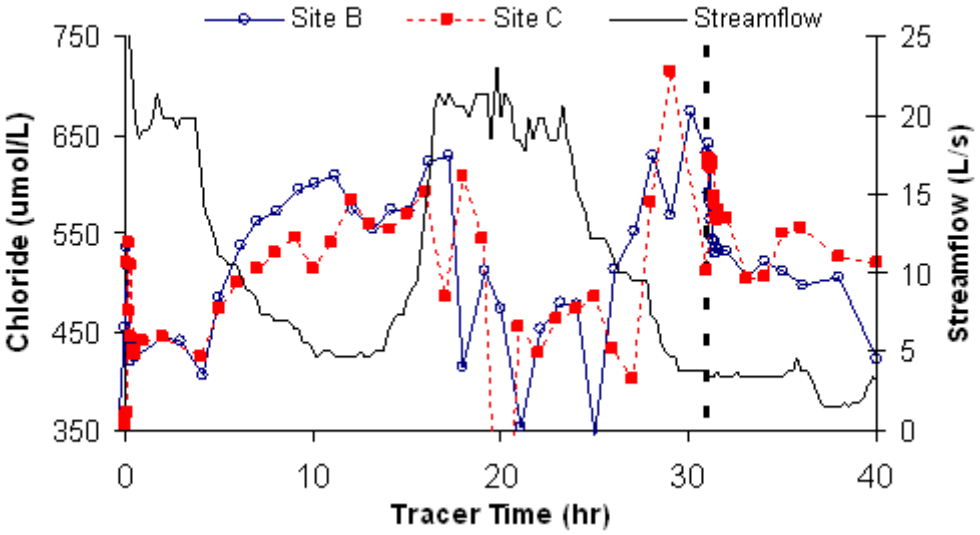

Figure 6: DOC concentrations measured at Sites B, D, and E, during high and low flows. Sample means were compared using the nonparametric Mann-Whitney Test. Error bars represent the range of values. The minimum detection limit (MDL) for DOC is 8.36 μM. Values below MDL were set to one half MDL. Letters represent populations that are not statistically different at the 0.90 level. During high flows, Sites B and D have significantly higher concentrations than Site E. The large ranges in Site B and D likely occur from the high DOC pulse measured upstream during the first hours of the injection. During low flows, Site D has significantly higher DOC concentrations than Sites B and Site E.

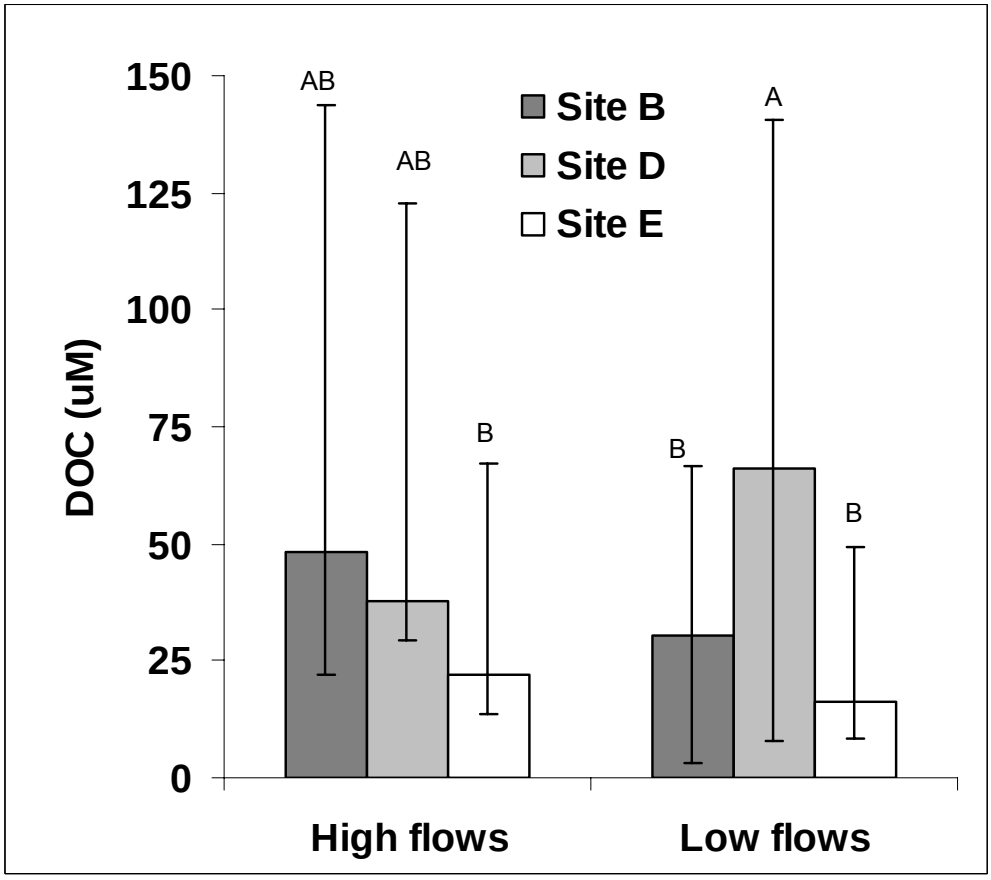

Figure 7: Areal uptake rates for reactive species between sites D and E. Positive values represent production. Calculations require steady state conditions, and were only calculated during low flow (Q < 15 L/s) periods. Error bars represent the maximum uncertainty for each calculation. The solid line represents streamflow. Vertical dashed lines denote cessation of the injection. Horizontal dashed lines indicate an aereal uptake rate of zero.

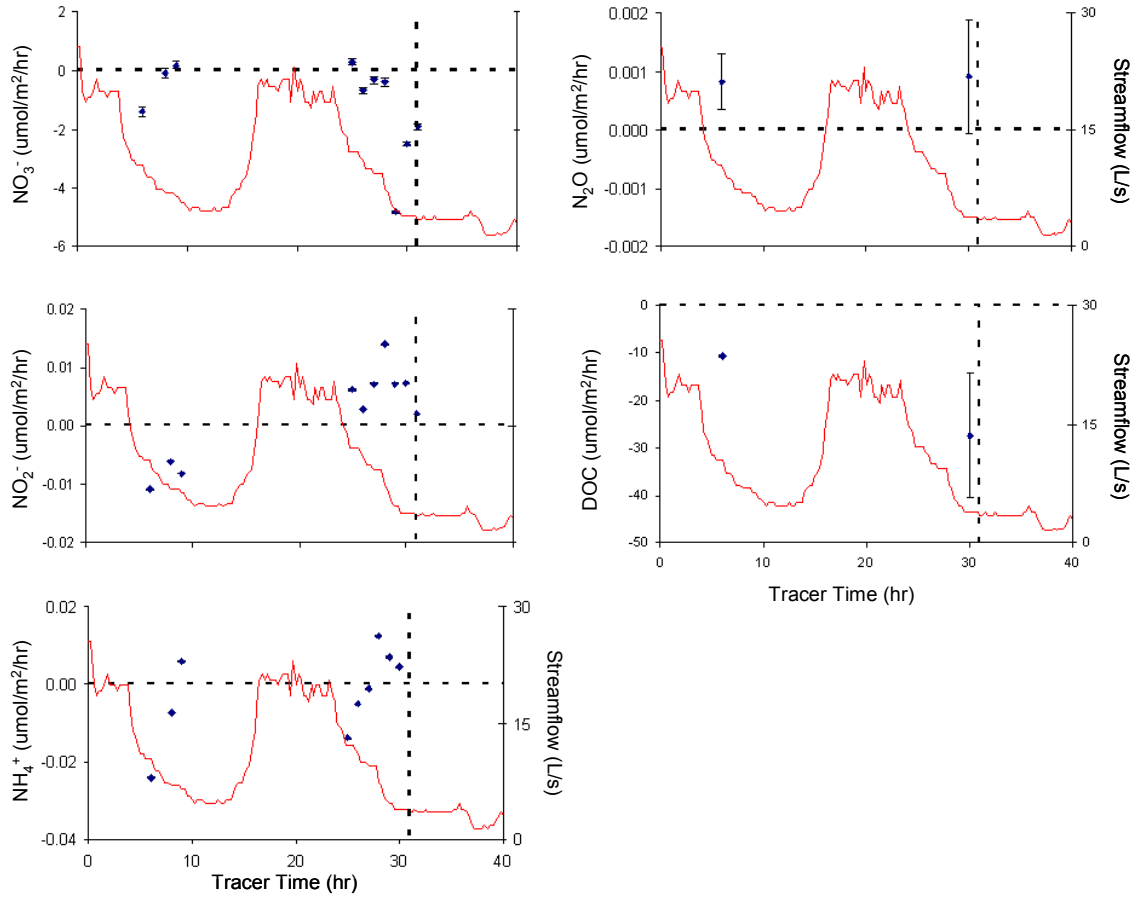

Figure 8: Total mass measured at sites A and E, integrated from time = 0 hr to time = 32 hr, which is one hour after the injection pump was shut off. Mass is expressed as a percentage of mass measured at Site A, just below the injection. Error bars represent the range of possible values for each measurement and consider both chemical analyses and flow measurement uncertainty

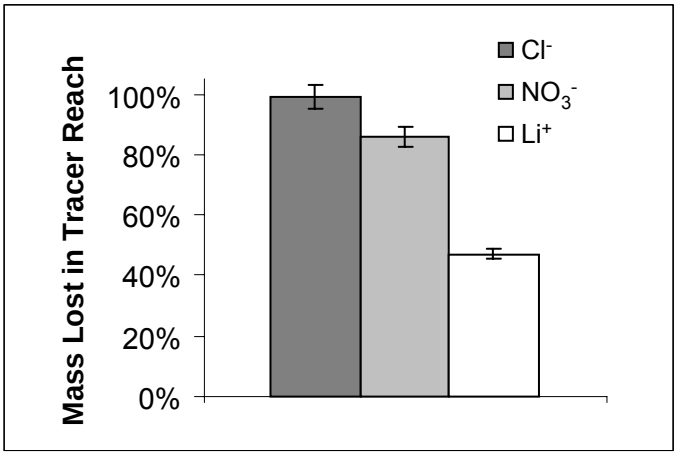

Figure 9a: Mass production (positive) and loss (negative), in moles, for species measured at each time interval. Samples were collected from time = 0 to 52 hr. The injection began at t = 0, and ended at t = 31 hr. Mass change is calculated as the difference in mass between the upstream and downstream sites. The solid line represents streamflow. Horizontal dashed lines represent the maximum level of uncertainty; therefore values outside of this range represent significant production/loss. The vertical dashed line represents the end of the injection period. Changes in Cl^- mass represent storage and exchange between the stream and anabranching/hyporheic zones. Major changes in N species that are not coincident with changes in Cl^- indicate microbial activity. Generally, Li^+, NO_3^-, and NO_2^- loss are coincident with high flow periods.

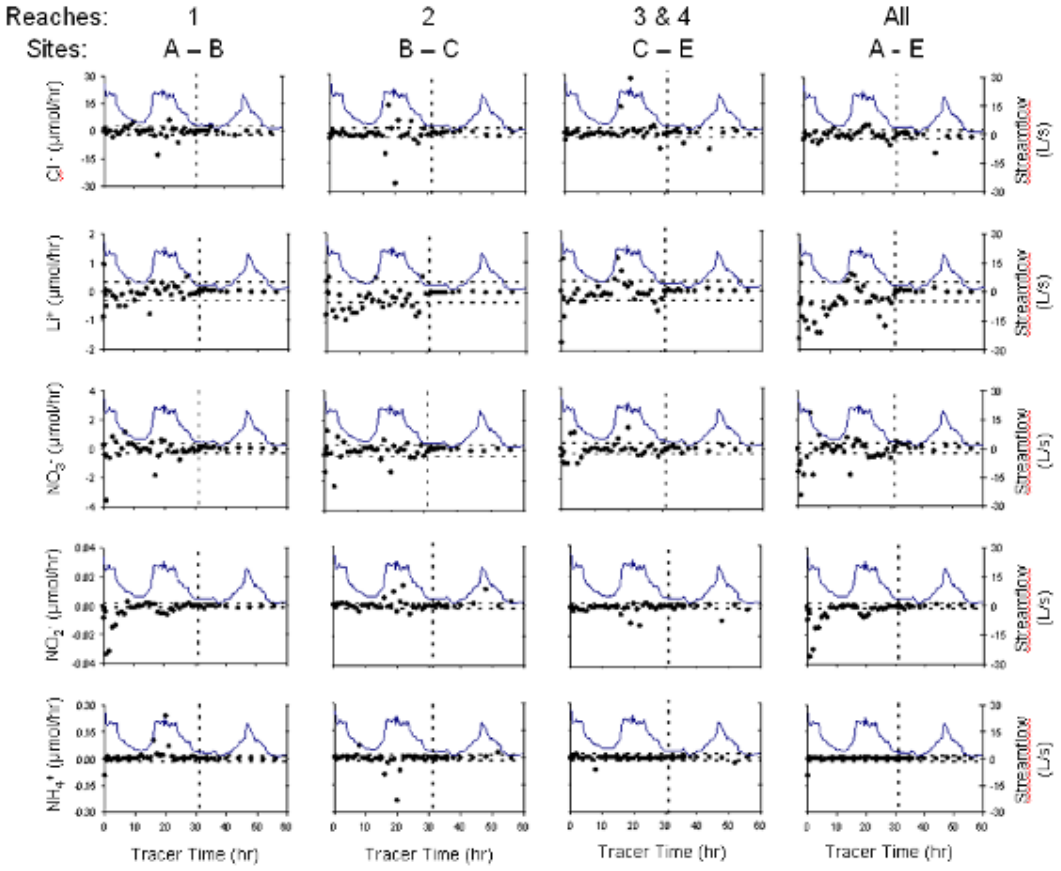

Figure 9b: Mass production (positive) and loss (negative), in moles, for species measured at each time interval. Samples were collected from time = 0 to 52 hr. The injection began at t = 0, and ended at t = 31 hr. Mass change is calculated as the difference in mass between the upstream and downstream sites. The solid line represents streamflow. Horizontal dashed lines represent the maximum level of uncertainty; therefore values outside of this range represent significant production/loss. The vertical dashed line represents the end of the injection period. DOC loss is greatest at early times in the upstream reach. DOC production is greatest in between Sites B and D (which includes the anabranching reach) during falling/low stream flow. The area of insignificant DOC change (ie the difference between the two, horizontal, dashed lines) is difficult to see because it is small relative to the plot scale.

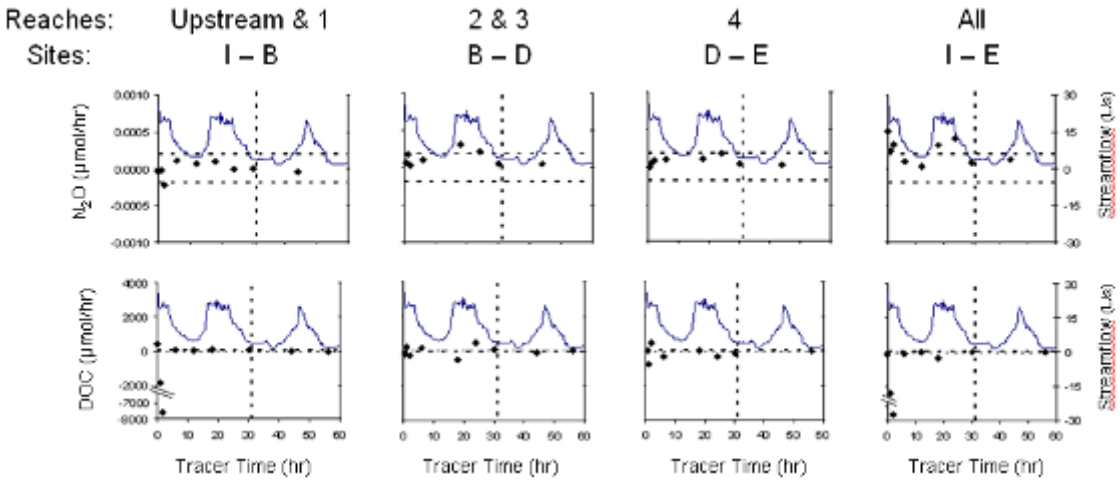

Figure 10: Conceptual model of unsteady flow and biogeochemistry in Huey Creek. Unsteady flow affects the interaction of water, solutes, and sediments, and subsequently hot spots and hot moments of N reactivity in Huey Creek. In the anbranching reach, high flows lead to significant storage in the subsurface, with exchange back to the stream at low flows. This return flow contains elevated DOC, which spurs activity in the downstream reaches. In the channels, N reduction is focused at high flows, when interaction between water and sediments is highest.

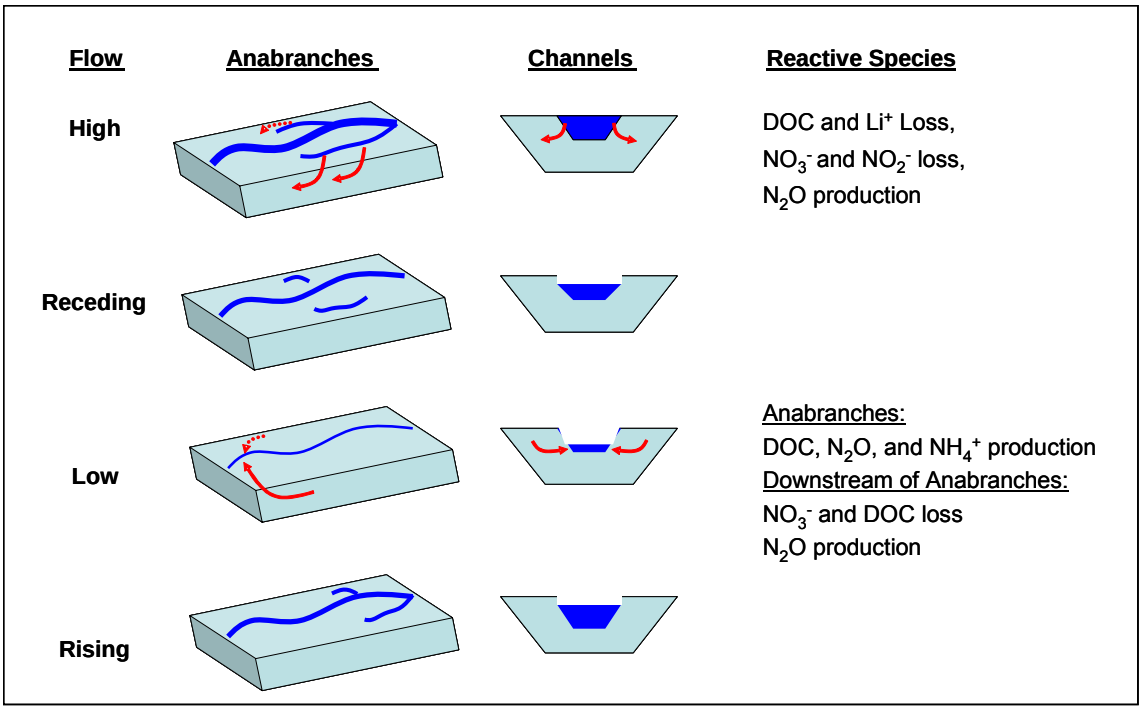

CHAPTER 4

Hydrologic Controls on Carbon and Nitrogen Cycling in a Sub-arctic Stream

Koch, J.C., R. Runkel, R. Striegl, and D.M. McKnight

Abstract

Boreal systems contain approximately one third of the world's carbon (C), much of which is locked in frozen soils and thus biologically unavailable. Whether C is mineralized in soils or flushed from catchments depends on the magnitude of precipitation/runoff events and has implications for ecosystem productivity and climate change feedbacks. Recent large-scale trends in the Yukon River Basin indicate increased C mineralization. We hypothesize that C cycling in soils and streams of this catchment is related to residence times in silt-dominated permafrost-bound hillslopes of interior Alaska, leading to high DOC export at all but the lowest hydrologic fluxes. We measured porewater chemistry and water discharge in tributaries and the stream draining a north-facing boreal hillslope. Synoptic sampling and conservative tracer additions were performed under varying flow conditions in the summers of 2008 and 2009. Our results were used to explore summer trends in hydrologic flux, and dissolved organic carbon (DOC) and nitrate loss in the soils and streams of this watershed. Stream DOC and nitrate concentrations were proportional to discharge, indicating greater leaching of organic material from the hillslope during wetter periods. Stream DOC and nitrate concentrations could not be explained by conservative transport, suggesting that C and N uptake/processing was occurring. These reactions were modeled as 1^{st} – order decay of DOC and nitrate concentrations. Uptake was greatest in reaches with substantial lateral inflows, and in the middle of the summer. Over the course of the summer stream subsurface inflows and total ion loads increased, suggesting that

decreased loss rates were related to deeper flowpaths and decreased water/organic soil interactions. We conclude that C and N cycling rates in this boreal catchment are primarily influenced by hydrologic flux and the contact time between water and organic soils.

Introduction

Boreal soils contain approximately one third of Earth's terrestrial organic carbon (C) [*Dixon, et al.*, 1994]. Much of this C exists in boreal peat soils, and has the potential to be mineralized through heterotrophic respiration in soils and streams. Recent studies recognize that climate warming is disproportionately affecting polar systems [IPCC, 2007], and Alaska specifically [*Hinzman, et al.*, 2005; *Schuur, et al.*, 2008]. Significant amounts of labile organic matter is soluble, which means that the balance between mineralization and transport is likely related to hydrologic fluxes. Understanding the fate and transport of organic matter in boreal systems is necessary for calculating accurate ecosystem C and nitrogen budgets, as well as for predicting possible climate warming feedbacks.

The Yukon River Basin is approximately 853,300 km^2 and is the fifth largest river that feeds the Arctic Ocean. The Yukon River Basin project of the USGS has quantified aqueous C loads and aquatic and terrestrial CO_2 efflux across the interior Alaska, and recognized a shift in the timing of discharge, which may be caused by longer/deeper flowpaths related to increased warming [*Walvoord and Striegl*, 2007]. This trend may be related to increased C mineralization in the basin [*Striegl, et al.*, 2005].

While these large – scale studies have successfully documented the signature of a changing system, finer – scale work is needed in order to identify the hydrologic and ecosystem processes responsible for changing water and C dynamics, and to inform conceptualization of

how these processes will change as a result of continued warming. Given that stream biogeochemical activity is often focused in the lowest order streams [*Mulholland, et al.*, 2008; *Peterson, et al.*, 2001], studying 1st- order catchments may provide insight into trends observed at the larger scale. This work aims to quantify C and N mineralization and export in a representative upland catchment underlain by permafrost that is tributary to the Yukon River.

Silt-loess is areally the most extensive surfacial deposit in Alaska [*Muhs, et al.*, 2003]. Above this silt, soils are dominated by an organic layer, which grades from live vegetation at the surface to decaying plant material and thicker peat at the organic-mineral boundary. Hydraulic conductivity in the boreal organic layers varies greatly with depth, and can be several orders of magnitude higher than in the underlying mineral soil [*Quinton and Marsh*, 1999]. The low conductivity of silt results in perched water tables, and water flowing predominantly through the organic layers [*Carey and Woo*, 2001; *Quinton and Marsh*, 1999]. Seasonality in catchment precipitation and stream discharge result in variable stream source area, with greater connectivity between the organic soils and the stream at high stage [*Carey and Woo*, 2001] and a greater proportion of flow through preferential flowpaths at low flows and later in the season [Chapter 5].

Seasonal changes in precipitation and thawed soil thickness may play an important role in catchment hydrology and biogeochemistry. Soils are commonly frozen to the surface in May, and may thaw to a meter or more by late summer. Thawing soils may initially contribute water and solutes to surface streams, and once drained may allow greater storage of precipitation and buffering of runoff. Increased storage potential has implications for the transport of nutrients and solutes, and may affect C and N budgets [*Ãgren, et al.*, 2007; *Carey*, 2003; *Edwardson, et*

al., 2003; *Maclean, et al.*, 1999; *O'Donnell and Jones*, 2006; *Petrone, et al.*, 2006; *Prokushkin, et al.*, 2005; *Waddington and Roulet*, 1997].

Stream tracer experiments are a useful tool for quantifying solute transport and inflows to the stream. Transient storage models provide a mechanism for relating solute transport to advective/dispersive properties of the stream, as well as to transient storage in pools and the hyporheic zone [*Bencala and Walters*, 1983; *Runkel*, 1998]. When coupled with independent measurements of surface water discharge, tracer dilution [*Kilpatrick and Cobb*, 1985] can be used to elucidate interactions between stream and subsurface water [*Harvey, et al.*, 1996; *Payn, et al.*, 2009].

Coupled conservative and nutrient/reactive stream tracer additions have been used to quantify microbial processes and nutrient uptake potential in many streams [*Dahm, et al.*, 1998; *McKnight, et al.*, 2004; *Mulholland, et al.*, 2008; *Peterson, et al.*, 2001; *Valett, et al.*, 1996]. Coupled tracer additions can be used to quantify nutrient spiraling length and velocity, which provide significant information about stream ecosystems [*Fisher, et al.*, 1998; *Newbold, et al.*, 1983]. While such studies have significantly improved our understanding of stream ecosystems, the spiraling metrics combine hydrologic and biogeochemical information, making comparisons between different stream ecosystems difficult [*Runkel*, 2007]. This mixing of hydrologic and biogeochemical information is especially problematic, because stream discharge variations commonly lead to increased/altered biogeochemical reaction rates [*Dent, et al.*, 2007; *Holmes, et al.*, 1998; *Koch, et al.*, 2010]. The addition of nutrients above ambient background conditions also leads to unnaturally elevated reaction rates [*Dodds, et al.*, 2002]. Given these challenges, this study focuses on ambient or naturally-elevated reactive solute concentrations and the spiraling metrics identified by Runkel [2007] to be free of hydrologic effects.

The goal of this work is to use synoptic sampling of pore and stream water chemistry and tracer additions to quantify the location and seasonal changes in DOC and nitrate transport and reaction in a small, boreal catchment. We hypothesize that reaction rates are affected by seasonal trends in catchment residence times and nitrogen availability. Residence times, in turn, are controlled by hydrologic conditions (ie. drought vs. flood) and soil thaw. By comparing water chemistry from soil pores and low-order streams, we identify the location and scale of dominant biogeochemical reactions. Tracer additions quantify C and N sources and flux rates to the stream, and are used to calculate in-stream DOC mineralization and nitrate assimilation / reduction rates.

Site Description

The Richardson Catchment is located 1.5 km southwest of the Hess Creek gaging station in the Yukon River Basin, AK (Figure 1). This catchment is drained by Richardson Tributary (RT), which appears as an unnamed 1st – order stream on USGS 1: 63,360 scale quadrangles. This stream is approximately 10 km long and flows into Richardson Creek, then Hess Creek, and eventually to the Yukon River. Our investigations are focused on a 1.2 km reach of RT that flows along the base of a steep, north-facing hill with a shallow floodplain on the north bank. Vegetation consists primarily of grasses/sedges, which grade into an approximately 10 cm thick organic layer. Below 10 to 20 cm, the catchment is composed of homogeneous silt-loess, which is seldom saturated, and generally acts as an aquitard [Chapter 5]. The shallowest layers of the silt may provide pathways for water and solute flux, especially near streams where preferential flowpaths may exist [Chapter 5].

The Richardson catchment burned in 2007, resulting in many downed and blackened trees and a lack of significant understory except around wetter gulleys. The tributary is incised several meters below the valley fill level. Incision led to significant bank erosion and fallen conifers lining the channel. Several tributaries flow into RT, including two major perennial inflows, which have eroded the organic soils and flow on top of the mineral soil, and three ephemeral tributaries that have been observed flowing only after large storm events. Dissolved organic carbon (DOC) in this stream and surrounding catchments is quite high relative to many streams, ranging from approximately 2000 to 4000 μM.

Methods

Discharge in Richardson Tributary was measured continuously during the summers of 2008 and 2009 at sites RT-0 and RT-829, and on the three largest tributary inflows, which entered the stream at 190, 855, and 1023 m. Seasonal hydrographs were developed using minitroll or level logger 100 pressure transducers (In-Situ, Fort Collins, CO) placed in stilling wells or gage pools above the flumes. Pressure was logged every 15 min, and field calibrated by independently measuring pool or flume staff plates during site visits. On RT, discharge often exceeded 67.4 L/s, which is the maximum flume capacity. During these high flows, discharge was modeled using Manning's equation:

$$Q = \frac{1}{n} S^{\frac{1}{2}} A R^{\frac{2}{3}}, \qquad (1)$$

where Q is discharge [m^3/s], n is Manning's roughness coefficient [s/m^2], S is the stream slope [m/m], A is channel area [m^2], and R [m^2/m] is the hydraulic radius of the stream. A rod and

level were used to survey the channel cross section at the two flume locations. Channel area and roughness were calculated by coupling the cross section with water height from the pressure transducer records. Slope was calculated from a GPS survey of the stream banks. Manning's roughness coefficient was calculated for instances when discharge greater than 67.4 L/s was independently measured with a rod and pygmy meter by rearranging equation 1. Discharge was also calculated via tracer dilution during continuous tracer additions.

Synoptic Sampling

Synoptic samples were collected five times over the course of the summers of 2008 and 2009 as indicated in Figure 2, and at up to twelve locations in RT. Additional samples were collected at the upstream and downstream flumes on May 31, and July 9, and August 19, 2009. Samples and field parameters including pH, specific conductance, dissolved oxygen content, and temperature were collected from the RT and any tributaries, as well as from porewater locations when possible. Two perennial tributaries were sampled during each synoptic sampling. A total of five tributaries were sampled during the June, 2008 synoptic sampling, which closely followed a large precipitation event. Porewaters were sampled by digging a pit and collecting any water that filled the pit. Anion, cation, DOC, specific ultraviolet light absorbance measured at 254 nanometers (SUVA), and water isotope samples from all sources were filtered through a 0.45 μm Gelman capsule filter. Samples were chilled and stored in the dark immediately following collection. Anion samples were frozen upon returning from the field.

All chemical analyses were conducted in the USGS laboratories in Boulder, CO. Anion, cation, and Br- samples were analyzed on a Dionex DX – 120 Ion Chromatograph. DOC samples were analyzed on an OI – 700 Total Organic Carbon Analyzer. $\delta^{18}O$ and $\delta^{2}H$ were

analyzed on a Los Gatos Research spectrometer. Nitrate samples below detection on the Ion Chromatograph were analyzed on a Nitric Oxide Analyzer.

C-mineralization and N-cycling Incubations

Biodegradable dissolved organic carbon (BDOC) samples were collected at the upstream and downstream flumes (RT-Inj and RT-829, respectively) during each 2009 synoptic sampling. BDOC incubations were set up by collecting 40 mL of unfiltered stream water in an amber glass bottle. The incubations were stored in a 10 C incubator, and analyzed for DOC weekly for one month after the initial measurement. BDOC decay coefficients were calculated as a first-order process based on the initial concentration.

Nitrification/mineralization and denitrification incubations were set up from samples collected during the 2008 synoptic samplings. These incubations consisted of a 50-50 mixture of streambed or streambank sediments and filtered streamwater, all of which had been stored in the dark during transport from the field site to the laboratory. Denitrification incubations were set up inside of an anaerobic glovebox and amended with acetylene. Samples were analyzed several times over the next days and weeks by removing 50 uL of gas and analyzing on an HNU gas chromatograph. Nitrification/mineralization experiments were set up aerobically. Half were amended with 1 mL of NaNH. Samples were placed in a 10 C incubator on a rotator to ensure total mixture of the water and sediments. Incubations were subsampled weekly by removing 4 mL of water. This water was filtered and placed into 2 separate vials. One vial was acidified with H_2SO_4 and stored in a cooler until analysis on a Scalar colorimetric ammonium analyzer. The other vial was frozen and analyzed on an NO Analyzer for nitrate and total N. Nitrate loss from the incubations was calculated as the total N lost from the denitrification incubation minus the nitrate produced in the nitrification/mineralization incubations.

Tracer Additions

In 2008, tracer was added to the stream at site RT-0 and monitored at three downstream locations (T1, T2, and T3). Tracer additions were performed for two purposes: steady state tracers were coupled with synoptic sampling to observe longitudinal variability in discharge and chemistry, and slug injections were performed to quantify transient storage parameters under varying discharge conditions.

Two continuous sodium bromide (NaBr) additions were performed in June and August, 2008 and coupled with synoptic samplings. Synoptic sampling chemistry was collected at several locations between the injection and approximately one km downstream (Table 1). Injection rates were maintained using a CR10 datalogger and two flow rate - sensing FMI pumps. Bromide concentrations were measured at site T1 using a Br^- - specific electrode, and at sites T1, T2, and T3 by collecting samples for laboratory analysis.

Slug additions were conducted at varying discharge conditions to aid development of a predictive relationship between discharge and stream transport (advection and dispersion). When combined with discharge measurements from the tributary and two flumes on RT, this information allowed us to run steady state simulations without conducting a constant rate tracer addition. Two rhodamine slug injections were performed for this purpose in 2008. 150 mL of rhodamine dye was poured slowly into the stream over a period of 3.5 minutes. Rhodamine concentration was measured at site T2 or T3 using an instream Sonde datalogger with a rhodamine specific probe.

Table 1: Synoptic sampling sites, distances from the injection site, and descriptions. Sites labeled with a "T" were locations where bromide or rhodamine were monitored for determining tracer transport.

Site	Distance (m)	Description
RT0	-20	Upstream Flume
RT Inj	0	Injection Location
RT 20	20	
RT 35	35	Ephemeral Inflow
RT 73	73	
RT131	131	Ephemeral Inflow
RT173	173	T1
USRa	264	
USRb	269	
USPa	270	
USPb	272	
RT 372	372	
RT 493	493	T2
RT 589	589	Seep
RT 726	726	
DSRa	805	
DSRb	809	
DSPa	811	
DSPb	813	
RT 829	829	T3, Downstream Flume
RT 855	855	Perennial Inflow, ST
RT 932	932	
RT 942	942	Ephemeral Inflow
RT 1015	1015	
RT 1023	1023	Perennial Inflow, BT
RT 1123	1123	
RT 1226	1226	

In June 2009, NaBr slug injections were performed in shorter reaches focused near the upstream and downstream flumes, because the 2008 injections indicated that they experience differing magnitudes of subsurface inflows. NaBr slug tracers were performed by instantaneously pouring 500 mL of NaBr into the stream, and measuring the associated response in specific conductance at a downstream location. This method allows comparison of discharge at individual locations, assuming injectate mass is equal for each slug. By performing one slug at a location of known discharge (ie. near the flume), the discharge in subsequent reaches can be calculated as:

$$Q_2 = A_{C1} / A_{C2} / Q_{1,} \qquad (2)$$

where Q is discharge [m^3/s], A_C is area under the breakthrough curve [µM*s], and 1 and 2 represent adjacent reaches where the test is performed.

Transient Storage Modeling

We used OTIS (one dimensional transport with inflows and storage, [*Runkel*, 1998]) to simulate tracer breakthroughs and DOC and nitrate reactivity. This transient storage model utilizes a form of the advection-dispersion equation to simulate concentrations in the main channel and a storage zone:

$$\frac{\partial C}{\partial t} = -\frac{Q}{A}\frac{\partial C}{\partial x} + \frac{1}{A}\frac{\partial}{\partial x}\left(AD\frac{\partial C}{\partial x}\right) + \frac{q_L}{A}(C_L - C) + \alpha(C_S - C) - \lambda C, \qquad (3)$$

$$\frac{\partial C_S}{\partial t} = \alpha\frac{A}{A_S}(C - C_S) - \lambda C_S, \qquad (4)$$

where A is main channel cross-sectional area [m^2], A_S is the storage zone cross-sectional area [m2], C is the main channel solute concentration [μM], C_L is the lateral inflow solute concentration [μM], C_S is the storage zone solute concentration [μM], D is the dispersion coefficient [m2/s], q_L is the lateral inflow rate [m^3/s/m], t is time [s], x is distance [m], α is the storage zone exchange coefficient [1/s], and λ is the 1^{st} – order decay coefficient [1/s]. The model was used to simulate tracer breakthrough curve chemistry measured at one transport site during rhodamine injections and three transport sites (T1, T2, and T3) during NaBr injections. The uncertainty in model parameters was assessed by running OTIS-P, which combines OTIS with STARPAC, an automated parameter-estimation method [*Donaldson and Tryon*, 1990]. The June, 2008 bromide tracer occurred on the tail of a large flood, which resulted in different physical stream characteristics between the beginning and end of the injection period. Therefore, the tracer was simulated using the unsteady flow option in OTIS, and the rising and falling tracer breakthroughs were simulated separately. Synoptic data was modeled with parameters from the falling breakthrough curve, because samples were collected within several hours of shutting off the injection pump. The five parameter sets obtained in 2008 were used to create regressions between the discharge and other model parameters. This information was used to estimate steady state parameters for the June 2009 NaBr slug injections and the July 2009 synoptic samplings based on observed discharge.

Tracer dilution allowed us to accurately quantify inflows to the stream for the June and August 2008 synoptic samplings. Inflows were separated into surface and subsurface fractions by subtracting gaged inflows from the total inflow volume. Ungaged tributaries were small enough that their exclusion from this analysis would not negatively affect the results.

The steady state form of OTIS was used to estimate first order reaction rates using synoptic chemistry data. In the steady state mode, OTIS simulations are controlled primarily by advection and inflows, with little effect from transient parameters such as dispersion and the exchange rate. The steady state model was run for several potentially conservative species (chloride, specific conductance, $\delta^{18}O$, and $\delta^{2}H$) to ensure that model parameters were correctly calibrated to recreate the synoptic chemistry. Reaction rate coefficients were estimated by running the same model, and allowing OTIS-P to adjust the rates until the best fit with reactive species synoptic sampling data was obtained. Reaction rate coefficients were estimated for reaches T1 and T3, and labeled "base" and "pulse", to highlight that T1 was generally devoid of inflows, while T3 experienced larger increases in discharge. Lateral inflow concentrations for the TSM were estimated as the average concentration in the perennial surface inflows. Effective inflows (C_{lateff}) were used to determine if observed surface inflow concentrations are representative of total (surface and subsurface) inflow concentrations. Effective inflows were calculated from discharge and conservative solute concentrations, following:

$$C_{Leff} = \frac{Q_{DS}C_{DS} - Q_{US}C_{US}}{Q_{DS} - Q_{US}}, \qquad (5)$$

where *US* and *DS* represent the upstream and downstream components, respectively. Differences between the conservative solute observed (surface) and effective (total) inflow concentrations indicate that surface and subsurface concentrations are different. We assumed that subsurface inflows had DOC and nitrate chemistry similar to porewaters, and adjusted inflow chemistry (C_L) to account for the proportion of subsurface water. Several lines of evidence suggest that residence time correlates to reactivity, which will be shown in the results

and discussed. Assuming that the difference between the fastest runoff (perennial inflows) and slowest runoff (porewaters) represent reactivity, we modeled hillslope DOC and nitrate reactivity as a first order process based on concentration:

$$\lambda_{hillslope} = -\frac{\ln(C_{Lpw}) - \ln(C_{HILL})}{t_R}, \quad (6)$$

where C_{Lpw} is average porewater concentration; C_{HILL} is the average perennial tributary concentration, which represents the fastest hillslope flowpath and thus least-processed, pre-reaction solute concentration; and t_R is the residence time of water in the catchment [s]. Residence time was calculated as:

$$t_R = \frac{Lz}{q_L}, \quad (7)$$

where L is the average flowpath length estimated as the straight line distance from the hill top to the stream [m], and z is the thickness of the organic soil [m].

Areal rates of DOC and nitrate loss were calculated to facilitate comparison between in-stream and hillslope biogeochemistry, and fluvial catchment export. Areal uptake was calculated as:

$$U = \lambda z C, \text{ and} \quad (8)$$

$$U = \frac{QC}{A}, \quad (9)$$

for biogeochemical processes and fluvial catchment export, respectively.

Results

Hydrologic Fluxes

Stream discharge varied substantially over the course of both summers (Figure 2). Generally, discharge was greatest in June and early July, and very low in late July and August. Ephemeral inflows were observed during the June 2008 synoptic sampling, which occurred within days of a large precipitation and flooding event. In 2009, discharge displays a late-season increase related to typically higher late summer precipitation.

Synoptic Samples

Conservative and reactive solute chemistry of pore waters, two gaged tributaries and the RT appears in Figure 3. Pore water was difficult to obtain because soils were typically unsaturated (see Chapter 5), leading to a small number of samples per site visit. Soil pits often filled with water flowing from the mineral/organic boundary, suggesting that this water represented organic soil flow. Hyporheic wells usually would not produce, and in the rare instances when they did, field parameters suggested that stream water was entering the well flowing downwards along the casing. We present data for four time periods, DOY = 154, 180, 192, and 241. There were 2, 1, 1, and 0 porewater samples for these four dates, respectively. Generally, there is a trend of increasing specific conductance and decreasing δ^2H moving from the pore water to RT. There is also a trend of increasing specific conductance with the day of the year. DOC and nitrate concentrations were higher in the perennial tributaries than in the 1st-order stream. Nitrate was low or below detection limits in porewaters. SUVA values were usually similar between subsurface and surface waters, except on DOY 192, when values were

significantly higher in the porewater relative to the surface waters. This is the same date on which porewater nitrate concentrations were below detection limit. Nitrate concentrations in the five tributaries from the June, 2008 synoptic sampling correlated to an ordinal ranking of their relative size, with the highest concentrations in the largest streams (Figure 4A). The smallest tributaries have nitrate concentrations similar to porewater samples, while the largest tributaries are similar to the 1st-order stream concentrations.

1st-order stream DOC concentrations were always in the range of 2500 to 4200 μM, which is high relative to most streams, while nitrate concentrations varied considerably, from below detection to 32 μM. DOC and nitrate significantly correlated to the natural logarithm of discharge (DOC: $R^2 = 0.84$, $p < 0.01$, nitrate: $R^2 = 0.91$, $p < 0.01$, Figure 4B). Two DOC samples collected at low discharge when much of the stream was stagnant were excluded from this regression. These low/no discharge points were significantly higher than expected given the aforementioned trend and may result from instream primary production in the warm stagnant pools. These high DOC values will be addressed further in the discussion section. SUVA values in the 1st-order stream ranged from 2.8 to 3.8. SUVA displayed a significant inverse correlation to the day of the year ($R^2 = 0.53$, $p < 0.005$, $n = 13$) between DOY 151 and 241.

Incubations

Initial and biodegradable DOC were highly variable between June and July, 2009. Initial DOC concentrations for the incubations were 45.9 and 44.1 mg/L in June, and 30.8 and 30.5 mg/L in July. Biodegradable DOC accounted for 49 and 48% in the upstream and downstream samples in June, and for 6 and 4% in July.

Nitrous oxide production in dentrification incubations occurred quickly, and generally reached equilibrium at about 20 hours. Decay rates were similar for all samples, averaging

6.99E-6 and 6.92E-5 s^{-1} in June and September 2008, respectively. Nitrate production in nitrification/mineralization experiments increased at a near-linear rate over the entire month of the incubation, averaging 2.37E-6 and 7.94E-7 s^{-1} in June and September 2008, respectively.

Conservative Tracer Data

Figure 5 displays observed and simulated concentrations for the two rhodamine additions (Figure 5A and 5B), and the two constant rate sodium bromide additions, sampled at three locations (Figure 5C and 5D). Stream velocities ranged from 0.005 to .251 m/s. Despite a constant tracer addition, the June, 2008 tracer experiment displays rising concentrations, due to the falling stream flow. The bite out of the plateau between 10 and 14 hr indicates a period of pump failure and a low tracer addition rate. In all cases OTIS was able to accurately simulate the breakthrough curves. Simulations were used to create exponential correlations between discharge and the OTIS parameters (Figure 6), for the purpose of estimating stream parameters for synoptic samplings not coupled with tracer additions. Measured and estimated parameter sets for all tracers and synoptic samplings are summarized in Table 2. In general, storage area and exchange rates were less certain than advection and dispersion.

Continuous tracer additions in June and August 2008 indicated that inflows were greatest in Reach 4, accounting for 65 % of the total inflows during both additions (Figure 7). Subsurface inflows were substantial, providing 51 and 66% of the Reach 4 inflow, respectively. Surface water from the largest, gaged inflows at RT-855 and RT-1015 accounted for 32% and 22% of the total inflows for the June 2008 and August 2008 tracers, respectively.

Effective Inflows

Effective inflow calculations displayed similar trends for specific conductance, $\delta^{18}O$, $\delta^{2}H$, and potassium. The difference between total and surface water inflows is significantly

correlated to DOY ($R^2 = 0.96$, $p < 0.0001$, Figure 8), with the largest differences in the early and late summer. DOY 154 inflow concentrations averaged 15 $^{+}$/- 9% lower/more depleted than effective inflows, and DOY 241 inflows averaged 22 $^{+}$/- 18% greater/more enriched than effective inflows. DOY 180 and 192 inflows were not significantly different from the effective inflows. We adjusted DOC and nitrate inflow concentrations, by assuming that the unsampled portion of the lateral inflows has a reactive solute chemistry similar to the mean porewater concentrations. Inflow concentrations were therefore adjusted assuming that 15 and 22% of the water in June, 2009 and August, 2008, respectively contained 3195 uM DOC and 2.5 uM nitrate.

Steady State Simulations

Steady state simulations were run for bromide, potassium, DOC, and nitrate (Figure 9). Potassium acted conservatively in the stream and thus provides evidence that modeled parameter are accurate. DOC and nitrate data could not be accurately fit to conservative transport simulations, indicating reactivity of these species in the stream. A better model fit was obtained by including first order decay in the simulations. Adjusting the DOY 154 and 241 reactive species lateral inflow concentrations changed DOC concentrations only slightly, and substantially affected nitrate (Table 3). These adjustments significantly affected the nitrate reaction rate coefficient.

Reaction Rates

Reaction rate coefficients varied seasonally for the base, pulse, and hillslope scenarios (Figure 10). DOC reaction rate coefficients varied widely, especially in the base samples, while nitrate values only ranged over several orders of magnitude, with similar variability between base, pulse, and hillslope rates. Generally, base reactions decreased over the season and rebounded on DOY 241. Pulse reactions increased between DOY 156 and 181, and then

Table 2: Hydrologic parameters from the transient storage modeling. Values in italics were calculated from relationships displayed in Figure 7.

Tracer Number	1	2a	2b	3	4	5	
Method	Slug	Plateau-Rise	Plateau-Fall	Slug	Plateau	Slugs	Regression
Injectate	Rhodamine	Bromide	Bromide	Rhodamine	Bromide	Bromide	NA
Date	June 24, 2008	June 29, 2008	June 30, 2008	August 25, 2008	August 30, 2008	June 4, 2009	July 11, 2009
Discharge (m^3/s)	0.014	0.41	0.25	0.003	0.002	0.045	0.0001
Velocity (m/s)	0.010	0.183	0.251	0.005	0.005	0.035	*0.011*
Dispersion (m^2/s)	0.03	0.69	1.46	0.02	0.02	*0.04*	*0.03*
Area (m^2)	1.5	2.23	1.00	0.6	0.3	*1.28*	*0.01*
Storage Area (m^2)	0.07	1.49	0.23	0.04	0.08	*0.08*	*0.06*
Exchange Rate (1/s)	7.5E-06	1.66E-02	1.84E+00	5.8E-06	6.6E-04	*4.1E-05*	*3.7E-05*
Lateral Inflows ($m^3/s/m$)	4.3E-07	1.32E-05	1.32E-05	8.0E-06	1.4E-06	1.3E-02	4.2E-03
Rhodamine Decay (1/s)	9.21E-06	NA	NA	7.38E-06	NA	NA	NA

decreased through the end of the season. Hillslope reactions were only calculated on DOY 156 and 241, because these were the two periods when significantly different subsurface inflow chemistries were identified. Hillslope reactions had the largest decay rate coefficients for both DOC and nitrate on DOY 156, and the smallest rate for both constituents on DOY 242. Generally, BDOC incubation rate coefficients were intermediate between base and pulse values and decreased between DOY 156 and 188. Nitrate loss incubation rate coefficients increased between DOY 181 and 242, and were most similar to the base reaction rate coefficients.

Table 3: Initial and adjusted inflow concentrations (C_{LIN} in micromoles per liter) for the two tracers, August, 2008 and June, 2009, where effective inflows suggested a second water source.

Constituent	Surface Inflow Chemistry	Subsurface Inflow Chemistry	Subsurface Contribution	Inflow Concentration
DOY 156 - DOC	3622	3195	15%	3555
DOY 156 - Nitrate	31.0	2.5	15%	26.7
DOY 242 - DOC	3722	3195	22%	3597
DOY 242 - Nitrate	23.0	2.5	22%	18.5

Incubations are of limited utility, due to the methodological differences that will be addressed in the discussion.

Areal uptake rates were calculated for DOC and nitrate (Figure 11) and generally follow the trends seen in the reaction rate coefficient plots. Maximum DOC uptake tended to be higher than nitrate uptake, due to the high concentrations of DOC in catchment waters. DOC uptake was are plotted with terrestrial and aquatic chamber CO_2 efflux data collected by Wickland in

2009 (unpublished). While chambers fluxes are several orders of magnitude larger than base rates, pulse rates are even greater. The utility of comparing instream/hillslope DOC loss and CO_2 efflux will be addressed further in the discussion.

Discussion

Data from this study provides insight into the relative importance of pore, inflow, and stream waters to the transport and processing of C in an upland boreal catchment. The direct correlation between discharge and C indicate the large pool of leachable organic matter that exists in boreal soils. We provide evidence of the relative importance of the surface and subsurface flow C mineralization, and explore the meaning of trends and deviations in the relationship between discharge and reactive solutes. Tracer addition results allow us to quantify surface and subsurface inflow chemistry and DOC and nitrate reactivity. Because our data combines both ambient and enriched DOC and nitrate values, we feel that it is more representative of natural rates of C mineralization and nitrate uptake than are values published in nutrient enrichment studies. We have summarized our interpretation of the results in Figure 12, and support our suppositions in the following discussion.

Differences between hillslope, tributary, and stream chemistry

Trends in specific conductance, $\delta^{18}O$, and $\delta^{2}H$ along a flowpath from pore water to tributary to stream (Figure 3) indicate the evolution of catchment runoff, providing the hydrologic information necessary to interpret our reactive solute results. Specific conductance increases along the flowpath, indicating continual contact with mineral soils. The seasonal increase in specific conductance indicates even greater mineral contact, likely due to deeper thaw and greater stream water / mineral soil contact in soil pipes (Chapter 5). Given the low hydraulic

conductivity of the silt mineral soil, we expect that increased mineral soil contact also correlates to decreased organic soil contact, surface/subsurface water interactions, and potentially biogeochemical cycling. The enrichment of $\delta^{18}O$ and $\delta^{2}H$ along a flowpath indicates evapotranspiration acting on the flowing water, and provides evidence of relative catchment residence times. The large range in porewater isotope values on DOY 154 indicates that water and solute residence times may vary greatly in the shallow soils, and that tributary chemistry is not always related to porewater concentrations. This disconnect between porewater and streamwater is explored further in Chapter 5, and has implications for reactivity in this catchment.

Synoptic samples of C quantity and quality and nitrate highlight the disconnect between porewater and surface waters, and indicate reactivity in both surface and subsurface pools. Further evidence that tributary water is not simply the sum of porewaters is supplied by nitrate data from DOY 154, 180, and 192, as well as by DOC and SUVA data from DOY 192. While DOC quantities are exceptionally high in boreal catchments, nitrate concentrations in Richardson are often low and/or below detection limits, resulting in C:N ratios that range well above the Redfield ratio, thereby indicating the potential for nitrate limitation of ecosystem processes. On DOY 192, depleted porewater nitrate concentrations coincide with decreased DOC concentrations and elevated SUVA, suggesting ecosystem utilization of labile DOC. Porewater concentrations suggest rapid C-mineralization and N-depletion in instances when solute pools cannot be replenished by hydrologic fluxes. Surface water C and N concentrations are substantially elevated relative to the porewaters. The decrease in DOC and nitrate between the tributary and stream may indicate biogeochemical processes in this system. To support this

supposition we first consider evidence in the relationship between C and N concentrations and discharge, and then simulate stream transport and reactivity with a transient storage model.

Discharge-controlled organic matter flushing and processing

The direct correlation between boreal catchment DOC and nitrate concentrations versus surface water discharge has been documented previously [*Carey*, 2003; *Petrone, et al.*, 2007], and attributed to organic matter leaching by runoff. In boreal soils, the majority of catchment runoff occurs at or very near the land surface [*Carey and Woo*, 2001], allowing water to leach significant amounts of organic material from the shallow soils. Runoff has little interaction with deeper mineral soils [*Quinton and Marsh*, 1999] [Chapter 5], leading to low catchment residence times and minimal biogeochemical processing. Larger events / higher stream stage may lead to increased organic material / streamwater contact, and could thus explain the relationship between organic matter and discharge displayed in Figure 4.

Concurrently, the direct correlation between DOC, nitrate, and discharge may indicate higher mineralization/processing of organic material at low discharge. This supposition is supported by evidence from tributary inflows sampled in June 2008 (Figure 4A). The larger perennial tributaries flow down established channels that are somewhat incised where any organic soils have been eroded, whereas the smaller, ephemeral tributaries are moving at very low velocities and discharges estimated at or below 1 L/s, and are still in contact with organic soils. The importance of water/soil contact for biogeochemical activity has been previously recognized [*Harvey and Wagner*, 2000; *Mulholland, et al.*, 2008; *Peterson, et al.*, 2001], and in the tributaries, the perennial inflows (855 and 1023m) display nitrate concentrations similar to the 1st-order stream while the small, ephemeral inflows (131, 35, and 942m) have lower concentrations, similar to porewaters. Further evidence of biogeochemical processes at low

discharge comes from the 1st-order stream (Figure 4B). Low to absent nitrate concentrations in the 1st-order stream during low flows may indicate nitrate limitation in low-velocity flows or in stagnant pools. The very high DOC concentrations may indicate increased autochthonous production in the warm, almost stagnant pools, or it may indicate decreased ecosystem productivity and subsequently decreased C-mineralization related to nitrate limitation.

Tracer Additions and Transient Storage modeling

In this study, tracer additions were used primarily for quantifying inflow magnitude and chemistry, and instream DOC and nitrate reaction rates. The large range of discharge over which tracer additions were performed provides us with significant information about the changing hydrologic conditions of Richardson Tributary and drainage of the adjacent hillslope. Generally, storage area and exchange rates were low, except surrounding the June, 2008 tracer which took place on the tail end of the large flood event. Given the low hydraulic conductivity of the silt streambanks, and the lack of slope breaks, riffle-pool morphology, dominant laminar flow, and inability to recover samples from substream wells, we believe that the gross majority of transient storage in this stream is related to in-stream pools and low-velocity zones. The strong correlation between discharge and transport and storage parameters (Figure 6) may be further evidence that stream morphology is the dominant control on advective/dispersive and storage hydrology. Uncertainty associated with our transient storage parameters have little effect on our results, because we focused primarily on steady state modeling, which is only significantly affected by advection, reactive solute concentrations, and inflow magnitude.

Temporal trends in inflow location, magnitude, and major ion chemistry

Tracer dilution coupled with effective inflow calculations provides evidence of seasonal shifts in the distribution and chemistry of surface vs. subsurface inflows. Sixty five percent of

the inflows to the stream occur in the furthest downstream reach (Chapter 5), which contains two gaged tributaries. This is likely due to the proportionally larger drainage area at the downstream end of our study reach. The shift from balanced surface/subsurface inflows to 2/3^{rds} from subsurface in Reach 4 between DOY 180 and 241 may be related to the thawing of subsurface flowpaths, to the large difference in hydrologic conditions between the two dates. The DOY 180 sampling was preceded by a large storm event, while the DOY 241 sampling occurred late in the season, under very dry conditions. Trends in the difference between tributary and effective inflow chemistry add support for a seasonal change in the proportion of surface to subsurface inflows, which are discussed extensively in Chapter 5.

Seasonal trends in the difference between observed and effective inflows (Figure 8) supports a shift in flowpaths related to melting of active layer water that has been frozen since the previous fall. At DOY 154, the mean surface water has a lower concentration than the total inflows, indicating a higher ion load and more depleted $\delta^{18}O$ and $\delta^{2}H$ in the subsurface water. In the early summer, subsurface water has likely been frozen on slopes all winter, resulting in long residence times and substantial mineral soil contact. Thaw depths are still shallow at this point in the year, which may allow water to readily flow through the subsurface near the organic/mineral soil boundary. At DOY 241, surface water concentrations have higher concentrations than the total inflows. This trend is consistent with uranium concentrations and activity ratios, which indicate substream preferential flow that has greater contact with mineral soils [Chapter 5] relative to matric flow moving through hillslope organic soils. The differences between surface and subsurface solutes may inform our calculation of inflow chemistry for the transient storage modeling.

Calculating subsurface inflow C and N chemistry

Reactive solute chemistry can not be calculated from effective inflows, leading to some uncertainty in DOC and nitrate concentrations in subsurface flowpaths. Given lower reactive solute chemistry in porewaters relative to tributaries (Figure 3), and the correlation between low reactive solute concentrations and low discharge (Figure 4), we estimate that this subsurface inflow has chemistry similar to porewater concentrations. We adjusted our model inputs to account for the lower concentrations of DOC and nitrate in the subsurface portion of the lateral inflow.

C and N Reactivity in catchment porewaters

The relationships between discharge and DOC and nitrate (Figure 4) provide further evidence that low velocities/high catchment residence times promote biogeochemical activity. Figure 4A indicates that large tributaries contain high concentrations of nitrate. We believe that this water is most indicative of leached organic matter that has had little time for reaction, relative to the smaller, slower moving tributaries that have lower nitrate concentrations. Because hillslope waters are created by the same process – leaching of organic material by precipitation, we assume that their concentrations similarly begin quite high. The difference between these initial concentrations and measured porewater/small stream concentrations indicate a loss of DOC and nitrate presumably related to hillslope biogeochemical processes.

Temporal trends in C and N reactivity

Figures 10 and 11 indicate seasonal changes in the base, pulse, and hillslope decay coefficients and areal uptake rates. Hillslope reactions become less important as the season progresses. This may be because this water is flowing through shallow, organic soil flowpaths, wherease in the late season hillslope water flows through deeper, mineral soil flowpaths [Chapter 5]. The mid-season increase in pulse reactions and decrease in base reactions may be related to

the hydrograph seasonality. Mid summer tends to be the driest time of the year. Discharge and stage in the 1st-order stream is quite low, and is probably in less contact with organic material relative to any other time of year. Furthermore, inflows are also extremely low, meaning that there is little to no incubation of the stream water with leached organic material. Therefore, the pulses of warm, nutrient-rich tributary water that does make it to the 1st-order stream is even more critical, and able to spur in-stream productivity. Late season decreases in pulse rates may correlate to increased subsurface flow and subsequently less water / organic soil interaction. These trends are accompanied by a decrease in SUVA, which may indicate that the organic matter exiting the drainage is less processed at the end of the season.

C and N cycling uncertainties

While our data provides evidence of DOC and nitrate loss, there is still substantial uncertainty concerning these rates. DOC loss and N-cycling incubation are useful for identifying the processes that may be occurring, but the differences in the timescales between the incubations and stream/hillslope processes, and the artificial conditions under which incubations are performed lead to inherent difficulty in comparing the two methods. Therefore, we present incubations not to prove that our rates are accurate, but to provide evidence that our calculated rates are of the correct order of magnitude. Given that DOC loss was measured over a four-week period, we imagine that the present decay coefficients are unnaturally low when compared to instream processes (base and pulse categories), and more representative of hillslope processes, which occur on a longer timescale. Denitrification incubations were sampled every few hours, which is a much more relevant timescale. While nitrification/mineralization incubations were only sampled weekly, the constant nitrate increase suggests that similar rates would have been measured regardless of timescale.

Despite the uncertainties in decay rate coefficients, comparisons with published data and CO_2 chamber flux data suggest that areal uptake rates for DOC and nitrate are reasonable. Methodological differences lead to uncertainty in the comparison of areal uptake and chamber measurements. Chambers measure CO_2 efflux from a soil plot or stream. This CO2 production represents heterotrophic respiration, but also includes the signature of autotrophic/root respiration and degassing from any inorganic carbonate reactions, and may also depend on diffusion rates through soils/stream water. Therefore, we would not be surprised by chamber measurement rates that are significantly larger than our DOC-loss rate calculations. Indeed, chamber measurements are several orders of magnitude greater than base rates. The fact that pulse rates are greater than chamber measurement data is surprising, and may indicate the high-level of ecosystem activity associated with natural incubations of stream water by warm, nutrient-rich inflows. Our DOC uptake rates span a large range, which is grounded by DOC uptake in the hyporheic zone reported by Battin [2003] and benthic respiration data published by Newbold [1997] for a temperate stream, at 1.3 and 1.5 mmol/m^2/hr, respectively. Nitrate areal uptake rates span a much smaller range, and are similar to ambient rates published by Claessens and Tague [2009] and mean rates for 52 first-order streams compiled by Ensign and Doyle [2006], at 0.51 and 0.24 mmol/m^2/hr, respectively.

Conclusion

Synoptic sampling and tracer injections indicate that ecosystem processes are occurring on the hillslopes and in the streams of the Richardson Catchment. Because this system is characterized by a steep hillslope, an active vegetated/organic horizon, and very limited subsurface storage potential, precipitation events lead to flushing of dissolved organic matter

from the hillslopes. The results of our tracer injections and synoptic sampling illustrate the dual role of water, which fuels hillslope biologic processes by providing necessary moisture, and which limits activity by transporting DOC and nitrate from hillslopes. Small tributaries are of critical importance to in-stream C and N cycling, providing heat energy and nitrogen, a primary limiting nutrient to the 1st-order stream. DOC and nitrate loss rates decrease later in the season, which may be related to greater subsurface flow. Our results support studies recognizing the importance of soil/water interactions for biogeochemical processes, and indicate that the smallest streams and lowest discharges promote DOC and nitrate uptake in boreal streams.

Acknowledgements

This work was supported by NSF grant OCE-BE 0628348. We thank G. Aiken, K. Butler, R.L. Smith, D. Repert, C. Hart, P. Schuster, and B. Kimball for analytical help; and K. Wickland, G. Aiken, D. Halm, M. Dornblaser, S. Ewing, R. Spencer, and M. Bourret for assistance with field sample collection.

References

Ãgren, A., et al. (2007), Importance of seasonality and small streams for the landscape regulation of dissolved organic carbon export, *Journal of Geophysical Research G: Biogeosciences*, *112*.

Battin, T. J., et al. (2003), A mixing model analysis of stream solute dynamics and the contribution of a hyporheic zone to ecosystem function, *Freshwater Biology*, *48*, 995-1014.

Bencala, K. E., and R. A. Walters (1983), Simulation of Solute Transport in a Mountain Pool-and-Riffle Stream - a Transient Storage Model, *Water Resources Research*, *19*, 718-724.

Carey, S. K. (2003), Dissolved organic carbon fluxes in a discontinuous permafrost subarctic alpine catchment, *Permafrost and Periglacial Processes*, *14*, 161-171.

Carey, S. K., and M. K. Woo (2001), Slope runoff processes and flow generation in a subarctic, subalpine catchment, *Journal of Hydrology*, *253*, 110-129.

Claessens, L., and C. L. Tague (2009), Transport-based method for estimating in-stream nitrogen uptake at ambient concentration from nutrient addition experiments, *Limnology and Oceanography: Methods*, *7*, 811-822.

Dahm, C. N., et al. (1998), Nutrient dynamics at the interface between surface waters and groundwaters, *Freshwater Biology*, *40*, 427-451.

Dent, C. L., et al. (2007), Variability in surface-subsurface hydrologic interactions and implications for nutrient retention in an arid-land stream, *Journal of Geophysical Research-Biogeosciences*, *112*.

Dixon, R. K., et al. (1994), Carbon pools and flux of global forest ecosystems, *Science*, *263*, 185-190.

Dodds, W. K., et al. (2002), N uptake as a function of concentration in streams, *Journal of the North American Benthological Society*, *21*, 206-220.

Donaldson, J. R., and P. V. Tryon (1990), User's guide to STARPAC - The standards, time series, and regression package.

Edwardson, K. J., et al. (2003), The hydraulic characteristics and geochemistry of hyporheic and parafluvial zones in Arctic tundra streams, north slope, Alaska, *Advances in Water Resources*, *26*, 907-923.

Ensign, S. H., and M. W. Doyle (2006), Nutrient spiraling in streams and river networks, *Journal of Geophysical Research G: Biogeosciences*, *111*.

Fisher, S. G., et al. (1998), Material spiraling in stream corridors: A telescoping ecosystem model, *Ecosystems*, *1*, 19-34.

Harvey, J. W., and B. J. Wagner (2000), Quantifying hydrologic interactions between streams and their subsurface hyporheic zones, in *Streams and Ground Waters*, edited by J. B. Jones and P. J. Mulholland, Academic Press, San Diego.

Harvey, J. W., et al. (1996), Evaluating the reliability of the stream tracer approach to characterize stream-subsurface water exchange, *Water Resources Research*, *32*, 2441-2451.

Hinzman, L. D., et al. (2005), Evidence and implications of recent climate change in Northern Alaska and other Arctic regions, *Climatic Change*, *72*, 251-298.

Holmes, R. M., et al. (1998), The impact of flash floods on microbial distribution and biogeochemistry in the parafluvial zone of a desert stream, *Freshwater Biology*, *40*, 641-654.

IPCC, et al. (2007), Technical Summary, in *Climate Change 2007: The Physical Science Basis. Contribution of Working Group 1 to the Fourth Assessment Report of the Intergovernmental Panel on Climate Change*, edited by S. Solomon, et al., Cambridge University Press, Cambridge, United Kingdom and New York, NY, USA.

Kilpatrick, F. A., and E. D. Cobb (1985), Measurement of Discharge Using Tracers, Techniques of Water Resources Investigations, Book 3, Chapter A16, 52 pp, U.S.Geological Survey.

Koch, J. C., et al. (2010), Effect of unsteady flow on nitrate loss in an oligotrophic, glacial meltwater stream, *Journal of Geophysical Research G: Biogeosciences*, *115*.

Maclean, R., et al. (1999), The effect of permafrost on stream biogeochemistry: A case study of two streams in the Alaskan (U.S.A.) taiga, *Biogeochemistry*, *47*, 239-267.

McKnight, D. M., et al. (2004), Inorganic N and P dynamics of Antarctic glacial meltwater streams as controlled by hyporheic exchange and benthic autotrophic communities, *Journal of the North American Benthological Society*, *23*, 171-188.

Muhs, D. R., et al. (2003), Stratigraphy and palaeoclimatic significance of Late Quaternary loess-palaeosol sequences of the Last Interglacial-Glacial cycle in central Alaska, *Quaternary Science Reviews*, *22*, 1947-1986.

Mulholland, P. J., et al. (2008), Stream denitrification across biomes and its response to anthropogenic nitrate loading, *Nature*, *452*, 202-205.

Newbold, J. D., et al. (1997), Organic matter dynamics in White Clay Creek, Pennsylvania, USA, *Journal of the North American Benthological Society*, *16*, 46-50.

Newbold, J. W., et al. (1983), Phosphorus dynamics in a woodland stream ecosystem: a study of nutrient spiralling, *Ecology*, *64*, 1249-1265.

O'Donnell, J. A., and J. B. Jones (2006), Nitrogen retention in the riparian zone of catchments underlain by discontinuous permafrost, *Freshwater Biology*, *51*, 854-864.

Payn, R. A., et al. (2009), Channel water balance and exchange with subsurface flow along a mountain headwater stream in Montana, United States, *Water Resources Research*, *45*.

Peterson, B. J., et al. (2001), Control of nitrogen export from watersheds by headwater streams, *Science*, *292*, 86-90.

Petrone, K. C., et al. (2007), The influence of fire and permafrost on sub-arctic stream chemistry during storms, *Hydrological Processes*, *21*, 423-434.

Petrone, K. C., et al. (2006), Seasonal export of carbon, nitrogen, and major solutes from Alaskan catchments with discontinuous permafrost, *Journal of Geophysical Research-Biogeosciences*, *111*.

Prokushkin, A. S., et al. (2005), Climatic factors influencing fluxes of dissolved organic carbon from the forest floor in a continuous-permafrost Siberian watershed, *Canadian Journal of Forest Research-Revue Canadienne De Recherche Forestiere*, *35*, 2130-2140.

Quinton, W. L., and P. Marsh (1999), A conceptual framework for runoff generation in a permafrost environment, *Hydrological Processes*, *13*, 2563-2581.

Runkel, R. L. (1998), One-dimensional tranpsort with inflow and storage (OTIS): a solute transport model for streams and rivers, U.S. Geological Survey, Denver, CO.

Runkel, R. L. (2007), Toward a transport-based analysis of nutrient spiraling and uptake in streams, *Limnology and Oceanography-Methods*, *5*, 50-62.

Schuur, E. A. G., et al. (2008), Vulnerability of permafrost carbon to climate change: Implications for the global carbon cycle, *BioScience*, *58*, 701-714.

Striegl, R. G., et al. (2005), A decrease in discharge-normalized DOC export by the Yukon River during summer through autumn, *Geophysical Research Letters*, *32*.

Valett, H. M., et al. (1996), Parent lithology, surface-groundwater exchange, and nitrate retention in headwater streams, *Limnology and Oceanography*, *41*, 333-345.

Waddington, J. M., and N. T. Roulet (1997), Groundwater flow and dissolved carbon movement in a boreal peatland, *Journal of Hydrology*, *191*, 122-138.

Walvoord, M. A., and R. G. Striegl (2007), Increased groundwater to stream discharge from permafrost thawing in the Yukon River basin: Potential impacts on lateral export of carbon and nitrogen, *Geophysical Research Letters*, *34*.

Figure 1: A) Map of Alaska with the red square indicating the location of the contour map. B) The study area, with 10 m contours. The line represents Richardson Tributary, a 2nd – order tributary in which tracer additions and synoptic samplings were performed. Circles indicate major tributaries that flowed most/all of the summer. Squares indicate the approximate paths of ephemeral tributaries that only flowed during the June, 2008 tracer injection. Stars represent the locations of flumes. T1, 2, and 3 are the locations where samples were collected during the tracer injections for bromide analysis.

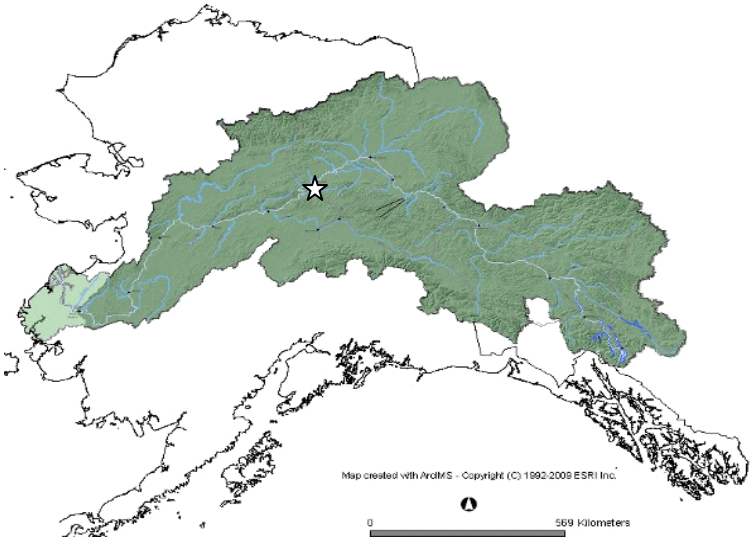

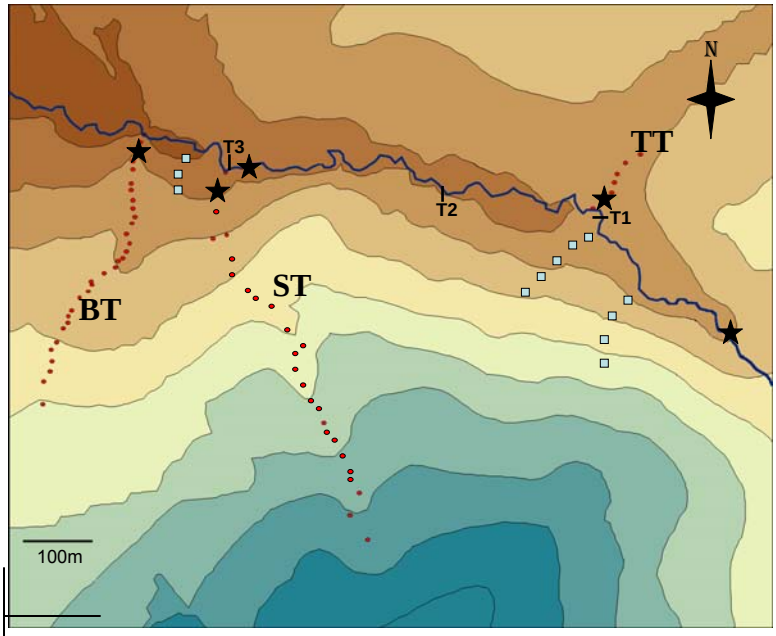

Figure 2: Discharge records from the downstream Richardson Tributary gaging station during the summers of 2008 and 2009. Vertical lines represent tracer additions and/or synoptic samplings.

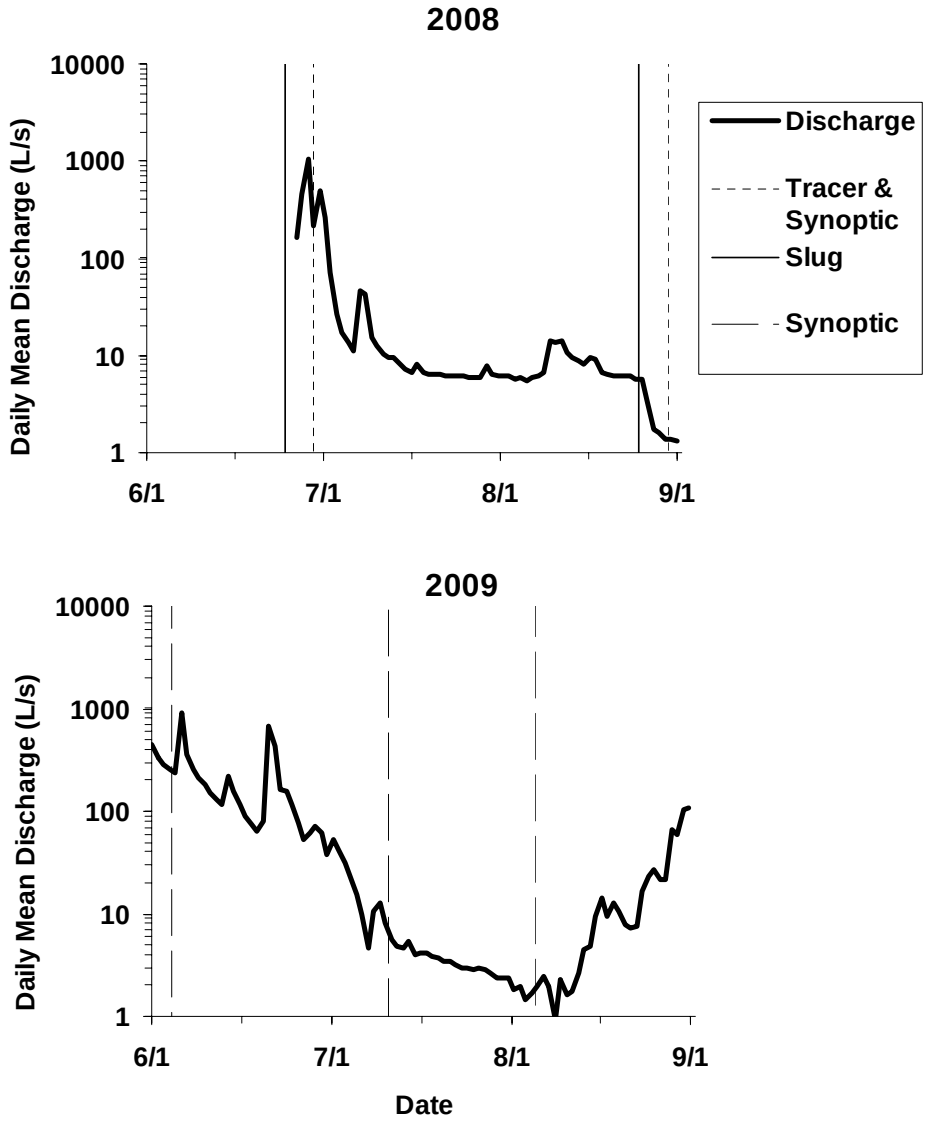

Figure 3: Conservative (A) and reactive (B) solute concentrations in streams and soils in Richardson Catchment. Bars represent the full sample range. No bars indicate that only one sample was collected. There is no porewater sample for DOY 241, because soils were unsaturated.

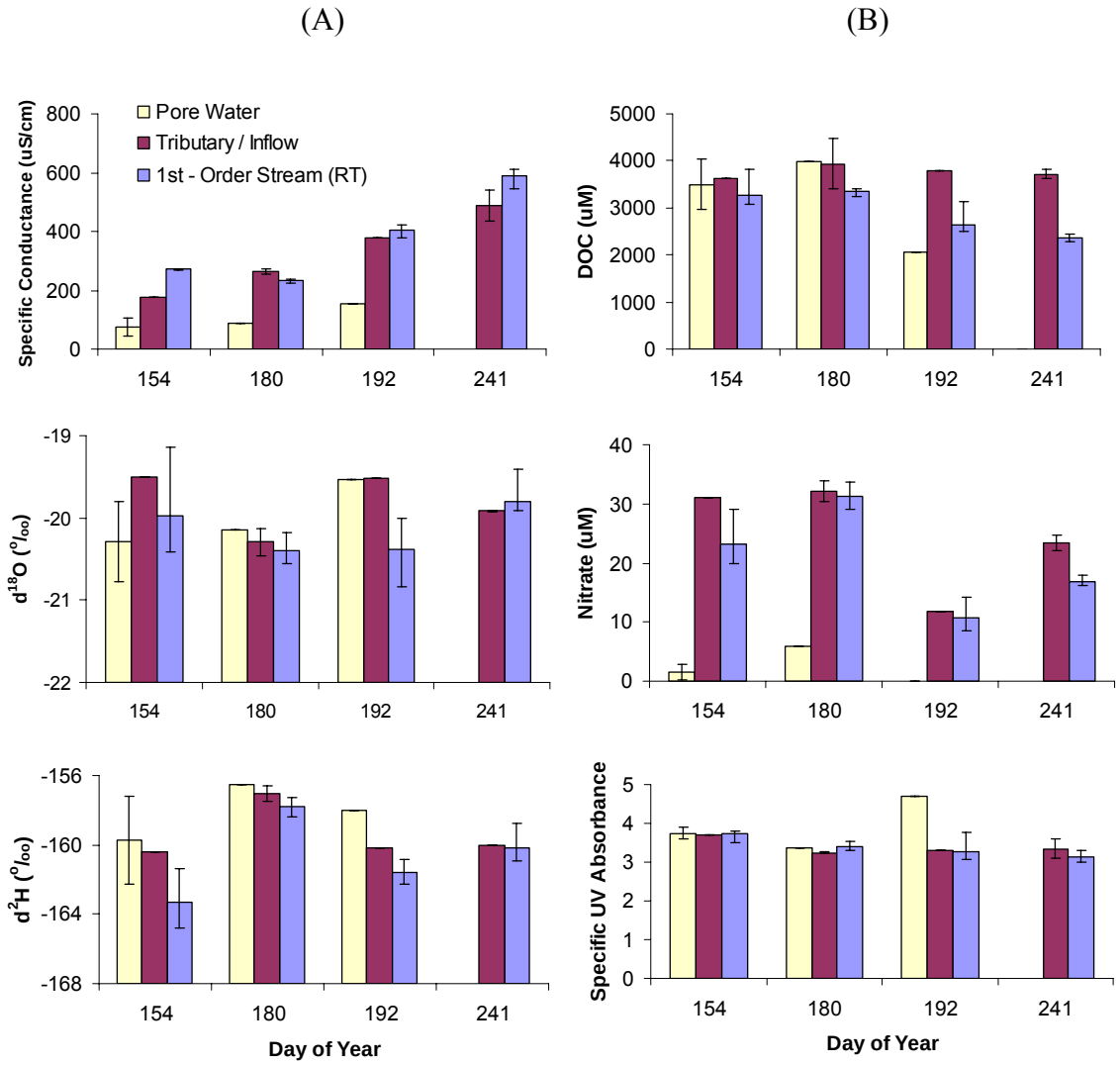

Figure 4: Reactive solutes correlate to discharge A) Nitrate concentration correlates to the relative size of the 1st - order inflows during the June, 2008 synoptic sampling. B) DOC and nitrate in Richardson Tributary (RT) correlate to discharge over two seasons, with deviations of DOC concentrations from the trend at the lowest discharge.

A)

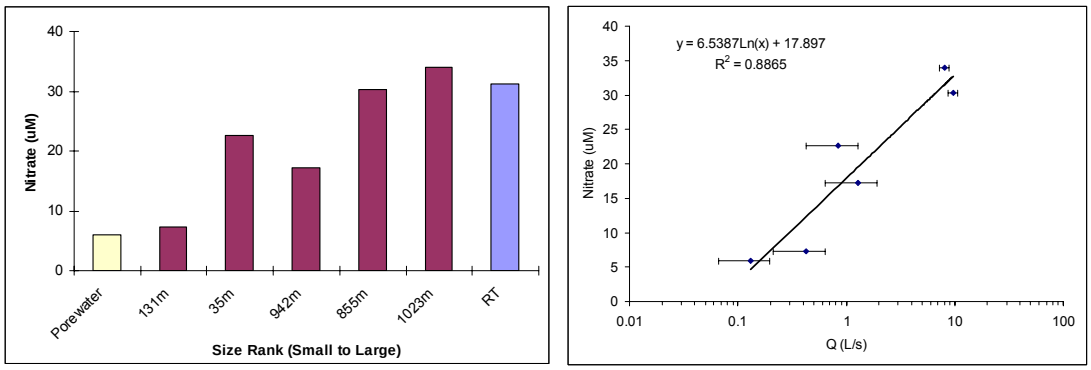

B)

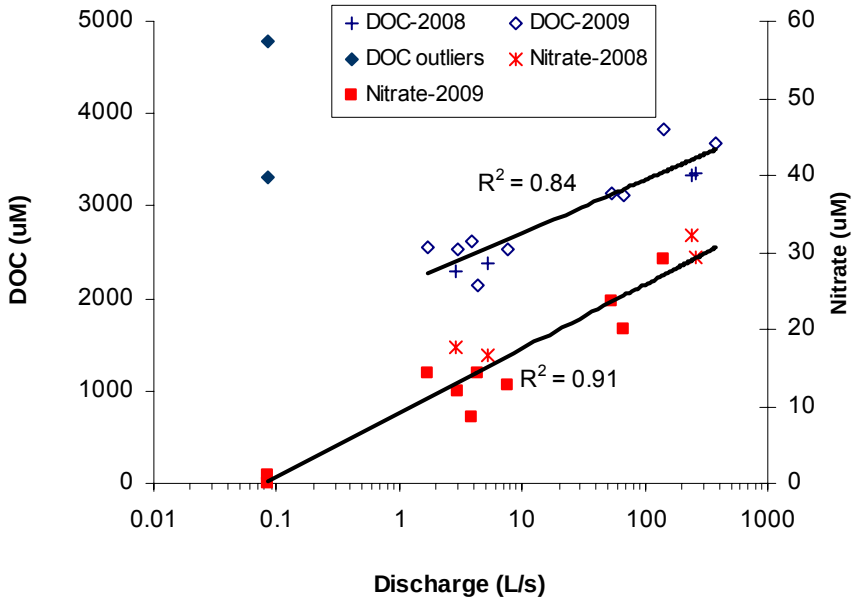

Figure 5: Tracer breakthrough curves and modeling for the 2008 injections. A) the July, 2008 tracer, monitored at Site T3 (829 m) and B) the August, 2008 tracer, monitored at Site T2 (493 m). Bromide breakthrough curves for the C) June, 2008 tracer injection displaying an increasing concentration related to the receding flood and a dip related to a pump malfunction, and D) the August, 2008 tracer at Site T1 (173 m), Site T2 (493 m), and C) Site T3 (829m).

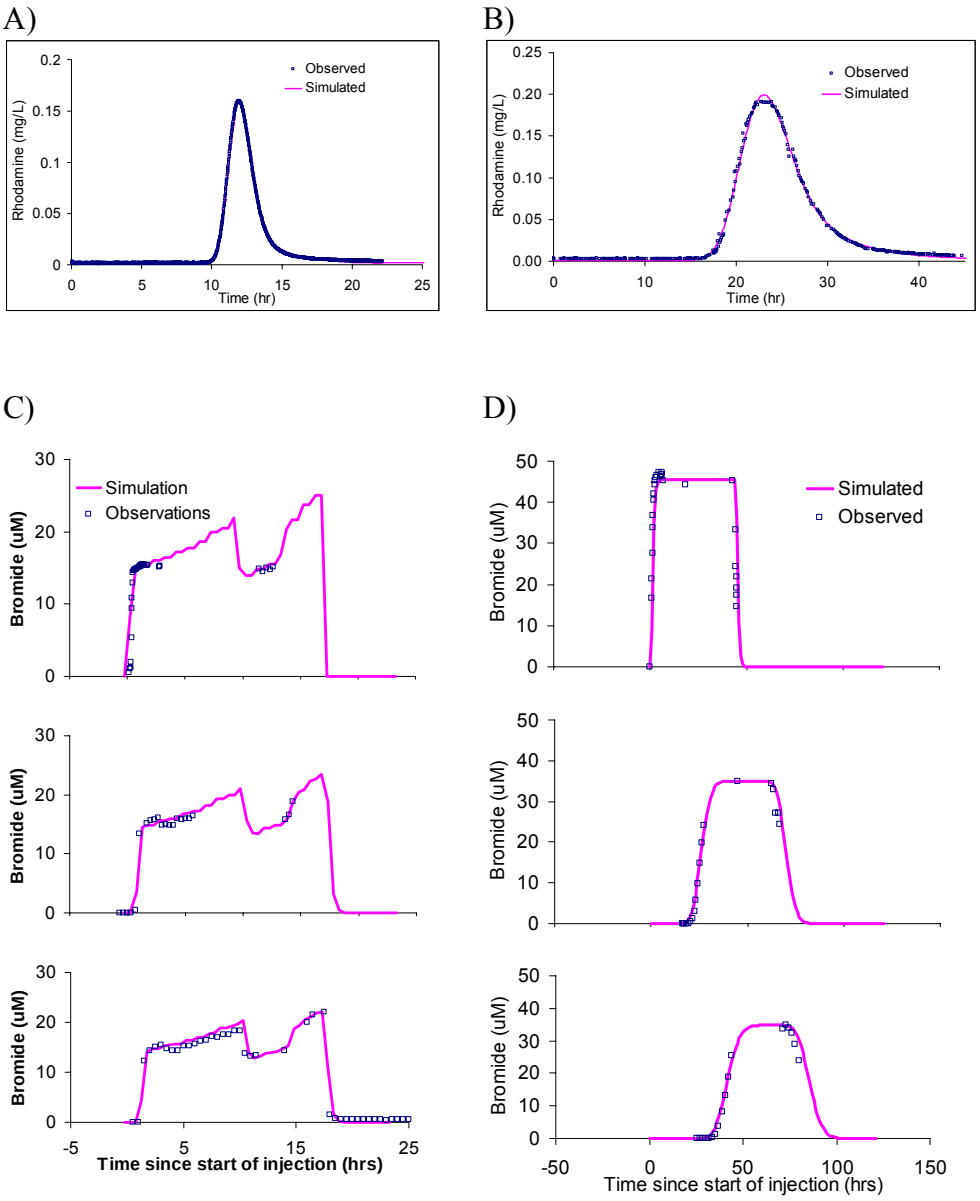

Figure 6: Correlations between discharge and transient storage model parameters for 5 simulations from the 2008 tracer injections. Error bars represent two standard deviations from the mean value based on STARPAC output.

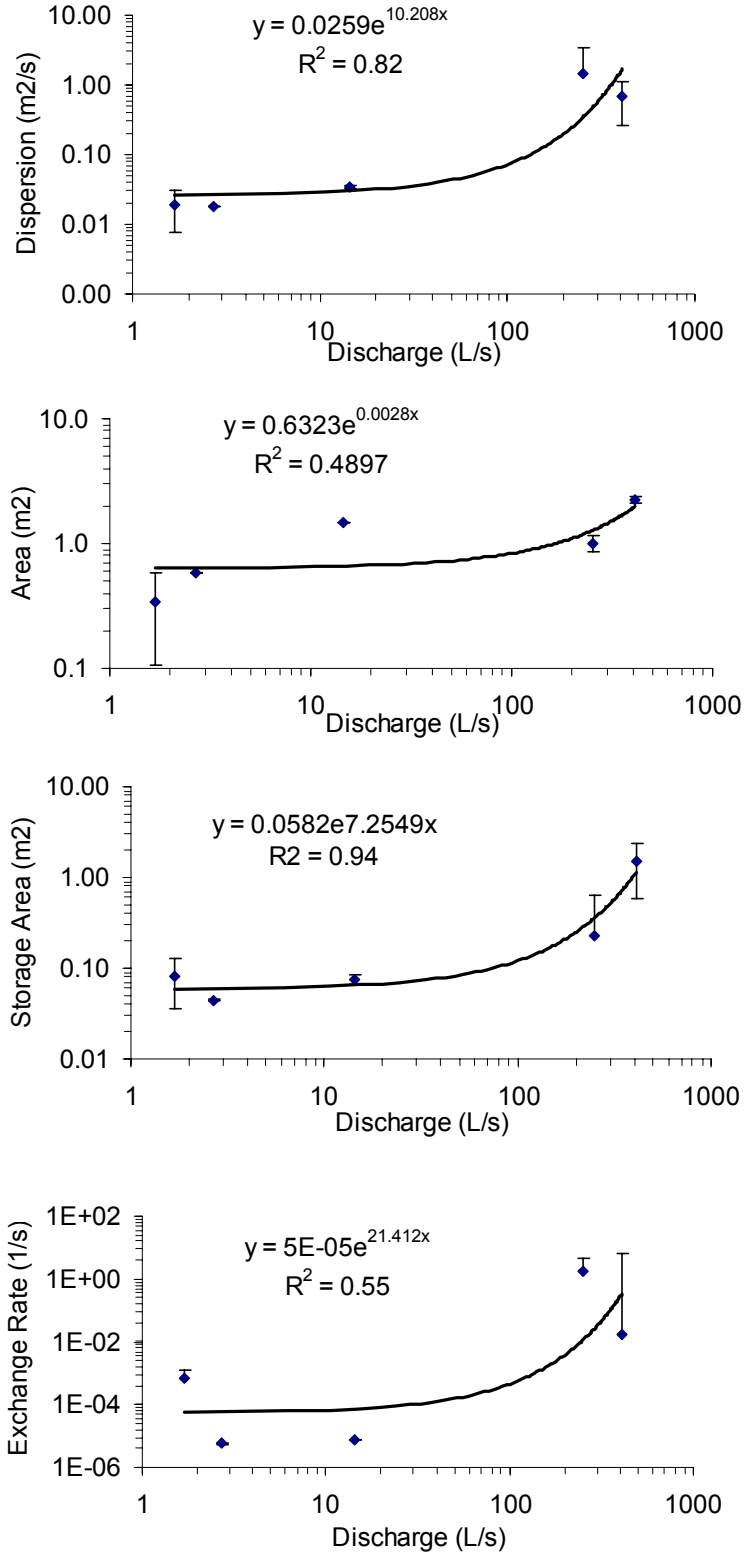

Figure 7: Proportional inflows indicate the location and proportion of surface water (SW) vs. subsurface or small, ungaged tributary inflows (GW). Sixty-four percent of the inflows occur in Reach 4 (829 – 1226 m) for both time periods. The proportion of subsurface water increases, from 61 to 78% of the total inflow between June and September, respectively.

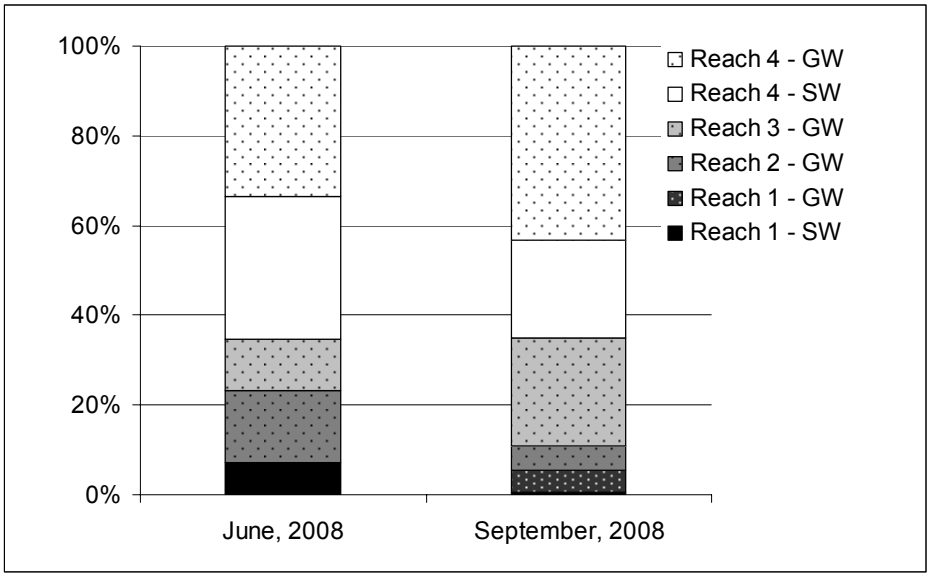

Figure 8: Comparisons of observed (surface water) and effective (total) inflows indicate a seasonal trend, with dilute subsurface inflows in the beginning of the summer, and higher ion load from subsurface inflows near the end of the summer.

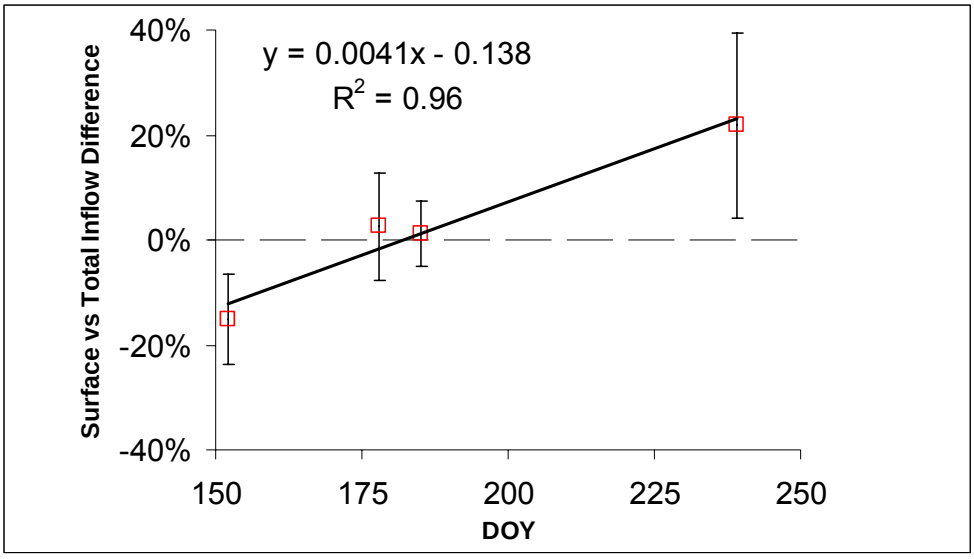

Figure 9: Steady state transient storage modeling results for DOC and nitrate from four time periods. Red squares represent Richardson Tributary stream concentrations, with error bars equal to analysis error. Black triangles represent surface water inflow concentrations. Thick black lines represent conservative transport. Dashed lines are shown when observed stream concentrations differed significantly from modeled conservative transport and represent simulated stream concentrations given first-order decay.

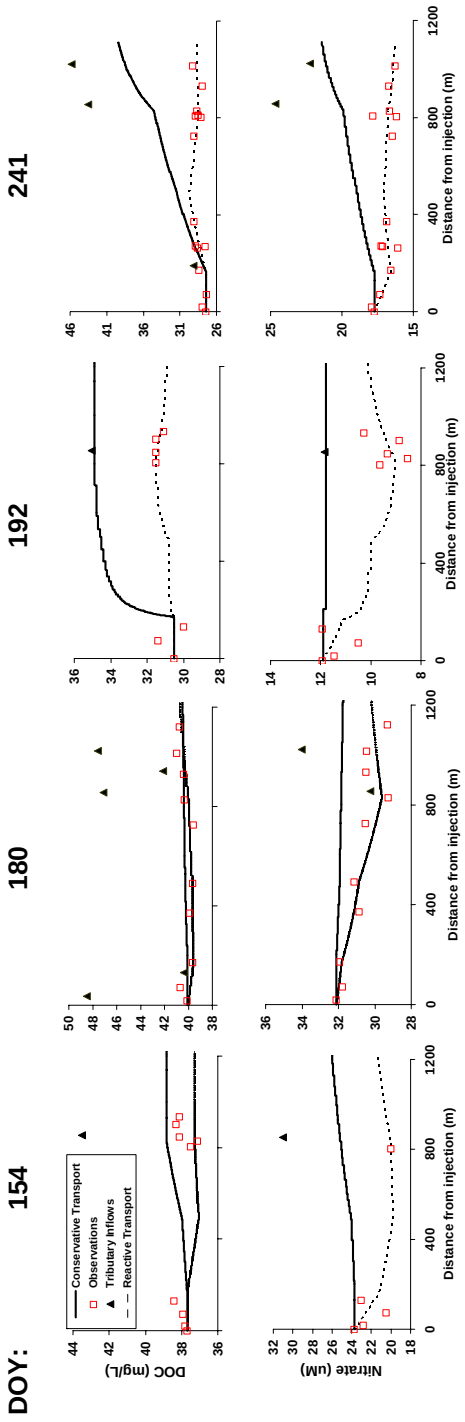

Figure 10: DOC and nitrate decay coefficients were calculated in the stream assuming no inflows (base) and inflows (pulse). Hillslope rates were calculated given estimated residence times and the difference between pore and exported water. DOC decay rate coefficients are compared to doc-loss incubations, and nitrate decay rate coefficients are compared to nitrogen cycling incubations (denitrification minus nitrification/mineralization).

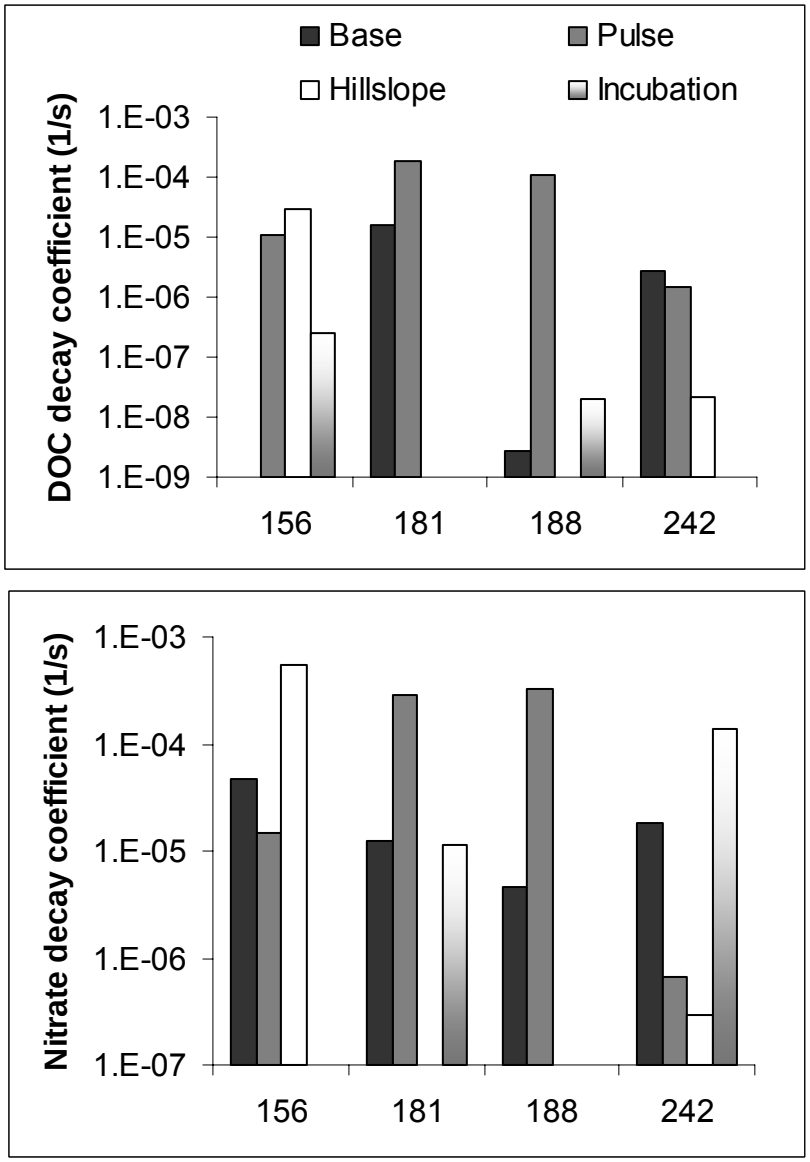

Figure 11: DOC and nitrate areal uptake under base (no inflows) and pulse (inflows) conditions. Export represents aqueous transport of DOC and nitrate past the downstream flume location. Aquatic and terrestrial chamber fluxes are presented to compare calculated C – loss to carbon dioxide efflux from the soils (Ch-terrestrial) and streams (Ch-aquatic) of the catchment.

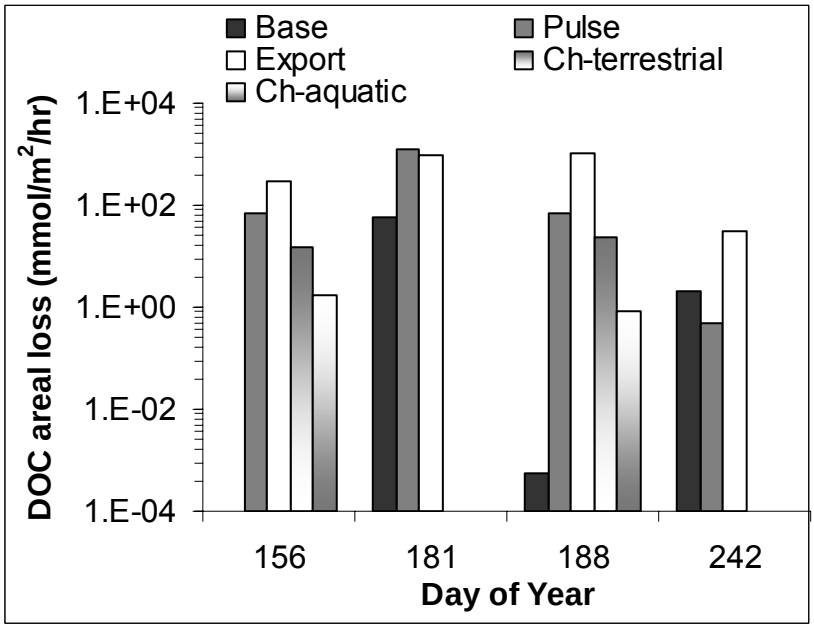

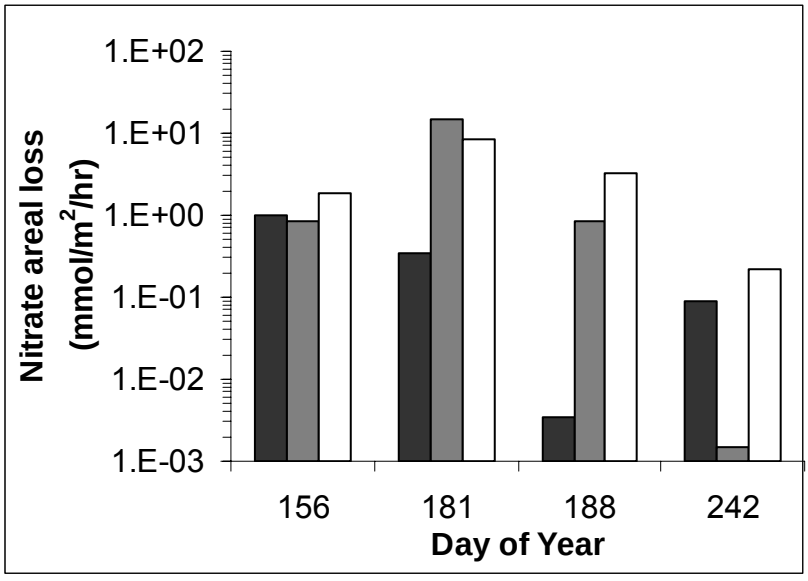

Figure 12: Conceptual model of hydrologic flux and biogeochemical reactions in the Richardson Catchment.

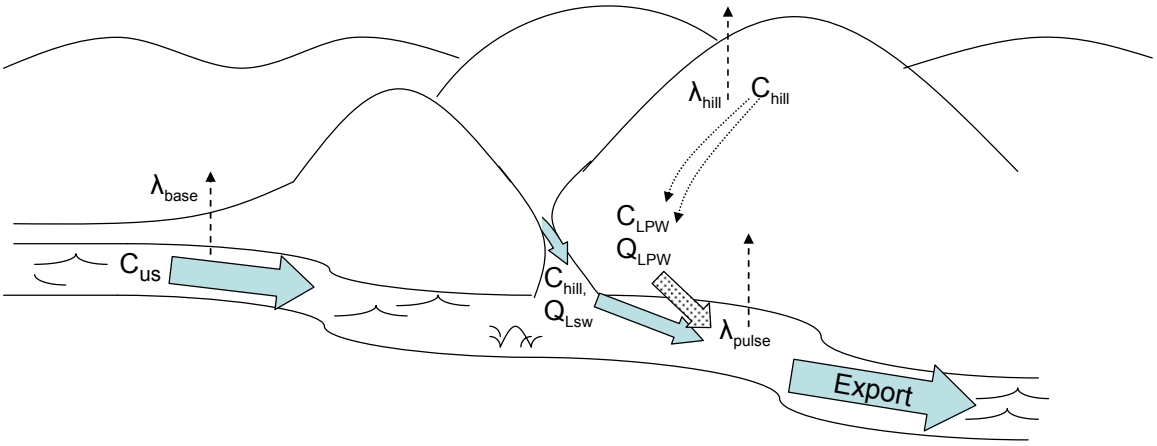

CHAPTER 5

Hydrologic and uranium isotope indicators of subsurface preferential flowpaths above continuous permafrost on a hillslope in interior Alaska

Koch, J.C., S.A. Ewing, R. Striegl, and D.M. McKnight

Abstract

The balance between runoff and storage is critical to biogeochemical processing of carbon (C) in boreal ecosystems. Whether C is mineralized in soils or flushed from catchments depends on catchment residence times and has implications for ecosystem productivity and climate change feedbacks. To understand the seasonal dynamics of catchment water storage and runoff, we monitored soil moisture, precipitation, stream/catchment interactions, and discharge in 1st - and 2nd -order streams from a north-facing hillslope in the Yukon River Basin, Alaska over the summers of 2008 and 2009. We also conducted two tracer dilution experiments and monitored major ion and uranium concentrations, and $^{234}U/^{238}U$ uranium activity ratios (UARs). Infiltration modeling and soil moisture measurements suggests that most of the precipitation that falls on the hillslope is lost to evapotranspiration. Runoff coefficients were related to soil moisture and active layer depth. U concentration and UARs were used as an indicator of water / mineral soil contact, and suggest soil piping / thermokarsting in otherwise similar tributaries. Using these results we create a conceptual model that highlights the near-stream, parafluvial environment as the dominant pathway for water and solutes to exit the drainage. The parafluvial zone has previously been recognized as a critical location for biogeochemical processes, and this work highlights its importance to hydrologic connectivity and catchment geomorphology. This model is useful in considering terrestrial carbon flux and stream export, and for predicting

changes in catchment hydrology, biogeochemistry, and geomorphology as the arctic becomes warmer and wetter.

Introduction

Northern hemisphere boreal soils contain as much as one third of the world's carbon (C) [*Dixon, et al.*, 1994]. Much of this C is stored in frozen soils and thus unavailable to ecosystems, while the remainder exists in the vegetation and organic soils that overlay mineral and frozen soils. High early-season stream discharge and flashy hydrographs in high latitude environments are often attributed to the presence of permafrost or frozen ground (Woo 1986), which precludes subsurface storage. Subsurface storage capacity may increase during the summer due to increased thawing of soils [*Prokushkin, et al.*, 2005] and the near-stream environment [*Brosten, et al.*, 2006].

Much of the important hydrology and biogeochemistry in boreal systems occurs in the shallow organic soil. Boreal soils are characterized by layers of moss and organic material overlying mineral soils. The hydraulic conductivity (K) of the organic layer varies greatly with depth, and has been shown to range from one to one thousand m/day [*Quinton and Marsh*, 1999]. Mineral soil K is often lower than the organic soils K by an order of magnitude or more. The abrupt change in K between the organic and mineral soil promotes lateral runoff, and may preclude infiltration into the mineral soil [*Carey and Woo*, 2001; *Quinton and Marsh*, 1999].

Preferential flowpaths are another potentially important mechanism by which water and solutes may move through boreal catchments. Preferential flow leads to rapid transport of water and solutes through high-velocity features including surface rills, soil pipes, macropores, and thermokarst features. Preferential flow through rills occurs in the early season, when frozen

ground focuses flow on and near the surface [*Carey and Woo*, 2000; 2001]. Soil piping tends to occur at the organic-mineral boundary, and more readily in ice-rich sediments [*Carey and Woo*, 2002]. Piping requires high enough velocities to move mineral grains, and therefore occurs predominantly on steeper slopes [*Quinton and Marsh*, 1998]. Piping has been recognized as a means of transporting solutes beneath streams, and may occur at high velocities similar to streamflow [*Cozzetto, 2009*].

Runoff coefficients provide information about catchment storage by comparing the ratio of discharge to precipitation. This method has been used to compare different catchments and consider the influence of different hydrologic events (snowmelt, convective thunderstorms, longer-duration storms) [*Merz, et al.*, 2006]. Runoff coefficients have also been used to consider the influence of variations in subsurface ice, indicating increased proportion of runoff with less thaw [*Wang, et al.*, 2009]. Runoff coefficients may provide information about seasonal changes in our study catchment.

Changes in the catchment residence times and stream/catchment interactions may be related to $^{234}U/^{238}U$ ratios in water, which have been used to indicate water/sediment contact time and are commonly elevated in groundwater [*Kigoshi*, 1971]. Variation in this ratio in sediments and water results from alpha decay of ^{238}U, which may eject a daughter product, ^{234}U out of a sediment grain, thereby enriching $^{234}U/^{238}U$ activity in the surrounding porewater. The deviation of this ratio from secular equilibrium, where $^{234}U/^{238}U$ activity equals one, is dependent on sediment age and size, and is greatest when grains are smallest and water concentrations are lowest [*DePaolo, et al.*, 2006]. Uranium activity ratios are an especially effective tracer when sediment size and shape are uniform. These measurements may be useful in identifying

subsurface flowpaths and areas of high water / mineral soil contact in the silt-dominated uplands of interior Alaska.

Many studies have considered C storage and transport in boreal ecosystems, invoking increasing thaw depth as the cause of trends in stream chemistry. Prokushkin et al. [2005] noted higher yields of dissolved organic carbon (DOC) from slopes with deeper active layers (south-facing) relative to adjacent slopes (north-facing), presumably due to increased leaching of sediments by infiltrating snow melt. Conversely, Petrone et al. [2007] witnessed lower yields of DOC from watersheds with larger active layers (deeper permafrost), and attributed this to storage and processing of these nutrients in deeper mineral soils. Striegl et al. [2005] found trends in the ratio of organic to inorganic C exports from the Yukon River Basin (YRB), and attributed this to greater processing of terrigeneous C in watersheds. Work by Walvoord and Striegl [2007] indicates that increased C processing in the YRB may be related to longer, deeper flowpaths related to subsurface thaw. While these studies infer a deepening thaw depth as the cause of biogeochemical trends, few have rigorously examined the hydrologic flowpaths that move water and solutes from catchments into streams.

We hypothesize that in the silt-loess dominated catchments of interior Alaska, thaw depth is of little importance to hydrology and solute transport, because water is unable to flow through the low hydraulic conductivity silt. Therefore, we expect that runoff is topographically controlled, and that low points and concavities in the landscape will dominate hillslope runoff. We support the lack of hillslope runoff using soil moisture data and infiltration modeling results. Seasonal trends in runoff coefficients suggest evolution of flowpaths, which is further supported by U isotope data. By coupling tracer dilution data presented in Chapter 4 with U inflow calculations, we identify areas of high sediment/water contact and present a conceptual model of

runoff from silt-loess catchments of the YRB Our model is relevant to considering C and N flushing and reactivity, and may be useful in predicting geomorphic, hydrologic, and biogeochemical changes as the Alaskan interior becomes warmer and wetter.

Site Description

The Richardson Catchment is an 11 km^2 watershed located 1.5 km southwest of the Hess Creek gaging station in the Yukon River Basin, AK (Figure 1). This catchment is drained by Richardson Tributary (RT), a 1^{st} order stream incised several meters below the valley fill level. This tributary flows along the edge of steep, north-facing hills, with a shallow, south-facing floodplain. The mineral soils are exclusively silt-loess and underlain by continuous permafrost. Maximum thaw depths have been measured at approximately 70 cm. Vegetation consists primarily of mosses and grasses, which grade into an approximately 10 cm thick organic layer on top of the mineral soil. This catchment burned in 2007, resulting in standing dead trees and a lack of significant understory except around wetter landscape positions. The northern stream bank is characterized by minimal topographic relief, no major inflows, and dry soils, precluding significant inflows from this half of the watershed. Many 1^{st}-order tributaries drain into RT on the south side. Several perennial inflows exist, which have eroded the organic soils, and flow on top of the mineral soil. Ephemeral tributaries have been observed flowing during the early summer, when soils are wetter. Ephemeral stream bed-type varied, with some tributaries flowing over mineral soil and others flowing directly on organic soils. There is evidence of small land slides and slumps along steeper slopes at the toe of the hillside near surface water inflows. Tracer dilution results from Chapter 4 indicate that the majority of inflows into the 2^{nd}-order tributary occur in the downstream reaches, which have larger catchment areas and perennial tributaries (Figure 2). Inflows to the stream were predominantly subsurface water, which

comprised 61 and 78% of the total recharge in the wetter early summer and drier late summer, respectively. Tracer addition and synoptic sampling results indicate that surface and subsurface inflows are well-mixed in the middle of the summer, but that dilute subsurface water accounted for 18 % of the inflows in early June, and that at the end of the season as much as 22% of the inflowing water may contain a significantly elevated solute load.

Methods

Field Measurements

Discharge was monitored at two locations in Richardson Tributary and in three perennial inflows during the summers of 2008 and 2009 using Level Logger 100 or Minitroll pressure transducers (In-Situ, Fort Collins, CO) placed in stilling wells in or above flumes. Pressure was logged every 15 min, corrected for atmospheric pressure, and field calibrated by independently reading flume staff plates during site visits. Discharge was calculated using flume rating curves and pressure logs. Discharge often exceeded 67.4 L/s, which is the maximum flume capacity. During these high flows, discharge was modeled using Manning's equation:

$$Q = \frac{1.49}{n} S^{\frac{1}{2}} A R^{\frac{2}{3}}, \qquad (1)$$

where Q is discharge, n is Manning's roughness, S is the stream slope, A is channel area, and R is the hydraulic radius of the stream. A rod and level were used to survey the channel cross section at the two flume locations. Channel area and roughness were calculated by coupling the cross section with water height from the pressure transducer records. Slope was estimated from a GPS survey of the stream banks. Manning's roughness was calculated for instances when discharge

greater than 67.4 L/s were independently measured with a rod and pygmy meter by rearranging equation 1. Precipitation was measured at the Hess Creek Gage, operated by the US Geological Survey and located several kilometers from the catchment. Runoff coefficients are defined as the ratio of discharge to precipitation, and were calculated for the Richardson Tributary for 2008 and 2009. Precipitation values less than 0.02 inches were removed to avoid false positive readings by the rain gage. Runoff coefficients (RC) were calculated as:

$$RC = \frac{Q}{P_{tot}}, \qquad (2)$$

where Q is the maximum average daily discharge measured at the downstream flume following the precipitation event, and P is the total event precipitation measured at the Hess Creek Gaging Station. Runoff coefficients were regressed with active layer depth and soil moisture. Regressions were created for the entire period of record, as well as for individual years to identify correlations that may explain seasonal shifts in runoff and infiltration.

Soil moisture and temperature were measured in three locations in the watershed in 2008 and five locations in 2009, delineated in Figure 1b. Soil moisture was measured with ECHO EC-5 probes, and temperature was measured with a 12-bit temperature Smart Sensor, both from Onset Computer Corporation. Measurements were logged with an Onset HOBO Micro Station.

The Green-Ampt model uses an approximation of Darcy's Law and a continuum equation to estimate infiltration into an initially unsaturated soil. We used this model to simulate infiltration into the mineral soil on the catchment hillslopes during the largest precipitation events in 2008 and 2009. The catchment's mineral soil is dominantly silt-loam based on particle

size distribution analysis. Soil hydraulic properties were obtained from Carsel and Parrish [1998]. Cumulative infiltration (F) and and infiltration rates (f) were calculated as:

$$F = Kt + \psi\Delta\theta \ln\left(1 + \frac{F(t)}{\psi\Delta\theta}\right), \quad \text{and} \qquad (3)$$

$$f(t) = K\left(\frac{\psi\Delta\theta}{F(t)} + 1\right), \qquad (4)$$

where K is hydraulic conductivity, t is time, ψ is the pressure head, $\Delta\theta$ is the change in water content from initial conditions measured by the moisture sensor and saturated water content, estimated as 0.45. The model was calculated for half hour timesteps. Infiltration rates were compared to precipitation rates and adjusted when necessary to account for ponding. The appropriate effective hydraulic conductivity for Green-Ampt modeling is uncertain [*Chow, et al.*, 1988; *Dingman*, 1994], and may range from saturated [*Dingman*, 1994], to one half of the saturated hydraulic conductivity [*Risse, et al.*, 1994]. Our simulations were executed using both of these extremes, and therefore considers the full range of potential infiltration. Initial soil moisture was estimated given the shallow sensor soil moisture measurements, and the Maulem-van Genuchten characteristic curve, which relates moisture to hydraulic pressure for a given soil type. The Green-Ampt model functions best in deep soils with constant depths, and therefore its utility is compromised in the shallow soils and variable initial moisture content over short vertical distances in this catchment. Our parameters were chosen to estimate the greatest potential infiltration, in order to show the shallow depth to which precipitation penetrates.

Tracer Addition

A continuous sodium bromide (NaBr) addition was performed in August, 2008, and is fully described in Chapter 4. Injection rates were maintained using a CR10 datalogger and two flow-rate sensing FMI pumps. Bromide and uranium samples were collected at multiple locations along the kilometer-long reach. Bromide samples were collected in June and August, 2008, and uranium samples were only collected in August, 2008. Samples were filtered with a Gelman capsule filter. Uranium samples were stored in a one liter acid-rinsed bottle. Uranium analysis was performed on a mass spectrometer. Uncertainty in uranium concentrations and activity ratios are on the order of 0.002 ppb and 0.004 ppb/ppb. Bromide samples were collected in a 60 mL nalgene bottle and chilled. Bromide concentrations were analyzed on a Dionex Ion Chromatograph in the Boulder, CO US Geological Survey office. Discharge at each location was calculated as:

$$Q_j = \frac{C_i Q_i}{C_j}, \qquad (5)$$

where Q represents the flow rate, C represents the bromide concentration, i is the injection location, and j is the location of interest. Q_i and C_i are known given the pumping rate and initial injectate concentration, and C_j was calculated given measured bromide concentrations. Subsurface inflows were determined by subtracting surface inflows measured at each flume from the total inflow, defined as the discharge difference for any given reach.

Effective inflow concentrations (C_{lateff}) represent the total, surface and subsurface concentrations of solute moving from the catchment into the stream. Effective inflow concentrations were calculated based on tracer dilution discharge and U concentrations, following:

$$C_{lateff} = \frac{Q_{DS}C_{DS} - Q_{US}C_{US}}{Q_{DS} - Q_{US}}, \quad (6)$$

where *US* and *DS* represent the upstream and downstream components, respectively.

Results

Daily total precipitation for the periods June 1st through September 1st for 2008 and 2009 are presented in Figure 3. Total precipitation values of 97.3 and 117.3 mm were measured for the two summers, respectively. Daily mean stream discharge varied substantially over the course of the summer (Figure 3. Discharge decreased from high early season measurements into the middle of the summer. July discharge remained fairly constant in 2008 and decreased steadily, and even ceased for several days at the upstream end of the study reach in 2009. In general, stream discharge increased between the upstream and downstream flumes, with the exception of water losses at the beginning of large flood events.

Mineral soil moisture logger data is plotted for two depths in 2008 and 2009 in Figure 4. Volumetric soil moisture was less than saturation (approximately 0.40 to 0.45 for silt-loess) for all locations and depths, except for TK1 during early June. Generally, soil moisture was higher in June, declined during July, and leveled or increased slightly towards the end of August, similar to stream discharge. Trends in soil moisture are greater at shallow depths. Shallow moisture sensors displayed large increases as a result of June precipitation/flood events, while deeper sensors displayed little to no increase in soil moisture. Given these data, hydraulic conductivities for shallow soils (averaging 8 cm deep in the silt-loess) varied from 1.65 to 0.008 cm/hr, while deeper soils (averaging 26 cm deep in the silt-loess) varied from 0.4 to 0.04 cm/hr.

Table 1: Green Ampt Infiltration Modeling Results for major precipitation events in (A) 2008, and (B) 2009.

A)

Event #	Date	Duration	Precipitation		Infiltration
		(hr)	Total (mm)	Max Rate (mm/hr)	Cumulative (mm)
1	6/27/08	1.5	7	13	
2	6/28/08	12	19	6.1	35.3
3	7/1/08	7	10.2	2.0	26.4
4	7/8/08	1.5	21.6	25.9	77.2
5	7/21/08	2	1.3	1.0	95.1

B)

Event #	Date	Duration	Precipitation		Infiltration
		(hr)	Total (mm)	Max Rate (mm/hr)	Cumulative (mm)
1	6/5/09	5	11.7	4.6	41.3
2	6/21/09	4	11.9	9.7	18.6
3	6/28/09	1.5	7.6	13.2	14.0
4	8/13/09	17.5	11.4	4.1	75.7
5	8/15/09	10.5	12.2	5.1	76.4
6	8/24/09	6.5	4.1	2.0	64.2

These values are many orders of magnitude lower than organic soil hydraulic conductivities reported by Quinton and Marsh [2001], which range from 100 to 100,000 cm/hr.

Green Ampt infiltration modeling results appear in Table 1. None of the storm events in 2008 or 2009 were able to produce runoff in a silt-loess with measured soil moisture (ie. precipitation rates never exceeded infiltration rates). Infiltration rates were greatest when the soils were driest, which is consistent with unsaturated zone flow modeling presented in Appendix A. Because this analysis did not consider the organic layer above the silts, precipitation rates likely over predict the amount and rate of water infiltrating the mineral soil. Even so, cumulative infiltration depths never exceeded 12 cm. These results therefore agree with the soil moisture logger data, indicating that storm events should not register in the deeper sensors. Consequently, mineral soils at depth have even lower conductivity, and thus act effectively as an aquitard, precluding water infiltration or movement through the seasonally-deepening thaw layer.

Discharge, uranium concentrations and UARs appear in Table 2. Tracer dilution indicates that the stream is always gaining water, and that the majority of inflows occur in the furthest downstream reaches (Figure 2), which are characterized by larger catchment sizes, surface streams, and associated topographic concavities and incision. While these 1st-order surface streams provide an observable hydrologic flux, the majority of inflow is through the subsurface. Uranium concentrations and UARs appear in Figure 5 and indicate significant shifts and mixing of at least three potential endmembers (identified in Figure 6). Uranium concentrations in the stream remain fairly stable with a mean around 1.2 ppb, but dropped to 0.6188 at the furthest downstream location. Effective inflow concentrations were always lower than stream concentrations, and showed a similar decrease with distance from the injection site.

Table 2: Discharge, uranium concentrations and UARs from the tracer experiments.

Site / Distance (m)	RT Discharge (L/s)	Surface Inflow Discharge (L/s)	U (ppb)	UAR ($^{234}U/^{238}U$)	Effective Inflow	U (ppb)	UAR ($^{234}U/^{238}U$)
0	2.10		1.2236	1.332			
20			1.2191	1.324			
73			1.2393	1.321			
173	2.93		1.2295	1.321	0.83	1.244	1.293
190		0.03	1.2690	1.289			
372	3.66		1.2269	1.331	0.74	1.217	1.372
493			1.2256	1.312			
726	5.03		1.2076	1.310	1.37	1.156	1.250
829	5.22		1.1904	1.313	0.19	0.736	1.471
855	5.27	0.05	1.9044	1.301			
932	6.66		1.1472	1.334	1.44	0.990	1.425
1015	9.43		0.6188	1.213	2.77		
1023		0.14	1.3498	1.223			

The lowest effective inflow concentrations occurred between sites 805 and 829. Generally, surface inflows had higher concentrations than the stream, with the large, downstream tributaries, RTST and RTBT displaying the highest concentrations. Uranium activity ratios displayed greater variability than U concentrations. Stream UARs were fairly constant, and displayed a large decrease at the furthest downstream end of the study reach. Effective inflow UARs were greater than stream UARs except between RT- 493 and RT-726. Inflow UARs were lower than the stream at RTTT and RTST, and higher than the stream at RTBT.

Runoff coefficients varied from 0.234 to 50.4 L/s/mm, suggesting a very large range in the stream response to storm events. Two convective thunderstorms, occurring on 6/30/08 and 7/1/08 were excluded from the analysis because they were more than an order of magnitude greater than the other runoff coefficients and skewed the statistical analysis of the rest of the data

set. It is likely that the convective nature of these events resulted in significant spatial variability, and that the skewness resulted from the several kilometer distance between the catchment and the precipitation gage. Runoff coefficients displayed significant positive correlation with soil moisture ($R^2 = 0.42$, $p < 0.01$) and a negative correlation with the day of the year ($R^2 = 0.56$, $p < 0.01$) (Figure 7).

Discussion

Hillslope Hydrology

Measured soil moisture and Green-Ampt modeling preclude the possibility that silt soils are a significant pathway of hillslope runoff. Soil moisture probes indicate that deeper mineral soils remain unsaturated throughout the summer, with a mean unsaturated hydraulic conductivity of 0.1 cm/hr. Shallow mineral soils are often drier, but they do respond to precipitation events, which leads to brief periods of higher hydraulic conductivity, although still well below the effective hydraulic conductivity of the organic soil. The fact that this response is not seen in moisture content or temperature at the deeper probes indicates that a wetting front has not reached these depths, and that matric flow potential remains very low compared to organic material, preferential/pipe flow, and surface water flow. Our Green-Ampt infiltration model ignores the thin, heterogeneous organic soil, thereby considering the greatest possible infiltration into the mineral soils. Even under such conditions, our results support the moisture content sensor data and show that infiltration into the mineral soils is minimal. The fact that mineral soils are usually drier at the surface than at depth implies an upward hydraulic gradient, which is likely related to the strong evapotranspiration potential caused by low relative humidity and high ecosystem activity in the organic soils and mosses [discussed further in Chapter 4]. Therefore,

even if water does infiltrate the mineral soil, it is likely to be lost back into the atmosphere rather than contributing to runoff.

Parafluvial Zone Processes

Results from the June and August, 2008 sodium bromide tracer injections indicate that the majority of inflows occur in the furthest downstream reach (Figure 2), which is also the reach with the largest surface water inflows. Coupled with the lack of hillslope runoff, the similarities between surface and effective inflow chemistry presented in Chapter 4, and the runoff model presented by Quinton and Marsh [1999], we suggest that the majority of this subsurface flow is associated with the saturated areas around surface water inflows. Streams account for 25 and 3% of the total inflow in June and August, respectively, which may signal a seasonal trend of increasing subsurface to surface flow. This is supported by major ion, δ^2H, and $\delta^{18}O$ values that indicate a seasonal evolution in surface water and total inflow chemistry [Chapter 4].

Runoff Coefficients

The direct correlation between runoff coefficients and soil moisture, and the inverse correlation to active layer depth provide information about rainfall/runoff hydrology in Richardson Catchment. Given soil moisture records and infiltration modeling data that assures us that this flow is not occurring in the mineral soils, we interpret these data as indicative of near-stream processes. For example, the relationship with soil moisture may indicate greater catchment hydrologic connectivity due to the increased accumulation area associated with higher tributary stage and a larger near-stream aquifer / hyporheic zone. The inverse relationship between runoff coefficients and the day of the year seems to indicate some increase in catchment storage potential. But, because we know this storage is not related to increasing thaw of hillslope mineral soils, we hypothesize that this trend indicates preferential flow in the near-stream

environment, most likely in sub-surface soil pipes that become active later in the year once the stream thaw bulb is more fully formed.

Uranium Concentrations and Isotope Ratios

There is significant variation in U concentrations in surface tributaries, total inflows, and even longitudinally in the main channel. Uranium isotope ratios are even more variable. We suggest that U can be used to indicate mineral soil contact and hillslope residence times, and that Richardson Tributary represents an integration of surface and subsurface inflows with varying topographically-derived signatures, as indicated in Figure 6.

Uranium concentrations at the upstream end of the stream are similar to the RTTT tributary. Both of these waters originate from the headwaters of the catchment and based on observations and elevated major ion loads, may be in contact with longer subsurface flowpaths that drain deeper mineral soils. Compared to this background level, we see inflow U concentrations are higher in surface waters than in the total inflows. Initially, this would appear counter-intuitive, but can be explained given the unique hydrology of this system. Surface water inflows in this catchment represent the hydrologically-connected near-stream portion of the watershed. Because this high-velocity water has eroded much of the organic layer, this fast flow occurs predominantly on top of the mineral soil, and so has greater interaction with the U source. Conversely, the subsurface flow is more likely to be distributed throughout the organic soils, precluding significant contact with the mineral soil and leading to low U concentrations. The furthest downstream sample displays a significant decrease in U concentration. Tracer dilution suggested that this is the largest inflow, and also represents a much larger contributing area than the upstream reaches. We believe that this signal represents precipitation that has not been

influenced by U. That is, this water has had a long organic soil residence time and has traveled through the drainage without much contact with the mineral soil.

Uranium activity ratio deviation from secular equilibrium stems from contact between water and sediments on a thousand year timescale. Given that residence times in this catchment range from hours to months, it is difficult to imagine that the elevated U ratios could indicate annual runoff processes. This signature must indicate movement of water that has emanated from deeper groundwater flowpaths, or represents a mixture of catchment runoff with thawing permafrost associated with channel incision or thermokarst features.

The regression of inverse U and UAR (Figure 6) allows us to infer mixing between water sources in Richardson Catchment. We assume that the farthest downstream samples represent precipitation that has had minimal contact with mineral soils. From this endmember, we can infer evolution towards observed stream or subsurface flows. The surface inflow with the lowest UAR represents stream water that has not experienced much fractionation, but has increased it's U load. We suggest that this represents mechanical weathering of mineral particles during stream transport, leading to higher concentrations of U, but the balance between the enriched water and the depleted grains results in an unchanged UAR. The other two streams show a similar entrainment signature, but with some level of UAR enrichment, as well. We argue that enrichment represents greater thermal or mechanical erosion of deeper sediments that contain an older and more-enriched UAR. RT-TT is known to flow through a large area of reworked silt, and may also emanate from a deep water flowpath (inferred from major ion chemistry and discussed in Chapter 4). Because RT-TT and RT-ST both fall on the same mixing line from precipitation, we believe that similar processes must be occurring in RT-ST as well. RT-ST displays the steepest slope of any of the streams and flows through at least one substantially

slumping hillslope. This combination of chemistry and physical factors suggest that RT-ST may be experiencing soil piping.

Our uranium data provide evidence of substream soil pipes and add credence to theories that pipes are an early indicator of rapid geomorphologic change. The presence of pipes in the parafluvial zone is consistent with the fact that pipes tend to occur in ice rich soil zones [*Carey and Woo*, 2002]. Piping in some streams and not others may be related to differences in slope, which must be greater than a certain threshold to promote piping (> 10˚ according to Quinton and Marsh [1998]). While pipes have been associated with slope failure in the past, it remains unclear whether they were a driver or consequence of major landscape change [Jenkins 1988]. The use of U and UAR provides evidence that soil piping may occur prior to slope failure, thus suggesting that pipes are a cause, and not a result of catchment evolution.

Our data provide compelling evidence that rainfall/runoff hydrology in the silt-dominated permafrost-bound catchments of interior Alaska is dependent on near-stream hydrologic connectivity and independent of moisture content or active layer depth in the hillslope mineral soils. Moisture content shows that silts are typically unsaturated (Figure 4), and therefore incapable of rapidly conducting water, especially in mid-summer, when evapotranspiration rates are likely at their maximum. Despite the fact that silts act as an aquitard, runoff coefficients correlate to directly to soil moisture and inversely with active layer depth, similar to observations in several other studies [*Jones and Rinehart, in press*], [*Wang, et al.*, 2009]. We argue that these correlations indicate processes occurring in the parafluvial zone, where soils are likely to stay saturated long after hillslopes dry out due to saturated conditions in the organic layer. U concentrations and UARs indicate different amounts of soil/water interactions among inflows, suggesting the potential for soil piping and thermokarsting in certain areas of the drainage.

Implications

Our new conceptual model (Figure 8) presents a view of boreal catchment runoff that focuses on topographic lows and the parafluvial environment. Our data show that surface flows are often representative of the inflow pathways, but only account for a fraction of the total flow. Flow is dominated by subsurface movement through the organic soils, and may be associated with soil pipes, which maintain high hydraulic conductivities and short hillslope residence times. As the season progresses the proportion of water moving through the subsurface increases, perhaps signaling greater importance of soil pipes that have thawed to a greater extent.

We propose that silt-dominated boreal catchments act much more like flumes than aquifers. High hydraulic conductivities of the organic material and a shallow confining unit allow water to quickly accumulate in topographic lows. This could lead to greater latitudinal hydrologic connectivity along the tributaries, and a smaller fraction of connectivity in the majority of the watershed relative to systems with deeper flowpaths.

Small streams have been implicated as disproportionately important to biogeochemical processes in terrestrial systems [*Mulholland, et al.*, 2008; *Peterson, et al.*, 2001] and in boreal catchment terrestrial DOC export [*Ãgren, et al.*, 2007], and this work expands their role as indicators of substantial subsurface flow and potential for piping and thermokarsting. Despite their critical role, the streams in this study are not delineated on the 1:63,360 topographic maps produced by the US Geological Survey, suggesting the need for greater mapping refinement, especially in high-latitude regions where a greater understanding of ecosystem potential is crucial in light of potential for biogeochemical activity [Chapter 4] and changes due to climate warming.

This work may also inform terrestrial ecosystem studies in the silt-dominated catchments of interior Alaska and elsewhere. Given soil moisture data and infiltration modeling that identify the shallow depth to which precipitation penetrates and the rapidity with which these same soils dry, we can narrow our focus on the dominant locations of catchment ecosystem processes. Our work identifies these shallowest soils as critically important to water cycling. And given that ecosystem productivity in boreal systems is so often water-limited (Wickland and Kelsey, unpublished), we imagine that this same zone is critically important to carbon cycling as well.

Conclusion

Our data lead to the creation of a new conceptual model that highlights topographic depressions, parafluvial flow, and preferential flow through subsurface soil pipes to explain catchment runoff. Our new conceptual model has implications for considering carbon transport and storage in boreal catchments. Many previous conceptual models correlate deepening active layers to greater hydrologic connectivity and transport through thawed area. In the silt-dominated catchments of interior Alaska, we see that the correlation between active layer and hydrologic connectivity is indicative of near-stream hydrology. The near-stream environment has been recognized as an important location of biogeochemical activity, and this work provides evidence of its importance to hydrology and geomorphology, too.

Acknowledgements

This work was supported by NSF grant OCE-BE 0628348 and NRC postdoctoral award to S. Ewing. We thank Jim Paces for assisting with the U isotope analysis.

References

Ãgren, A., et al. (2007), Importance of seasonality and small streams for the landscape regulation of dissolved organic carbon export, *Journal of Geophysical Research G: Biogeosciences*, *112*.

Brosten, T. R., et al. (2006), Profiles of temporal thaw depths beneath two arctic stream types using ground-penetrating radar, *Permafrost and Periglacial Processes*, *17*, 341-355.

Carey, S. K., and M.-K. Woo (2002), Hydrogeomorphic relations among soil pipes, flow pathways, and soil detachments within a permafrost hillslope, *Physical Geography*, *23*, 95-114.

Carey, S. K., and M. K. Woo (2000), The role of soil pipes as a slope runoff mechanism, Subarctic Yukon, Canada, *Journal of Hydrology*, *233*, 206-222.

Carey, S. K., and M. K. Woo (2001), Slope runoff processes and flow generation in a subarctic, subalpine catchment, *Journal of Hydrology*, *253*, 110-129.

Chow, V. T., et al. (1988), *Applied Hydrology*, McGraw-Hill, Inc., New York.

DePaolo, D. J., et al. (2006), Sediment transport time measured with U-series isotopes: Results from ODP North Atlantic drift site 984, *Earth and Planetary Science Letters*, *248*, 379-395.

Dingman, S. L. (1994), *Physical Hydrology*, Prentice Hall, New Jersey.

Dixon, R. K., et al. (1994), Carbon pools and flux of global forest ecosystems, *Science*, *263*, 185-190.

Kigoshi, K. (1971), Alpha-recoil thorium-234: Dissolution into water and the uranium-234/uranium-238 disequilibrium in nature, *Science*, *173*, 47-48.

Merz, R., et al. (2006), Spatio-temporal variability of event runoff coefficients, *Journal of Hydrology*, *331*, 591-604.

Mulholland, P. J., et al. (2008), Stream denitrification across biomes and its response to anthropogenic nitrate loading, *Nature*, *452*, 202-205.

Peterson, B. J., et al. (2001), Control of nitrogen export from watersheds by headwater streams, *Science*, *292*, 86-90.

Petrone, K. C., et al. (2007), The influence of fire and permafrost on sub-arctic stream chemistry during storms, *Hydrological Processes*, *21*, 423-434.

Prokushkin, A. S., et al. (2005), Climatic factors influencing fluxes of dissolved organic carbon from the forest floor in a continuous-permafrost Siberian watershed, *Canadian Journal of Forest Research-Revue Canadienne De Recherche Forestiere*, *35*, 2130-2140.

Quinton, W. L., and P. Marsh (1998), The influence of mineral earth hummocks on subsurface drainage in the continuous permafrost zone, *Permafrost and Periglacial Processes*, *9*, 213-228.

Quinton, W. L., and P. Marsh (1999), A conceptual framework for runoff generation in a permafrost environment, *Hydrological Processes*, *13*, 2563-2581.

Risse, L. M., et al. (1994), Determining the Green-Ampt effect hydraulic conductivity from rainfall-runoff data for the WEPP model, *Transactions - American Society of Agricultural Engineers*, *37*, 411-418.

Striegl, R. G., et al. (2005), A decrease in discharge-normalized DOC export by the Yukon River during summer through autumn, *Geophysical Research Letters*, *32*.

Walvoord, M. A., and R. G. Striegl (2007), Increased groundwater to stream discharge from permafrost thawing in the Yukon River basin: Potential impacts on lateral export of carbon and nitrogen, *Geophysical Research Letters*, *34*.

Wang, G., et al. (2009), The influence of freeze-thaw cycles of active soil layer on surface runoff in a permafrost watershed, *Journal of Hydrology*, *375*, 438-449.

Figure 1: A) Map of Alaska with the star indicating the location of the contour map. B) Map of the study area with 10 m contours. The line represents Richardson Tributary, a 2nd – order stream. Small ircles indicate perennial 1st - order tributaries. Stars represent the locations of flumes. Large circles represent soil moisture and soil temperature sensors.

A)

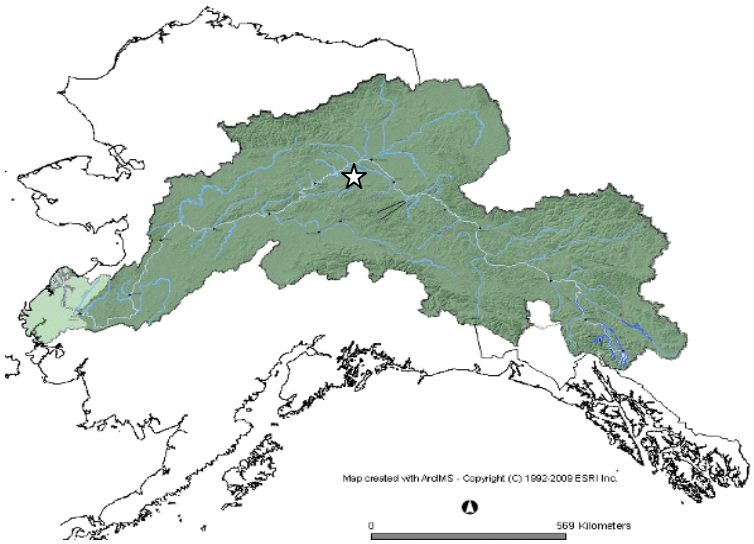

B)

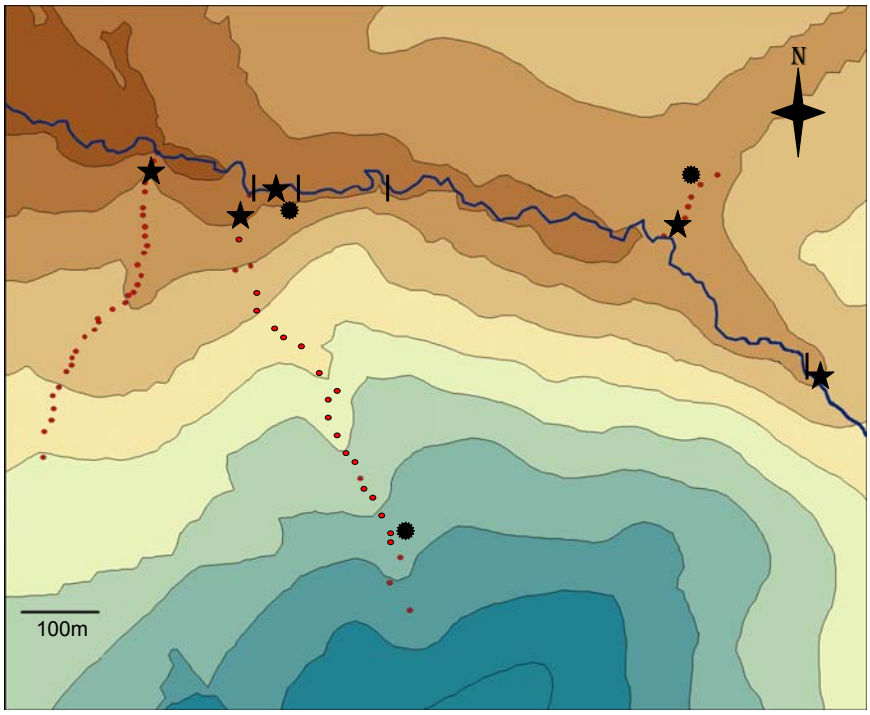

Figure 2: Discharge, as a percentage of total discharge measured at the downstream end of the study reach for two sodium bromide injections from Chapter 4.

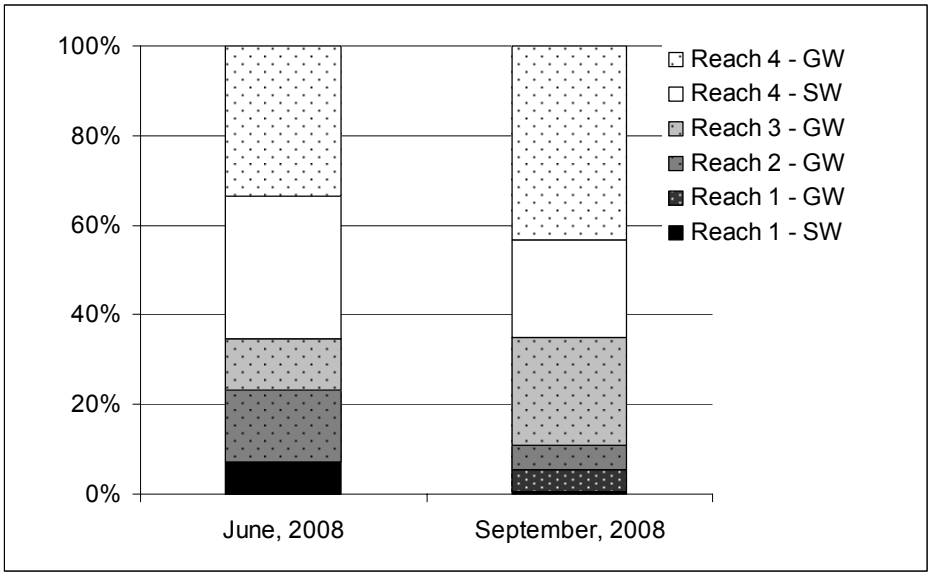

Figure 3: Precipitation from the Hess Creek Gage, located approximately 1.5 km from the center of the catchment., and discharge records from the downstream Richardson Tributary gaging station during the summers of 2008 and 2009.

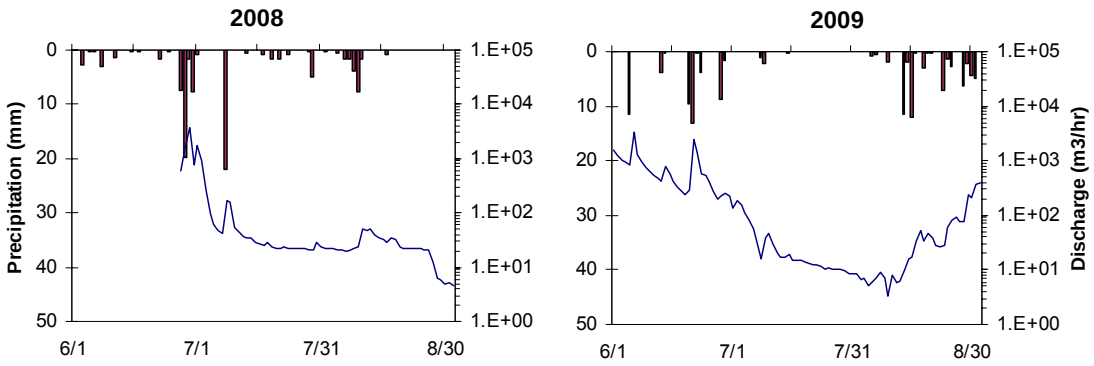

Figure 4: Volumetric soil moisture from loggers at two depths in A) 2008 and B) 2009. For a silt-loess soil, 0.40 to 0.45 represents saturation, which is only approached by the shallow soils early in the summer.

A)

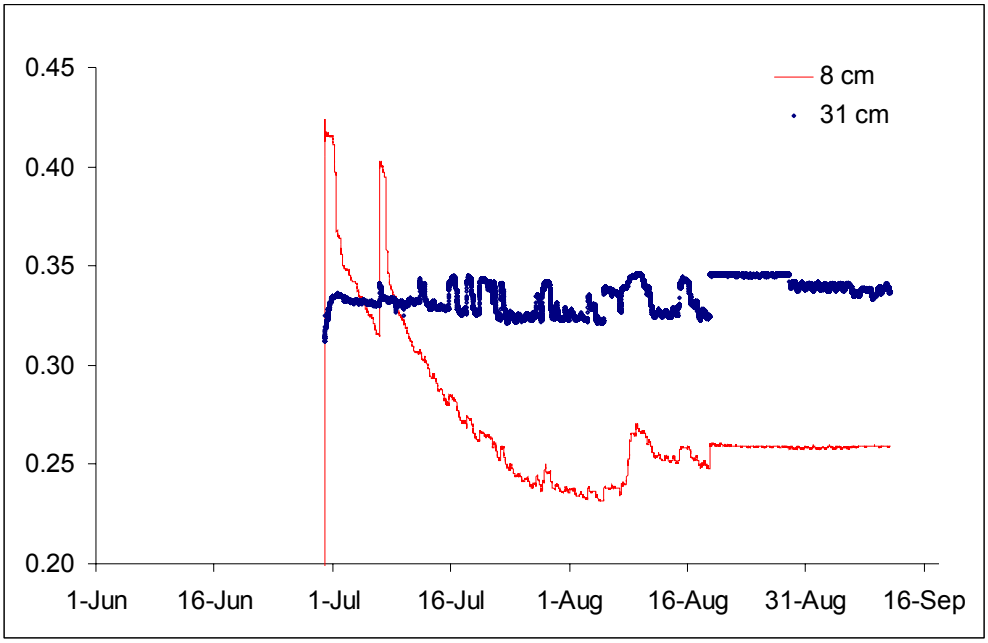

B)

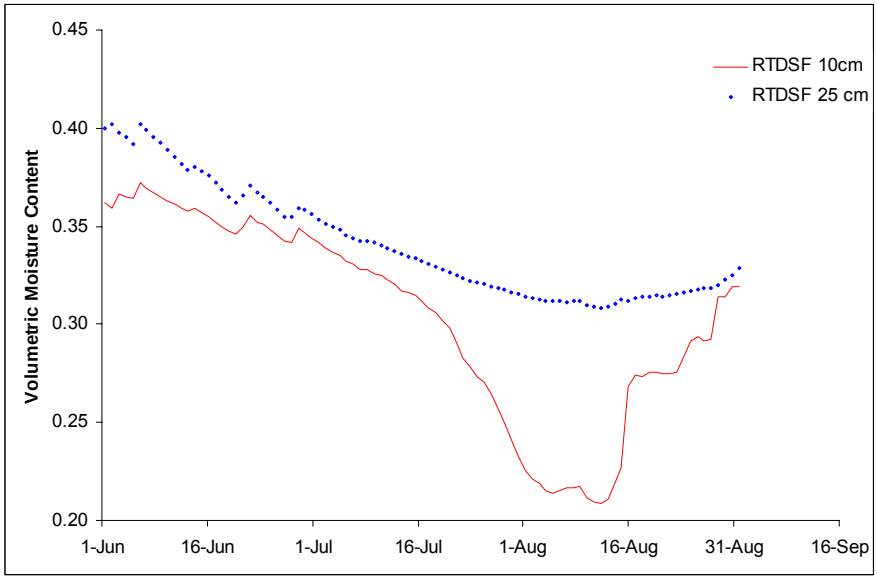

Figure 5: Uranium concentrations and ratios vs. distance along the stream reach. Streamflow and surface inflow values were measured, and effective inflow values were calculated given upstream, downstream, and surface inflow values.

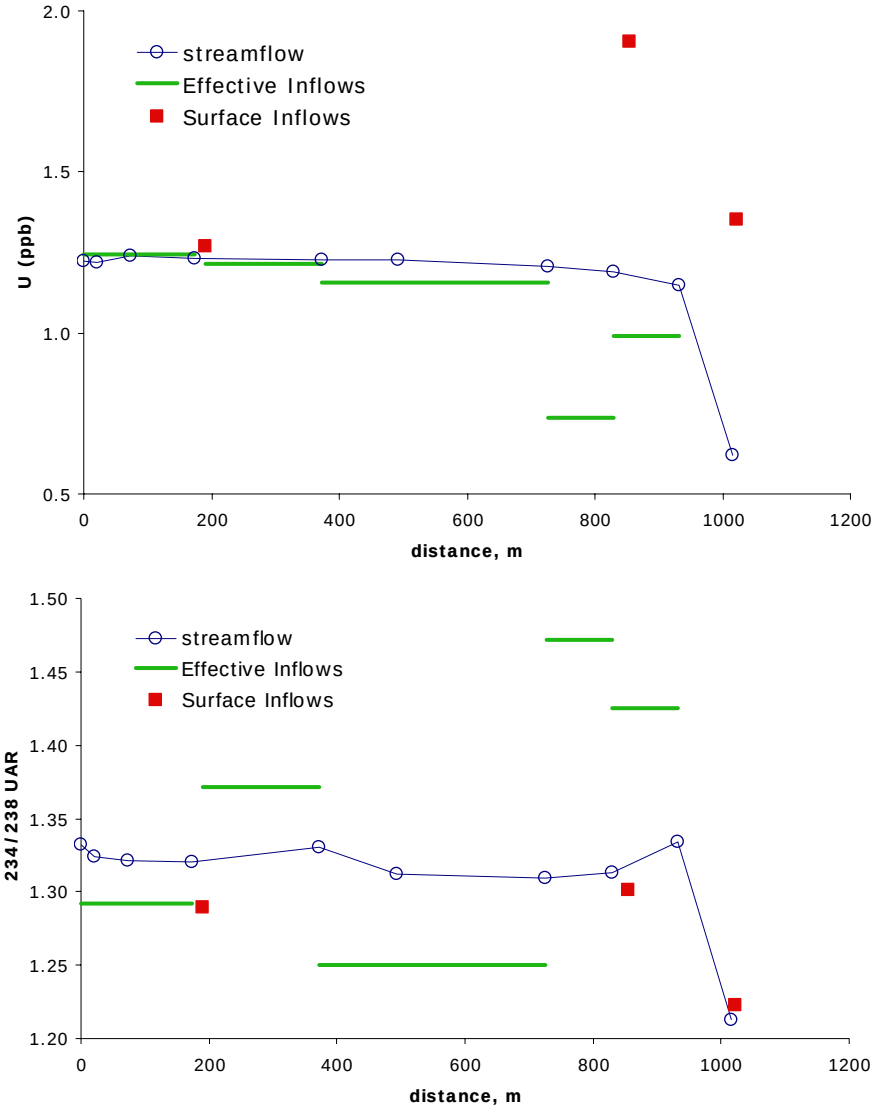

Figure 6: Ratios of $^{234}U/^{238}U$ in this small headwater catchment have evolved from a precipitation signal, which would have low U and low UAR. Higher concentrations with no isotopic enrichment in ^{234}U represent physical weathering of silt grains. Isotopic enrichment indicates contact between water and mineral soils, which is a function of residence time and contributing area. The dashed line represents one possible evolution pathway that very nearly describes two of the surface streams. One of these streams is known to have high soil/water contact due to active thermokarsting. The second has higher U concentrations and is characterized by a high slope, and slumping banks. This second stream seems like a potential location of soil piping.

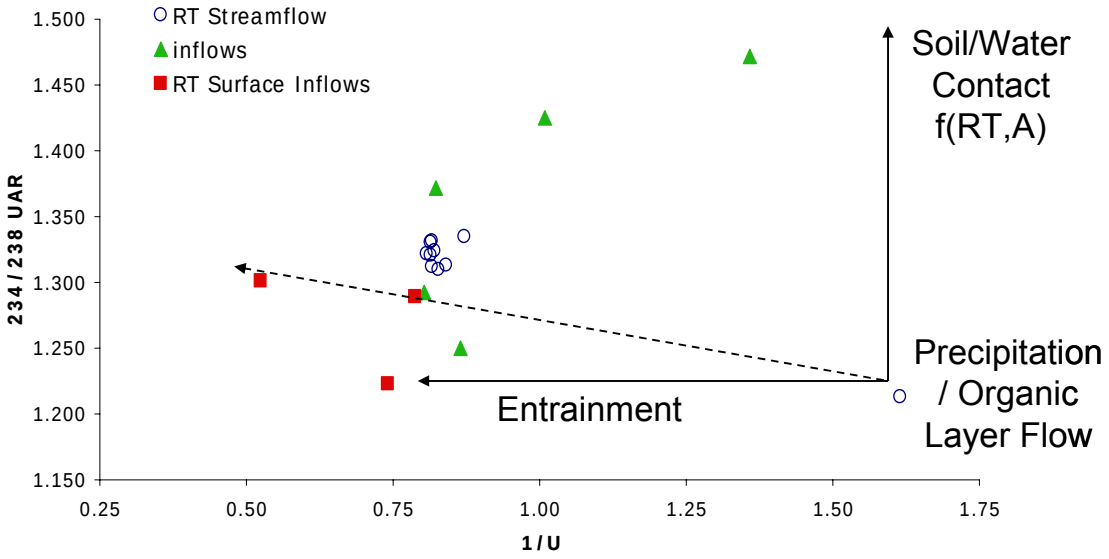

Figure 7: Runoff coefficients and for the summers of 2008 and 2009. Runoff coefficients displayed significant ($p < 0.01$) correlations to volumetric soil moisture and active layer depth.

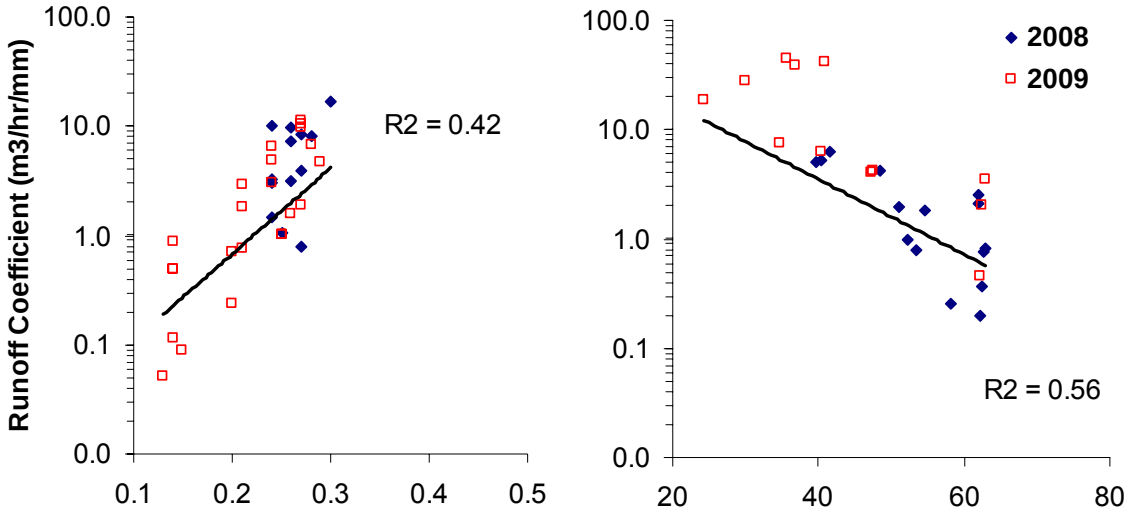

Figure 8: Conceptual model of subsurface hydrology in the silt-dominated catchments of Alaska. The water table is perched on top of the silt, and the interactions with the organic soil is highly dependent on stream stage. There is some amount of preferential flow through soil pipes beneath the stream, as evidenced by the uranium data. Precipitation that falls on the hillslope is generally lost to evapotranspiration, while precipitation near that infiltrates in the wetter area near the stream is more likely to runoff.

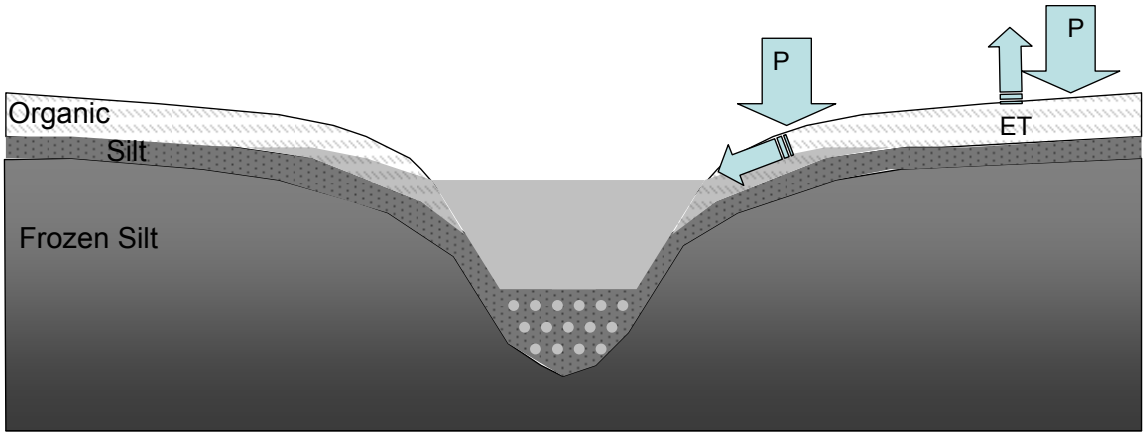

CHAPTER 6: CONCLUSION

Critical hydrologic thresholds in high-latitude catchment ecosystems

Abstract

In polar systems, hydrology and energy are tightly coupled. During the short polar summers, stream discharge is flashy, with hydrographs that can vary by orders of magnitude on hourly timescales. This variability is related to frozen soils and surface snow and ice, which may melt at higher temperatures and contribute to stream discharge, but also preclude significant subsurface water storage. In temperate and boreal systems, low-order streams are disproportionately important to biogeochemistry due to the high interactions between stream water and sediments, while larger rivers are viewed primarily as exporters – transporting water and solutes from reaction sites. Here we present hydrologic and biogeochemical data from a boreal arctic stream and a sub-polar Antarctic stream that provides evidence that individual streams may shift from reactors to exporters and vice versa depending on discharge. Such shifts are dependent on the relationship between flooding and stream catchment interactions, which can be linked in these two systems to geology and geomorphology. We identify critical discharge thresholds that cause these shifts, and consider how these relationships might change given climate warming. We hypothesize that these dynamics are particular to polar systems, because of the normally flashy discharge and short growing seasons that favor organisms capable of thriving in rapidly changing conditions.

Introduction

Water is a critical requirement of life on Earth. While water is necessary for metabolic processes, it is seldom available in the ideal form or quantity. This disparity is greater near the Earth's poles, leading to ecosystems that are increasingly water limited. The lack of polar water stems from several physical mechanisms that result in decreased liquid water sources and shorter catchment residence times. The high angle between the sun and the atmosphere in polar environments leads to less incoming shortwave radiation per area, and subsequently decreased atmospheric energy. This correlates to decreased precipitation and greater aridity. The low relative humidity also increases the potential for water on the landscape or in soils to be lost to evaporation. Low solar input energy also leads to low temperatures and a greater potential for water to exist in the solid phase. Ice is generally not accessible by organisms for metabolic purposes. Ice on the land or in soils precludes storage of liquid water, thereby increasing runoff and decreasing catchment residence times. During warmer periods, melting ice may contribute to streamflow, often leading to flooding. Permafrost-bound catchments tend to display flashy stream hydrographs, because of both the low storage potential and high melting capacity of liquid water.

Decreased precipitation, high evaporation rates, and flashy hydrographs present a "feast or famine" situation for high latitude ecosystems. Either there is no water, there is so much water that critical dissolved organic matter and nutrients are flushed from catchments before they can be utilized, or the organisms themselves are scoured from surfaces by the floods [*Holmes, et al.*, 1998]. Life has adapted in many ways to exist with limited water, to decrease metabolic function until water is readily available [*McKnight, et al.*, 1999], or to manipulate conditions in order to get or store water. Evidence abounds of life thriving in extremely cold and arid

conditions near the poles, with the recognition that a constant water supply is a necessity [*Alger, et al.*, 1997], and a steady water supply promotes species diversity [*Esposito, et al.*, 2006]. Similarly, intermediate soil moisture conditions are required for heightened rates of aerobic biogeochemical processes (Figure 1). These dynamics are very similar to semi-arid ecosystems, except that in sub-polar systems transmission losses are precluded by the presence of subsurface permafrost, or in the case of Alaska, a glacially-derived silt aquitard.

The smallest streams are disproportionately important to stream ecosystem function [*Mulholland, et al.*, 2008a; *Peterson, et al.*, 2001] As stream size increases, the interactions between water and sediments decrease [*Harvey and Wagner*, 2000], and streams become transporters rather than bioreactors, integrating the chemical signature of processes occurring in the smaller watersheds. Therefore rivers can be used to indicate catchment/watershed/basin ecosystem function. Brookshire et al [2009] argue that the majority of streams display in-stream nutrient cycling, leading to longitudinal evolution of stream chemistry as downstream ecosystems adjust to inefficiencies and nutrient loss from upstream systems. Wollheim et al. [2001] found that physical properties dominated over biogeochemical in controlling the chemical signature of a stream.

This work addresses the factors that control catchment residence time, storage, transport, and exchange in two polar drainages (Figure 2), and attempts to link these physical processes to biogeochemical activity in the water and the adjacent terrestrial ecosystem. While these two systems are different in terms of their location, water sources, geology, watersheds, and vegetation, their similarities in climate and rapid hydrologic flux provide an interesting comparison that sheds light on the fundamental controls on high-latitude ecosystems. We hypothesize that catchment water flux is a primary control on ecosystem productivity, and that

flashy hydrographs in polar regions result in streams with a unique ability to switch from exporters to bioreactors and vice versa. We test this hypothesis by considering physical changes in catchment connectivity and stream-catchment interactions in two high-latitude catchments. We provide chemical evidence that these physical changes result in altered biogeochemical cycling rates and processes.

Results/Discussion

Low-order streams in both coastal Antarctica and interior Alaska are subject to flooding, which alters hydrologic pathways, and results in measureable changes and trends in C and N species and reactivity.

DOM sources

In the McMurdo Dry Valleys, discharge variation occurs on a diel timescale, leading to higher stage and increased contact between stream water and sediments in channelized reaches, and a substantial increase in storage area and exchange rates in the anabranching reach. These heightened hyporheic dynamics lead to measureable increases in downstream DOC and denitrification rates. Figure 3 displays the increased DOC and N-species following flood pulses, and also shows the subsequent rapid assimilation of the pulse in the downstream reaches.

We hypothesize that maximum ecosystem benefit occurs when discharge exceeds the threshold necessary to leach DOM from the large overflow storage zones, but remains low enough to avoid significant transport limitation associated with flood wave velocities. A previous tracer in this same stream [*Runkel, et al.*, 1998] witnessed a much higher discharge, and much lower exchange rates and storage areas in the zone, than quantified in Chapter 2. Our study also notes that higher discharges can be expected in Huey Creek once the storage capacity

of the anabranching reach is overwhelmed. At this point, exchange rates may decrease rapidly, precluding the delivery/leaching of solutes to/from sediments. Furthermore, higher discharges and subsequent high velocities may exacerbate transport limitation. Concurrently, if discharge does not exceed the 65 m^3/hr threshold identified in Chapter 2, the large storage area will never fill, and the sediments cannot be fully flushed.

In interior Alaska, flooding is a result of precipitation events and rapid runoff through organic material and on top of a silt aquitard. These events leach DOM from the organic material, leading to a strong correlation between discharge and DOC and nitrate, which indicates that stream-catchment interactions and subsequently DOM flushing are directly proportional to discharge (Figure 4A). These dynamics are witnessed in the second-order Richardson Tributary, but are likely indicative of processes occurring in the first-order and ephemeral streams, because Richardson Tributary is incised and does not come in contact with floodplain/riparian organic material [Chapter 4].

C and N decay rates and synoptic concentrations in Richardson Tributary and its inflows suggest there is a switch from streams dominated by nutrient cycling to a stream characterized by export. We can see the evolution of this trend in the June, 2008 inflow concentrations, where nitrate concentrations – our proxy for ecosystem activity – increase in larger inflows. Further evidence comes from the decoupling of the discharge – DOC and nitrate relationship in Richardson Tributary at the lowest flows (Figure 4B). Usually, RT is an exporter. But at very low discharges nitrate is lost, and DOC concentrations are extremely high, suggesting autochthonous activity. Given this information we can identify a discharge threshold at which transport limitation dominates, precluding in-stream productivity.

Hydrologic Events and Soil Moisture

The flashy hydrographs and subsequent limited water availability in high latitude systems may enhance the importance of a regular precipitation/flood return interval to sustain soil moisture and biogeochemical activity. Intermediate levels of water-filled pore space have been found to lead to the highest respiration rates [*Linn and Doran*, 1984; *Lohse, et al.*, 2009] (Figure 1). In polar systems where water fluxes are high and storage is low, this balance is hard to achieve. Daily flood pulses in the McMurdo Dry Valleys may enhance ecosystem productivity by creating a larger zone of moist sediments, where both oxygen and water are available. This should lead to higher productivity than sustained high discharges, which more fully saturate sediments, thereby decreasing oxygen availability needed for high respiration rates. Interior Alaska would seem less favorable to ecosystem activity, because flood return intervals are less regular, leading to large extremes in soil water content, and only brief intervals at the optimal conditions. These extremes are buffered to some extent by the potential for the silt to hold some amount of water that is available for transpiration.

Geologic/Geomorphic Legacies

Findings from both Antarctica and Alaska provide evidence of the importance of geologic legacies on controlling hydrology and biogeochemical reactions. In both of these systems, permafrost precludes deeper flowpaths that may contribute altered chemistry or greater flood buffering capacity, either through increased storage or constant baseflow. The location of water in these systems is dictated by topography. In Antarctica this is related to the presence of shallow permafrost and the formation of the channel where glacial melt erodes the permafrost. A slope break near the valley floor leads to branching, playas, and pools in many of the MDV streams that has significant consequences for water storage, [Chapter 2] heat and solute transport [Cozzetto, personal communication], [*Joslin*, 2005] and biogeochemistry [Chapter 3]. In Alaska

the tendency of water to follow topography is related to the silt aquitard, and the potential for thermal erosion of this layer on steep slopes, and near water-gathering features such as depressions. This topographic control of water flow provides a predictive method for identifying saturated areas with heightened biogeochemistry and geomorphology in the high-latitude landscape.

Climate Change Implications

Geomorphologic change due to channel incision and thermokarsting may significantly affect stream ecosystems. Both interior Alaska and the McMurdo Dry Valleys display recent and significant channel geomorphology. Richarsdon Tributary flows several meters below the floodplain due to channel incision that may be related to a recent fire and/or to climate warming. Regardless of the cause, the result is a stream that is significantly shaded by tall stream banks and disconnected from the terrestrial ecosystem. Pre-incision, this stream likely interacted with its floodplain in a similar fashion to the interactions of the first order tributaries. Now, the stream is truly a drain. It is several meters below the phreatic aquifer, incapable of pushing water back up the slope, and thereby removing any potential interaction with biogeochemicallt-active organic soils. Pre-incision, flood events in Richardson Tributary may have increased stream/catchment interactions and promoted ecosystem activity following models presented by Junk et al. [1989], Holmes et al. [1998] and in Chapter 2. Now, floods simply increase stream stage, leading to higher discharge velocities, but only minimal exchange with subsurface water [Appendix A].

There is some evidence that McMurdo Dry Valley ecosystems may be experiencing thermal alteration and channel incision similar to what has been witnessed in interior Alaska. In Garwood Valley, Antarctica, a stream has recently incised into its bed, and now resides

approximately 50 m below the valley fill level, whereas before it flowed along the surface. This stream now receives minimal direct sunlight, and flows through a subterranean cavern. Soil pipes identified beneath Von Guerard Stream in Taylor Valley [Cozzetto, 2009] indicate the potential for stream advection of heat into the subsurface and subsequent thermal erosion in a stream with no visible signs of instability. Because the Dry Valleys have not experienced any fire activity, it seems more likely that these effects are a direct result of a changing climate.

Conclusion

Low-order catchments in the Richardson Tributary and in the McMurdo Dry Valleys of Antarctica are both characterized by ephemeral hydrologic fluxes and minimal storage potential. These factors are related to the tight coupling water and heat in polar systems, and exert substantial control on ecosystems: High discharges increase leaching and export of DOM and nutrients, whereas lower discharges may lead to higher ecosystem productivity. Both of these systems show evidence of stream morphology related to thermokarsting, which may decrease ecosystem productivity by removing the potential for stream/catchment interactions.

References

Alger, A. S., et al. (1997), Ecological processes in a cold desert ecosystem: the abundance and species of algal mats in glacial meltwater streams in Taylor Valley, Antarctica, *Institute of Arctic and Alpine Research, Occasional Paper 51*, 108.

Brookshire, E. N. J., et al. (2009), Maintenance of terrestrial nutrient loss signatures during in-stream transport, *Ecology*, *90*, 293-299.

Cozzetto, K. (2009), Dissertation, University of Colorado, Boulder.

Esposito, R. M. M., et al. (2006), Antarctic climate cooling and response of diatoms in glacial meltwater streams, *Geophysical Research Letters*, *33*.

Harvey, J. W., and B. J. Wagner (2000), Quantifying hydrologic interactions between streams and their subsurface hyporheic zones, in *Streams and Ground Waters*, edited by J. B. Jones and P. J. Mulholland, Academic Press, San Diego.

Holmes, R. M., et al. (1998), The impact of flash floods on microbial distribution and biogeochemistry in the parafluvial zone of a desert stream, *Freshwater Biology*, *40*, 641-654.

Joslin, J. C. (2005), Determining the role of chemical weathering reactions and hyporheic exchange on silicate concentrations in Dry Valley streams, Antarctica, University of Colorado, Boulder, CO.

Junk, W. J., et al. (1989), The Flood Pulse Concept in River-Floodplain Systems, paper presented at Proceedings of the International Large River Symposium, Can. Spec. Publ. Fish. Aquat. Sci.

Linn, D. M., and J. W. Doran (1984), Effect of water-filled pore space on carbon dioxide and nitrous oxide production in tilled and nontilled soils, *Soil Science Society of America Journal*, *48*, 1267-1272.

Lohse, K. A., et al. (2009), Interactions between biogeochemistry and hydrologic systems, *Annu. Rev. Environ. Resour.*, *34*, 65-96.

McKnight, D. M., et al. (1999), Dry valley streams in Antarctica: Ecosystems waiting for water, *Bioscience*, *49*, 985-995.

Mulholland, P. J., et al. (2008), Stream denitrification across biomes and its response to anthropogenic nitrate loading, *Nature*, *452*, 202-205.

Peterson, B. J., et al. (2001), Control of nitrogen export from watersheds by headwater streams, *Science*, *292*, 86-90.

Runkel, R. L., et al. (1998), Analysis of transient storage subject to unsteady flow: diel flow variation in an Antarctic stream, *Journal of the North American Benthological Society*, *17*, 143-154.

Wollheim, W. M., et al. (2001), Influence of stream size on ammonium and suspended particulate nitrogen processing, *Limnology and Oceanography*, *46*, 1-13.

Figure 1: Soil microbial processes are dependent on proper moisture content. Aerobic activity is enhanced by intermediate soil water contents (from Lohse et al. 2009).

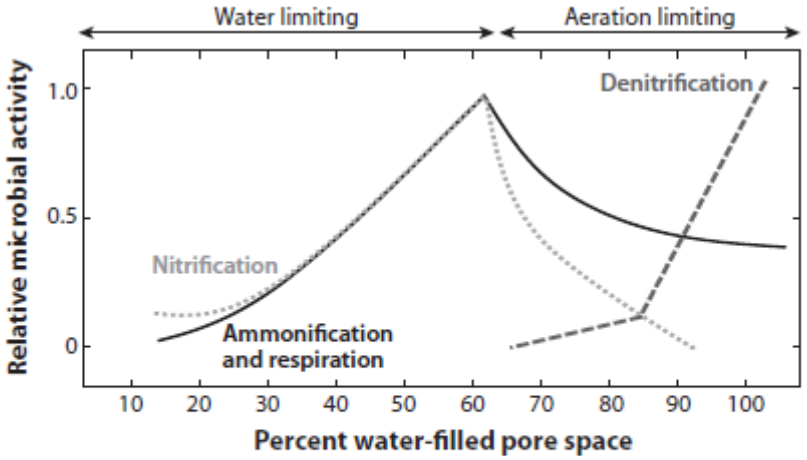

Figure 2: Site Locations in A) Antarctica and B) Alaska. Pictures from both systems illustrate the significant differences in watershed properties. The systems are similar in the ephemeral nature of hydrologic fluxes and minimal subsurface water and solute storage potential.

A)

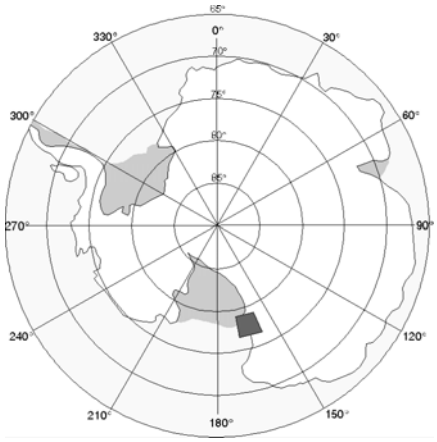

B)

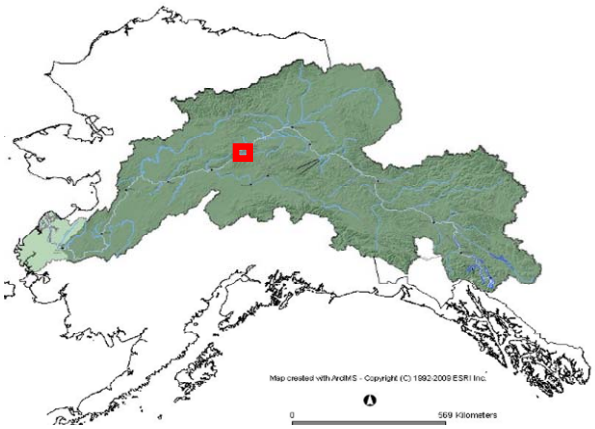

Figure 3: Trends in reactive solutes in Huey Creek are dependent on discharge. A) DOC is utilized as it moves downstream. A large pulse of DOC emanates from the anabranches at low flows and is quickly utilized. B) Solutes are most reactive during high flows. Li+ changes indicate sediment/water interactions, while N – cycling generally results in reduction of nitrate and nitrite, and production of ammonium and nitrous oxide.

A)

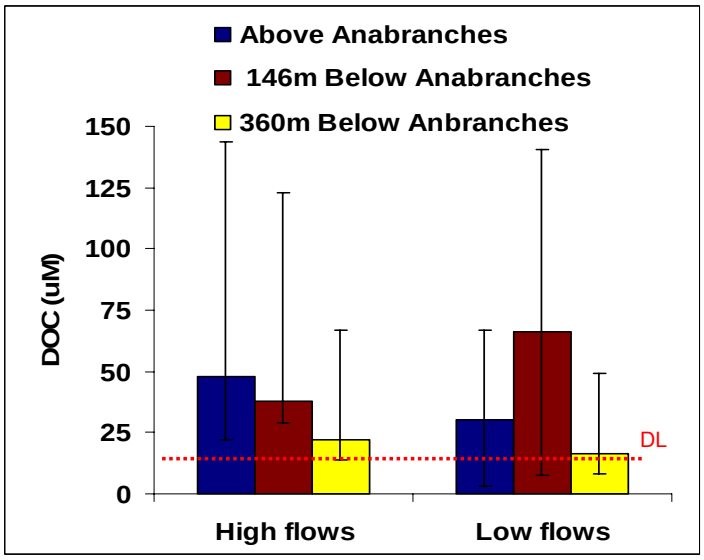

B)

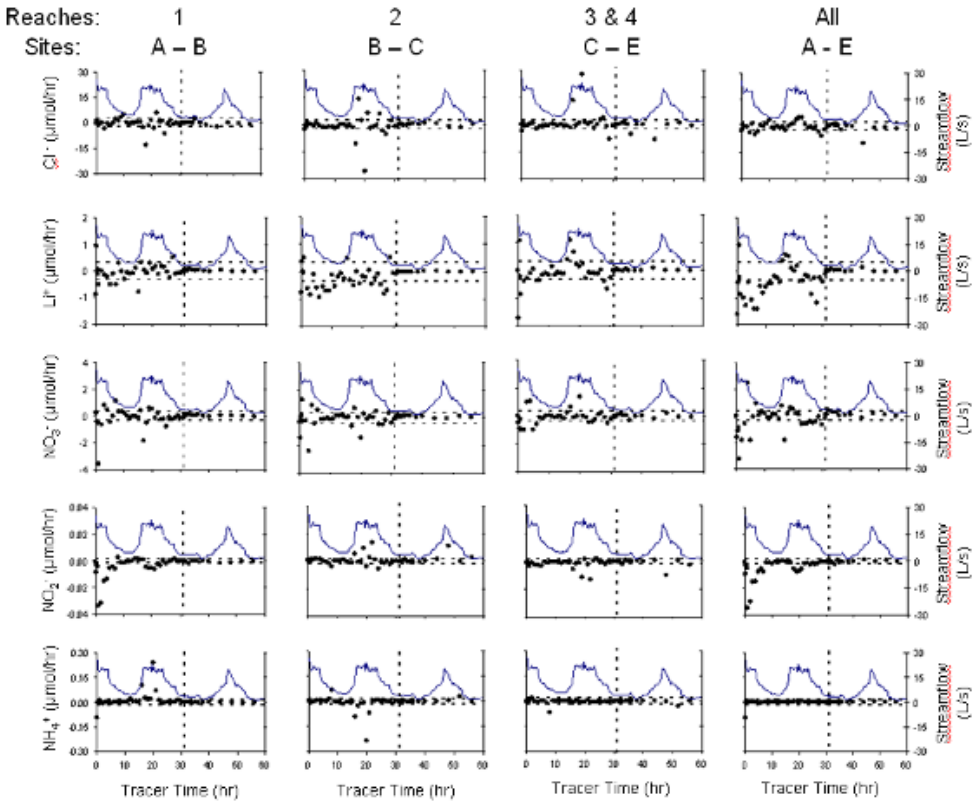

Figure 4: A) Significant correlation between discharge and DOC and nitrate in Richardson Tributary, Alaska. B) A shift in the relationship between DOC and nitrate indicates nitrate limitation at the lowest streamflows (open diamonds) in Richardson Tributary.

A)

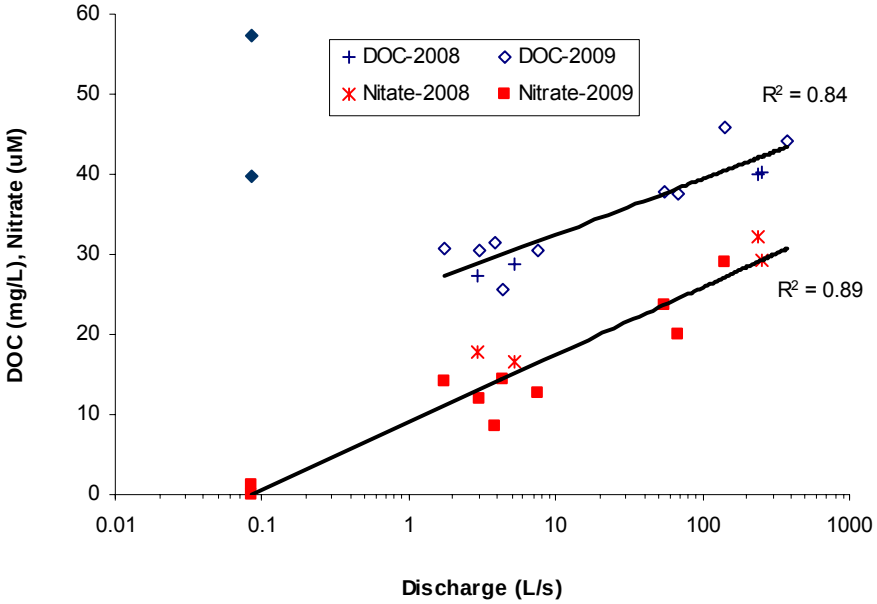

B)

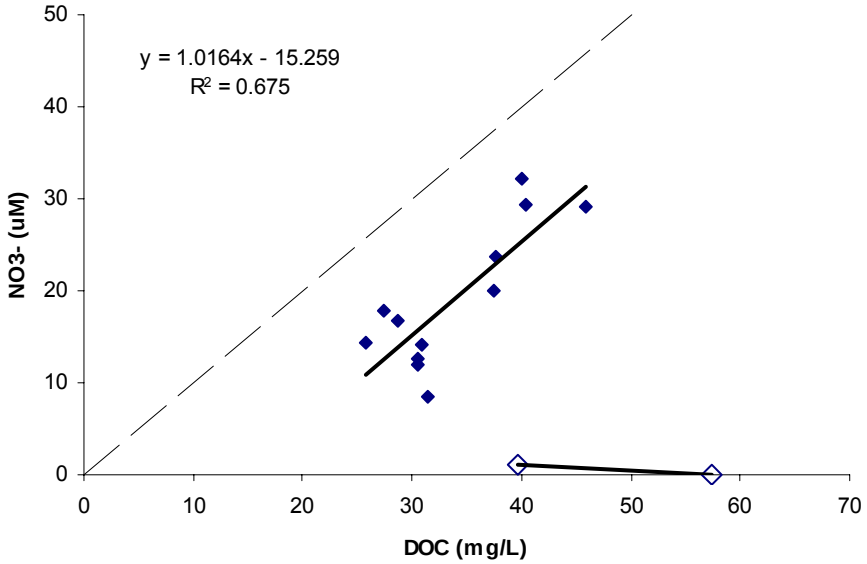

BIBLIOGRAPHY

Ãgren, A., et al. (2007), Importance of seasonality and small streams for the landscape regulation of dissolved organic carbon export, *Journal of Geophysical Research G: Biogeosciences*, *112*.

Alger, A. S., et al. (1997), Ecological processes in a cold desert ecosystem: the abundance and species of algal mats in glacial meltwater streams in Taylor Valley, Antarctica, *Institute of Arctic and Alpine Research, Occasional Paper 51*, 108.

Bencala, K. E., and R. A. Walters (1983), Simulation of Solute Transport in a Mountain Pool-and-Riffle Stream - a Transient Storage Model, *Water Resources Research*, *19*, 718-724.

Boano, F., et al. (2007), Bedform-induced hyporheic exchange with unsteady flows, *Advances in Water Resources*, *30*, 148-156.

Brookshire, E. N. J., et al. (2009), Maintenance of terrestrial nutrient loss signatures during in-stream transport, *Ecology*, *90*, 293-299.

Brosten, T. R., et al. (2006), Profiles of temporal thaw depths beneath two arctic stream types using ground-penetrating radar, *Permafrost and Periglacial Processes*, *17*, 341-355.

Brunke, M., and T. Gonser (1997), The ecological significance of exchange processes between rivers and groundwater, *Freshwater Biology*, *37*, 1-33.

Burkins, M. B., et al. (2001), Organic carbon cycling in Taylor Valley, Antarctica: quantifying soil reservoirs and soil respiration, *Global Change Biology*, *7*, 113-125.

Cardenas, M. B., et al. (2004), Impact of heterogeneity, bed forms, and stream curvature on subchannel hyporheic exchange, *Water Resources Research*, *40*.

Carey, S. K. (2003), Dissolved organic carbon fluxes in a discontinuous permafrost subarctic alpine catchment, *Permafrost and Periglacial Processes*, *14*, 161-171.

Carey, S. K., and M.-K. Woo (2002), Hydrogeomorphic relations among soil pipes, flow pathways, and soil detachments within a permafrost hillslope, *Physical Geography*, *23*, 95-114.

Carey, S. K., and M. K. Woo (2000), The role of soil pipes as a slope runoff mechanism, Subarctic Yukon, Canada, *Journal of Hydrology*, *233*, 206-222.

Carey, S. K., and M. K. Woo (2001), Slope runoff processes and flow generation in a subarctic, subalpine catchment, *Journal of Hydrology*, *253*, 110-129.

Choi, J., et al. (2000), Characterizing multiple timescales of stream and storage zone interaction that affect solute fate and transport in streams, *Water Resources Research*, *36*, 1511-1518.

Chow, V. T., et al. (1988), *Applied Hydrology*, McGraw-Hill, Inc., New York.

Conovitz, P. A., et al. (1998), Hydrologic processes influencing streamflow variation in Fryxell Basin, Antarctica., in *Ecosystem dynamics in a polar desert: The McMurdo Dry Valleys*, edited, pp. 93-108, American Geophysical Union, Washington, DC.

Cozzetto, K., et al. (2006), Experimental investigations into processes controlling stream and hyporheic temperatures, Fryxell Basin, Antarctica, *Advances in Water Resources*, *29*, 130-153.

Dahm, C. N., et al. (1998), Nutrient dynamics at the interface between surface waters and groundwaters, *Freshwater Biology*, *40*, 427-451.

Dent, C. L., et al. (2007), Variability in surface-subsurface hydrologic interactions and implications for nutrient retention in an arid-land stream, *Journal of Geophysical Research-Biogeosciences*, *112*.

DePaolo, D. J., et al. (2006), Sediment transport time measured with U-series isotopes: Results from ODP North Atlantic drift site 984, *Earth and Planetary Science Letters*, *248*, 379-395.

Dingman, S. L. (1994), *Physical Hydrology*, Prentice Hall, New Jersey.

Dixon, R. K., et al. (1994), Carbon pools and flux of global forest ecosystems, *Science*, *263*, 185-190.

Dodds, W. K., et al. (2002), N uptake as a function of concentration in streams, *Journal of the North American Benthological Society*, *21*, 206-220.

Donaldson, J. R., and P. V. Tryon (1990), User's guide to STARPAC - The standards, time series, and regression package.

Doran, P. T., et al. (2002), Valley floor climate observations from the McMurdo dry valleys, Antarctica, 1986-2000, *Journal of Geophysical Research-Atmospheres*, *107*.

Edwardson, K. J., et al. (2003), The hydraulic characteristics and geochemistry of hyporheic and parafluvial zones in Arctic tundra streams, north slope, Alaska, *Advances in Water Resources*, *26*, 907-923.

Esposito, R. M. M., et al. (2006), Antarctic climate cooling and response of diatoms in glacial meltwater streams, *Geophysical Research Letters*, *33*.

Fisher, S. G., et al. (1998), Material spiraling in stream corridors: A telescoping ecosystem model, *Ecosystems*, *1*, 19-34.

Fortner, S. K., et al. (2005), The geochemistry of supraglacial streams of Canada Glacier, Taylor Valley (Antarctica), and their evolution into proglacial waters, *Aquatic Geochemistry*, *11*, 391-412.

Fountain, A. G., et al. (1999), Physical controls on the Taylor Valley ecosystem, Antarctica, *Bioscience*, *49*, 961-971.

Fountain, A. G., et al. (2007), Evolution of cryoconite holes and their contribution to meltwater runoff from glaciers in the McMurdo Dry Valleys, Antarctica (vol 50, pg 35, 2004), *Journal of Glaciology*, *53*, 723-723.

Gooseff, M. N., et al. (2006), A modeling study of hyporheic exchange pattern and the sequence, size, and spacing of stream bedforms in mountain stream networks, Oregon, USA (Retraction of vol 19, pg 2915, 2005), *Hydrological Processes*, *20*, 2441-+.

Gooseff, M. N., et al. (2007), Relating transient storage to channel complexity in streams of varying land use in Jackson Hole, Wyoming, *Water Resources Research*, *43*.

Gooseff, M. N., et al. (2002), Weathering reactions and hyporheic exchange controls on stream water chemistry in a glacial meltwater stream in the McMurdo Dry Valleys, *Water Resources Research*, *38*.

Gooseff, M. N., et al. (2003), Determining long time-scale hyporheic zone flow paths in Antarctic streams, *Hydrological Processes*, *17*, 1691-1710.

Gooseff, M. N., et al. (2004a), Reach-scale cation exchange controls on major ion chemistry of an Antarctic glacial meltwater stream, *Aquatic Geochemistry*, *10*, 221-238.

Gooseff, M. N., et al. (2004b), Denitrification and hydrologic transient storage in a glacial meltwater stream, McMurdo Dry Valleys, Antarctica, *Limnology and Oceanography*, *49*, 1884-1895.

Green, W. J., et al. (1988), The Geochemistry of Antarctic Streams and Their Role in the Evolution of 4 Lakes of the Mcmurdo Dry Valleys, *Geochimica Et Cosmochimica Acta*, *52*, 1265-1274.

Grimm, N. B., and S. G. Fisher (1984), Exchange between Interstitial and Surface-Water - Implications for Stream Metabolism and Nutrient Cycling, *Hydrobiologia*, *111*, 219-228.

Haggerty, R., et al. (2000), On the late-time behavior of tracer test breakthrough curves, *Water Resources Research*, *36*, 3467-3479.

Harbaugh, A. W. (2005a), MODFLOW-2005, The U.S. Geological Survey modular ground-water model--the Ground-Water Flow Process, *U.S. Geological Survey Techniques and Methods 6-A16*.

Harbaugh, A. W. (2005b), MODFLOW-2005, the U.S. Geological Survey modular ground-water model -- the Ground-Water Flow Process, US Geological Survey.

Harms, T. K., and N. B. Grimm (2008), Hot spots and hot moments of carbon and nitrogen dynamics in a semiarid riparian zone, *Journal of Geophysical Research-Biogeosciences*, *113*.

Harvey, J. W., and K. E. Bencala (1993), The Effect of Streambed Topography on Surface-Subsurface Water Exchange in Mountain Catchments, *Water Resources Research*, *29*, 89-98.

Harvey, J. W., and B. J. Wagner (2000), Quantifying hydrologic interactions between streams and their subsurface hyporheic zones, in *Streams and Ground Waters*, edited by J. B. Jones and P. J. Mulholland, Academic Press, San Diego.

Harvey, J. W., et al. (1996), Evaluating the reliability of the stream tracer approach to characterize stream-subsurface water exchange, *Water Resources Research*, *32*, 2441-2451.

Hester, E. T., and M. N. Gooseff (2010), Moving beyond the banks: Hyporheic restoration is fundamental to restoring ecological services and functions of streams, *Environmental Science and Technology*, *44*, 1521-1525.

Hinzman, L. D., et al. (2005), Evidence and implications of recent climate change in Northern Alaska and other Arctic regions, *Climatic Change*, *72*, 251-298.

Holmes, R. M., et al. (1998), The impact of flash floods on microbial distribution and biogeochemistry in the parafluvial zone of a desert stream, *Freshwater Biology*, *40*, 641-654.

Holmes, R. M., et al. (1996), Denitrification in a nitrogen-limited stream ecosystem, *Biogeochemistry*, *33*, 125-146.

IPCC, et al. (2007), Technical Summary, in *Climate Change 2007: The Physical Science Basis. Contribution of Working Group 1 to the Fourth Assessment Report of the Intergovernmental Panel on Climate Change*, edited by S. Solomon, et al., Cambridge University Press, Cambridge, United Kingdom and New York, NY, USA.

Jones, J. B., et al. (1995a), Nitrification in the Hyporheic Zone of a Desert Stream Ecosystem, *Journal of the North American Benthological Society*, *14*, 249-258.

Jones, J. B., et al. (1995b), Vertical Hydrologic Exchange and Ecosystem Metabolism in a Sonoran Desert Stream, *Ecology*, *76*, 942-952.

Joslin, J. C. (2005), Determining the role of chemical weathering reactions and hyporheic exchange on silicate concentrations in Dry Valley streams, Antarctica, University of Colorado, Boulder, CO.

Junk, W. J., et al. (1989), The Flood Pulse Concept in River-Floodplain Systems, paper presented at Proceedings of the International Large River Symposium, Can. Spec. Publ. Fish. Aquat. Sci.

Kasahara, T., and A. R. Hill (2006), Hyporheic exchange flows induced by constructed riffles and steps in lowland streams in southern Ontario, Canada, *Hydrological Processes*, *20*, 4287-4305.

Kigoshi, K. (1971), Alpha-recoil thorium-234: Dissolution into water and the uranium-234/uranium-238 disequilibrium in nature, *Science*, *173*, 47-48.

Kilpatrick, F. A., and E. D. Cobb (1985), Measurement of Discharge Using Tracers, Techniques of Water Resources Investigations, Book 3, Chapter A16, 52 pp, U.S.Geological Survey.

Koch, J., et al. (in review), Simulating unsteady flow, anabranching, and hyporheic dynamics in a glacial meltwater stream using a coupled surface water routing and groundwater flow model, *Water Resources Research*.

Koch, J. C., et al. (2010a), Effect of unsteady flow on nitrate loss in an oligotrophic, glacial meltwater stream, *Journal of Geophysical Research-Biogeosciences*, *115*.

Lappala, E. G., et al. (1993), Documentation of computer program VS2D to solve the equations of fluid flow in variably saturated porous media, US Geological Survey, Denver, CO.

Lautz, L. K., and D. I. Siegel (2006), Modeling surface and ground water mixing in the hyporheic zone using MODFLOW and MT3D, *Advances in Water Resources*, *29*, 1618-1633.

Lautz, L. K., et al. (2006), Impact of debris dams on hyporheic interaction along a semi-arid stream, *Hydrological Processes*, *20*, 183-196.

Linn, D. M., and J. W. Doran (1984), Effect of water-filled pore space on carbon dioxide and nitrous oxide production in tilled and nontilled soils, *Soil Science Society of America Journal*, *48*, 1267-1272.

Lohse, K. A., et al. (2009), Interactions between biogeochemistry and hydrologic systems, *Annu. Rev. Environ. Resour.*, *34*, 65-96.

Maclean, R., et al. (1999), The effect of permafrost on stream biogeochemistry: A case study of two streams in the Alaskan (U.S.A.) taiga, *Biogeochemistry*, *47*, 239-267.

Marti, E., et al. (1997), Pre- and post-flood retention efficiency of nitrogen in a Sonoran Desert stream, *Journal of the North American Benthological Society*, *16*, 805-819.

McClain, M. E., et al. (2003), Biogeochemical hot spots and hot moments at the interface of terrestrial and aquatic ecosystems, *Ecosystems*, *6*, 301-312.

McKnight, D. M., et al. (1999), Dry valley streams in Antarctica: Ecosystems waiting for water, *Bioscience*, *49*, 985-995.

McKnight, D. M., et al. (2004), Inorganic N and P dynamics of Antarctic glacial meltwater streams as controlled by hyporheic exchange and benthic autotrophic communities, *Journal of the North American Benthological Society*, *23*, 171-188.

Meixner, T., et al. (2007), Influence of shifting flow paths on nitrogen concentrations during monsoon floods, San Pedro River, Arizona, *Journal of Geophysical Research-Biogeosciences*, *112*.

Merz, R., et al. (2006), Spatio-temporal variability of event runoff coefficients, *Journal of Hydrology*, *331*, 591-604.

Miller, M. P., et al. (2006), Hyporheic exchange and fulvic acid redox reactions in an alpine stream/wetland ecosystem, Colorado front range, *Environmental Science & Technology*, *40*, 5943-5949.

Minshall, G. W., et al. (1985), Developments in stream ecosystem theory, *Can. J. Fish. Aquat. Sci.*, *42*, 1045-1055.

Muhs, D. R., et al. (2003), Stratigraphy and palaeoclimatic significance of Late Quaternary loess-palaeosol sequences of the Last Interglacial-Glacial cycle in central Alaska, *Quaternary Science Reviews*, *22*, 1947-1986.

Mulholland, P. J., et al. (2008a), Stream denitrification across biomes and its response to anthropogenic nitrate loading, *Nature*, *452*, 202-205.

Mulholland, P. J., et al. (2008b), Stream denitrification across biomes and its response to anthropogenic nitrate loading, *Nature*, *452*, 202-U246.

Nanson, G. C., and A. D. Knighton (1996), Anabranching rivers: Their cause, character and classification, *Earth Surface Processes and Landforms*, *21*, 217-239.

Newbold, J. W., et al. (1983), Phosphorus dynamics in a woodland stream ecosystem: a study of nutrient spiralling, *Ecology*, *64*, 1249-1265.

Niswonger, R. G., and D. E. Prudic (2005a), Documentation of the streamflow-routing (SFR2) package to include unsaturated flow beneath streams - a modification of SFR1, 48 pp, US Geological Survey.

Niswonger, R. G., and D. E. Prudic (2005b), Documentation of the Streamflow-Routing (SFR2) Package to include unsaturated flow beneath streams - A modification to SFR1, *U.S. Geological Survey Techniques and Methods 6-A13*.

Niswonger, R. G., et al. (2008), Method for estimating spatially variable seepage loss and hydraulic conductivity in intermittent and ephemeral streams, *Water Resources Research*, *44*.

O'Donnell, J. A., and J. B. Jones (2006), Nitrogen retention in the riparian zone of catchments underlain by discontinuous permafrost, *Freshwater Biology*, *51*, 854-864.

Parkin, T. B. (1987), Soil Microsites as a Source of Denitrification Variability, *Soil Science Society of America Journal*, *51*, 1194-1199.

Payn, R. A., et al. (2009), Channel water balance and exchange with subsurface flow along a mountain headwater stream in Montana, United States, *Water Resources Research*, *45*.

Peterson, B. J., et al. (2001), Control of nitrogen export from watersheds by headwater streams, *Science*, *292*, 86-90.

Petrone, K. C., et al. (2007), The influence of fire and permafrost on sub-arctic stream chemistry during storms, *Hydrological Processes*, *21*, 423-434.

Petrone, K. C., et al. (2006), Seasonal export of carbon, nitrogen, and major solutes from Alaskan catchments with discontinuous permafrost, *Journal of Geophysical Research-Biogeosciences*, *111*.

Porazinska, D. L., et al. (2004), The Biodiversity and biogeochemistry of cryoconite holes from McMurdo Dry Valley glaciers, Antarctica, *Arctic Antarctic and Alpine Research*, *36*, 84-91.

Prokushkin, A. S., et al. (2005), Climatic factors influencing fluxes of dissolved organic carbon from the forest floor in a continuous-permafrost Siberian watershed, *Canadian Journal of Forest Research-Revue Canadienne De Recherche Forestiere*, *35*, 2130-2140.

Quinton, W. L., and P. Marsh (1998), The influence of mineral earth hummocks on subsurface drainage in the continuous permafrost zone, *Permafrost and Periglacial Processes*, *9*, 213-228.

Quinton, W. L., and P. Marsh (1999), A conceptual framework for runoff generation in a permafrost environment, *Hydrological Processes*, *13*, 2563-2581.

Risse, L. M., et al. (1994), Determining the Green-Ampt effect hydraulic conductivity from rainfall-runoff data for the WEPP model, *Transactions - American Society of Agricultural Engineers*, *37*, 411-418.

Runkel, R. L. (1998), One-dimensional tranpsort with inflow and storage (OTIS): a solute transport model for streams and rivers, U.S. Geological Survey, Denver, CO.

Runkel, R. L. (2007), Toward a transport-based analysis of nutrient spiraling and uptake in streams, *Limnology and Oceanography-Methods*, *5*, 50-62.

Runkel, R. L., et al. (1998), Analysis of transient storage subject to unsteady flow: diel flow variation in an Antarctic stream, *Journal of the North American Benthological Society*, *17*, 143-154.

Schuur, E. A. G., et al. (2008), Vulnerability of permafrost carbon to climate change: Implications for the global carbon cycle, *BioScience*, *58*, 701-714.

Storey, R. G., et al. (2003), Factors controlling riffle-scale hyporheic exchange flows and their seasonal changes in a gaining stream: A three-dimensional groundwater flow model, *Water Resources Research*, *39*.

StreamSoluteWorkshop (1990), Concepts and Methods for Assessing Solute Dynamics in Stream Ecosystems, *Journal of the North American Benthological Society*, *9*, 95-119.

Striegl, R. G., et al. (2005), A decrease in discharge-normalized DOC export by the Yukon River during summer through autumn, *Geophysical Research Letters*, *32*.

Swanger, K. M., and D. R. Marchant (2007), Sensitivity of ice-cemented Antarctic soils to greenhouse-induced thawing: Are terrestrial archives at risk?, *Earth and Planetary Science Letters*, *259*, 347-359.

Tonina, D., and J. M. Buffington (2007), Hyporheic exchange in gravel bed rivers with pool-riffle morphology: Laboratory experiments and three-dimensional modeling, *Water Resources Research*, *43*.

Valett, H. M., et al. (2005), Biogeochemical and metabolic responses to the flood pulse in a semiarid floodplain, *Ecology*, *86*, 220-234.

Valett, H. M., et al. (1996), Parent lithology, surface-groundwater exchange, and nitrate retention in headwater streams, *Limnology and Oceanography*, *41*, 333-345.

Von Guerard, P., et al. (1995), Streamflow, water-temperature, and specific-conductance data for selected streams draining into Lake Fryxell, Lower Taylor Valley, Victoria Land, Antarctica, 1990-92, U.S. Geological Survey, Denver, CO.

Waddington, J. M., and N. T. Roulet (1997), Groundwater flow and dissolved carbon movement in a boreal peatland, *Journal of Hydrology*, *191*, 122-138.

Walvoord, M. A., and R. G. Striegl (2007), Increased groundwater to stream discharge from permafrost thawing in the Yukon River basin: Potential impacts on lateral export of carbon and nitrogen, *Geophysical Research Letters*, *34*.

Wang, G., et al. (2009), The influence of freeze-thaw cycles of active soil layer on surface runoff in a permafrost watershed, *Journal of Hydrology*, *375*, 438-449.

Welter, J. R., et al. (2005), Nitrogen transport and retention in an arid land watershed: Influence of storm characteristics on terrestrial-aquatic linkages, *Biogeochemistry*, *76*, 421-440.

Wollheim, W. M., et al. (2001), Influence of stream size on ammonium and suspended particulate nitrogen processing, *Limnology and Oceanography*, *46*, 1-13.

Wondzell, S. M. (2006), Effect of morphology and discharge on hyporheic exchange flows in two small streams in the Cascade Mountains of Oregon, USA, *Hydrological Processes*, *20*, 267-287.

Wondzell, S. M., and F. J. Swanson (1996), Seasonal and storm dynamics of the hyporheic zone of a 4th-order mountain stream .1. Hydrologic processes, *Journal of the North American Benthological Society*, *15*, 3-19.

Woolhiser, D. A. (1974), Unsteady free surface flow problems., in *Proc. of Institute on Unsteady Flow in Open Channels*, edited, pp. 195-213, Colorado State University, Fort Collins, CO.

Wroblicky, G. J., et al. (1998), Seasonal variation in surface-subsurface water exchange and lateral hyporheic area of two stream-aquifer systems, *Water Resources Research*, *34*, 317-328.

Zarnetske, J. P., et al. (2007), Transient storage as a function of geomorphology, discharge, and permafrost active layer conditions in Arctic tundra streams, *Water Resources Research*, *43*.

Appendix A:

Incised channel hyporheic dynamics

Introduction

Results and conclusions in Chapters 4 and 5 assume that hyporheic dynamics in the second order stream, Richardson Tributary are negligible, because of the low hydraulic conductivity of the silt-loess soils. This work addresses those assumptions, by measuring changes in stream bed hydraulic gradients and determining stream bank storage.

Methods

Upwelling hydraulic gradients were measured by installing wells at two different depths in the streambed in two locations in the study reach. Paired wells were installed at the base of the steepest hill in the study reach and further downstream in an area which tracer results revealed received substantial subsurface inputs. The paired wells were screened only in the subsurface and monitored with minitroll or level logger 100 pressure transducers that took readings every fifteen minutes. Upward hydraulic gradient (*UHG*) was calculated as:

$$UHG = \frac{P_L - P_U}{z_L - z_U}, \qquad (1)$$

where P is pressure, z is depth, and L and U represent the lower and upper pressure transducers, respectively. This relationship between these two pressure measurements was used to infer the direction of water flow in the stream's subsurface, with the expectation that the greatest response would occur during flood events.

Stream Bank Storage

Inflows to Richardson Tributary beneath the north-facing hillslope were calculated as the difference in discharge measured at the upstream and downstream flumes. Discharge difference was verified on June 30th, and September 1st, 2008 based on tracer dilutions methods described in Chapters 4 and 5.

The magnitude and timing of water storage and release in stream banks as a result of flooding was considered using VS2D, a 2 dimensional unsaturated zone flow model, which solves a form of Darcy's law for flow in variably-saturated media coupled with a continuum equation:

$$V\left[\rho\left(c_m + sS_s\right)\right]\frac{\partial H}{\partial t} - \rho\sum_{k=1}^{m} A_k K k_r\left(h\right)\frac{\partial H}{\partial x_k} - \rho q V = 0, \qquad (2)$$

where V is volume, ρ is density, c_m is the specific moisture capacity, s is liquid saturation, S_s is specific storage, H is hydraulic head, t is time, m is a number of faces of a curvilinear polygon, A_k is the area of the kth face, x_k is the direction orthogonal to the face, K is hydraulic conductivity, h is relative humidity, and q is a volumetric source-sink term. The model was set up as a two dimensional stream cross-section, and was used to simulate lateral flow moving from the stream into the banks as a result of changes in stream stage. Stream bank boundary conditions were set as constant head boundaries when they were at or below the stream stage, and seepage/no flow boundaries when they were above stream stage. Initial conditions were set up as an equilibrium profile based on a water table at the level of the initial/baseflow stream stage. Ice depth was represented as a no flow boundary, and set based on the average thaw depth measured at four transects of Richardson Tributary. The storage change for the simulated storm

events were compared to storage calculated from change in discharge between the upstream flumes

Results

Upwelling hydraulic gradients responded to storm events at each location, and displayed seasonal trends (Figure 1). The upstream well pair displayed the largest magnitude of upwelling during the large, storm event in late June, 2008. This upwelling decreased as the storm flow receded. Subsequent events lead to similar responses, but with smaller magnitudes. Seasonally, there was an increase in the seasonal upwelling hydraulic gradients. The downstream well pair displayed a sinusoidal response to storm events, with downwelling measured at the beginning of the recession, then upwelling, and finally no measureable response. This trend was evident for most events, but with different magnitudes. The largest magnitude occurred during the late June, 2009 flood. There was no measureable seasonal trend in the downstream well pair.

The differences in stream storage for the two measurement methods are displayed in Figure 2. Both methods agree that water moves into storage (out of the stream) during flood events. The difference in discharge shows a much larger and more rapid change in storage relative to the unsaturated flow modeling.

Discussion

Upwelling hydraulic gradients indicate that large changes in stream stage cause gradients in the streambed. Near a steep hillslope, this gradient is always towards the stream, likely because of the high gradient caused by the land surface elevation. The other transect has a shallower surrounding landscape and is probably more representative of most stream reaches. Here, the gradient is initially downwelling and then upwelling following storm events. These

gradients show that the potential for flow exists, but may still not be substantial due to the low hydraulic conductivities.

Storage modeling provides evidence of exactly how much water flow may occur for due to the measured hydraulic gradients. The subsurface hydrologic flow model provides evidence that some water is moving into the subsurface and back out as a result of the storm events, consistent with the pressure gradients measured at the 2009 data. These results also suggest that the change in storage potential is very small.

Storage change measured from flow loss between the gages is much larger, faster, and more uncertain than the unsaturated flow model results. This method measures all water losses between the two stream gages, and is likely larger due to substantial detention storage near the stream channel. Similarities in storage changes between the two models several days after flood events may indicate that detention ponds have drained and further exchange is a result of flood water draining from the streambank.

Conclusion

Both models indicate that flood events are moving water in to storage, with faster exchange into storage than out. The magnitude of storage is small (on the scale of 0.15 m^2) relative to the instream storage identified by transient storage modeling (up to 1.5 m^2 following the June 2008 Flood events).

Figure 1: Richardson Tributary hydrographs from 2008 and 2009 displaying major flood events. Upwelling hydraulic gradients are calculated from pressure measurements at two depths in the streambed. The upstream/hillside site is shown for 2008 and displays a decreasing upward gradient following storm events and a trend of increasing gradient seasonally. The downstream/floodplain site is shown for 2009 and displays rapid shifts from downwelling to upwelling following many storm events. Later in the season, the gradient is downwards.

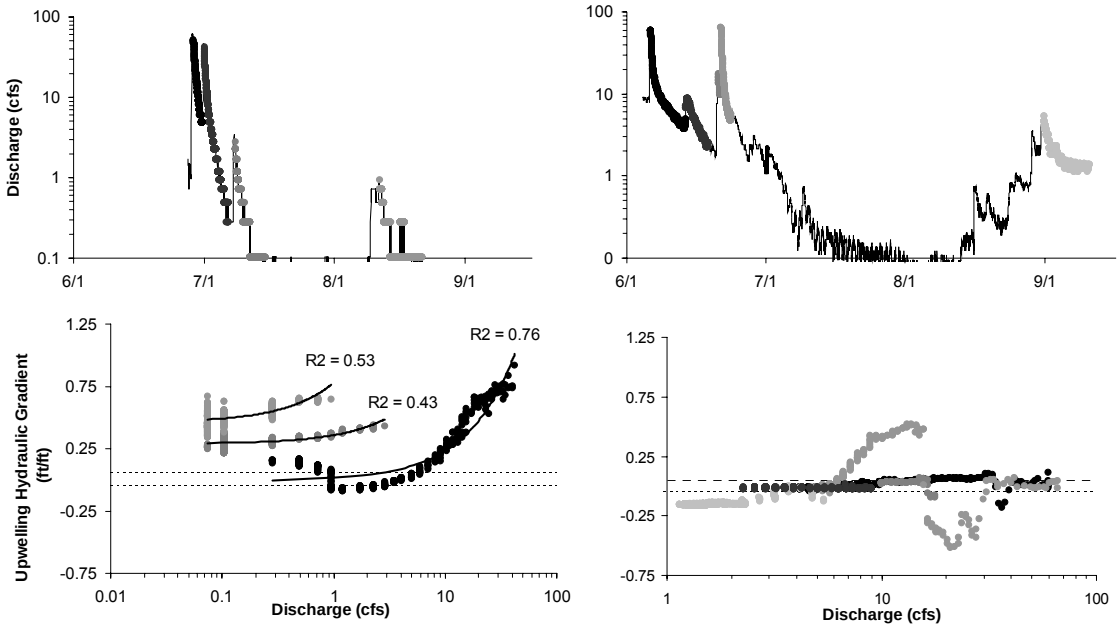

Figure 2: Stream stage and storage for three flood events in 2008. 'Bank infiltration storage' represents flood waters moving in and out of the stream banks as a result of the increased stream stage. 'Discharge loss storage' represents the change in discharge between the two flumes.